UNIVERSITY OF CALIFORNIA SAN DIEGO

Deep-ocean macrofauna assemblages on ferromanganese and phosphorite-rich substrates in the Southern California Borderland

A Thesis submitted in partial satisfaction of the requirements
for the degree Master of Science

in

Oceanography

by

Michelle Guraieb Casis

Committee in charge:

Lisa A. Levin, Chair
C. Anela Choy
Kira Mizell
Gregory W. Rouse

2024

The Thesis of Michelle Guraieb Casis is approved, and it is acceptable in quality and form for publication on microfilm and electronically.

University of California San Diego

2024

DEDICATION

a mis queridos padres,

su amor incondicional y apoyo han sido la fuerza detrás de este trabajo. este es nuestro logro.

con todo mi amor,

michelle

a nuestra Madre Tierra y sus Océanos, por su generosidad que nos sostiene y da vida.

EPIGRAPH

"People feel so separate from the oceans. What we want to do with storytelling is to create that connection and build that relationship. It is the only way we are going to be successful at protecting more of the ocean."

Cristina Mittermeier

TABLE OF CONTENTS

LIST OF FIGURES

LIST OF TABLES

LIST OF SUPPLEMENTAL FILES

Guraieb_Macrofauna_Taxonomy.xlsx

Guraieb_Macrofauna_Counts.xlsx

Guraieb_Macrofauna_Comparisons.xlsx

ACKNOWLEDGEMENTS

Our gratitude goes to NOAA OER for their support through grants NA19OAR110305 and NA23OAR0110520, which made this study possible. The Ocean Exploration Trust and Schmidt Ocean Institute played a crucial role by providing invaluable ship time, and we are grateful for the outstanding team, including captains, crew, ROV pilots, technicians, and science crew, aboard the E/V *Nautilus (NA124)* from October 28 to November 6 of 2020, and the R/V *Falkor (FK210726)* from July 26 to August 6 of 2021. Special thanks are also extended to the Rouse Lab and Jensen Lab for their collaborative contributions to the Levin Lab during the expeditions.

To the members of my thesis committee, Lisa Levin (chair), Greg Rouse, Anela Choy and Kira Mizell, thank you for generously sharing your knowledge with me. You have enriched my academic journey and I am grateful for the feedback and time you provided along the way.

Lisa, I am beyond grateful for the opportunity to be your student. Thank you for your insightful teachings about deep-ocean ecosystems, for taking me to sea, our trip to COP27, and for giving me the most amazing experiences that a few years ago I could've only dreamed of. As a scientist and co-founder of the Deep-Ocean Stewardship Initiative, you have become a tremendous source of inspiration and hope for me. Thank you for teaching me how to communicate effectively as a scientist and for sharing your knowledge with me. I deeply admire your dedication, courage, resilience, commitment, fortitude, knowledge, perseverance, and profound love for the ocean. It's a privilege to share a passion for the deep ocean with you and I look forward to doing more work with you in the future.

I am especially grateful to the taxonomic experts that provided support identifying specimens: Guillermo Mendoza, Greg Rouse, Oliver Ashford, Tim O'Hara, and Charlotte Seid. This work would not have been possible without your time and dedication to this work.

Thank you to Kira Mizell, from the United States Geological Survey (USGS) for identifying the rock substrates on both cruises.

To the members of the Levin Lab, thank you for bouncing off ideas with me, making lab work more fun, being supportive, and building lasting memories at sea with me. Special thanks to Olívia Pereira, thank you for answering my questions, big and small, for your feedback and knowledge of stats, you will always be a friend and inspiration to me. To Ailish, Devin and Angelica thank you for your friendship, for being amazing lab mates and for your support and feedback along the way.

Thank you to Ximena Flores and Ana Patricia Galindo of the ENLACE Program for their volunteer work sorting samples and for giving me my first experience as a mentor.

Thank you to director Margaret Leinen and the Comms team at Scripps Institution of Oceanography for an amazing trip to Egypt in November, 2022, where I was able to put my learned knowledge into practice at the UN Climate Change negotiations.

Special thanks to Dana Jimenez and Gilbert Bretado from the Graduate Office.

Lastly, I thank my friends and loved ones for being amazing. Johanna, Gabo, Zoltan and Alix, thank you for the home and meals we have shared this past year. To my friends around the world – Mireille, Dani, Ale, Andres, Vico, Amala, Andrea, Mariana, Fer, Sandra, Vale, Leticia, Caro, Michelle, Gauri, Jacqueline, Mirabai, Maca, Carol, Eesha, Aria, Damini, Eliza, Gitali, Vanna, Chaitanya, Abby – thank you for filling me with love and support during this time. Ryan, thank you for being the best coding teacher and for being there for me. To my sisters, Mariana and Chris, thank you for your love and support from afar, for visiting me and helping me adjust to a new home. To my parents, thank you for always believing in me, for your love, your immense generosity and for your financial support, without which I would not be presenting this work.

ABSTRACT OF THE THESIS

Deep-ocean macrofauna assemblages on ferromanganese and phosphorite-rich substrates in the Southern California Borderland

by

Michelle Guraieb Casis

Master of Science in Oceanography

University of California San Diego, 2024

Lisa A. Levin, Chair

The deep ocean, exceeding 200 meters in depth, represents Earth's largest habitable space, yet it remains its least explored region. This study focuses on the Southern California Borderland (SCB), an area characterized by uneven and heterogeneous topography; and varying depths, temperatures, and oxygen concentrations. Due to its variability, this environment serves as an optimal setting for investigating the relationship between mineral-rich hardgrounds and benthic fauna. The deep ocean plays a crucial role in resource provisioning, but human activities, including deep-seabed mining, may threaten these oceanic functions. Two mineral-rich substrates, ferromanganese (FeMn) crusts and phosphorite rocks, are among the deep ocean mineral types being considered for their resource potential due to their enrichment in valuable metals in some regions. However, these geological features support deep-ocean biodiversity by acting as specialized substrates for macrofaunal communities and enabling key biogeochemical processes. This study aims to characterize macrofaunal (> 300 μm) density, diversity, and community

composition on mineral-rich substrates in the SCB, focusing on FeMn crusts and phosphorite rocks. Macrofaunal samples were collected using remotely operated vehicles (ROVs) during expeditions in 2020 and 2021. Through quantitative analysis, I explore the faunal association with different substrate types, sites in the SCB, and various environmental variables, including oxygen, depth, temperature, and proximity to shore. Additionally, I assess the relationship between megafauna presence and macrofaunal density and diversity. A total of 3,555 macrofauna individuals were counted and 417 different taxa were identified from 82 rocks from depths between 231 m and 2,688 m. Average density for SCB macrofauna was 11.08 ± 0.87 individuals /200 cm^2 and mean diversity per rock was $H'_{(loge)}$ = 2.22 ± 0.07. A relationship was found between site, substrate type, and macrofaunal communities. Phosphorite rocks had the highest diversity on a per-rock basis and when pooled, FeMn crusts had the highest number of species. Of all the environmental variables, depth explained the largest variance in macrofauna community composition. Macrofauna density and diversity had similar values at sites within and outside the oxygen minimum zone (OMZ). Understanding the intricate relationships between macrofaunal assemblages and mineral-rich substrates is essential, especially in the context of environmental disruptions associated with deep-seabed mining or climate change. This study is the first to analyze the macrofaunal communities of mineral-rich hard substrates in the SCB. The findings contribute crucial baseline information for effective conservation and management of the SCB and will support scientists in monitoring changes in these communities due to environmental disturbance or human impact in the future.

INTRODUCTION

The Deep-Ocean Floor: Mineral-Rich Resources and Their Biological Importance

The deep ocean (> 200 m deep) is the largest habitable space on Earth and it remains the least explored and understood area of the ocean. With an average depth of 3,800 m, the ocean consists mostly of deep water, which represents over 95% of the volume on earth that is available for living organisms to thrive (Danovaro et al., 2020). The ocean plays a vital role in regulating our climate and providing essential services and resources to humanity (Thurber et al., 2014; Baker et al., 2020). However, human activities are increasingly impacting the natural functions that occur in the ocean, and as a result, the deep-ocean ecosystem services provided to humankind are under pressure (Baker et al., 2020). Advancing our knowledge of the deep ocean through baseline studies is a vital step toward developing conservation initiatives and effective marine ecosystem management strategies. Addressing these gaps in knowledge is especially urgent as cumulative impacts, from climate change to deep-seabed mining, pose complications for the proper management of the deep ocean (Levin et al., 2016; Baker et al., 2020).

Two deep-ocean minerals types being considered for their resource potential are ferromanganese (FeMn) crusts and phosphorite rocks. Due to the economic potential of some of these mineral occurrences, these mineral-rich rocks are of interest to the deep-ocean mining industry (Hein et al., 2016; Conrad et al., 2017). FeMn crusts, which were first studied as a resource for cobalt in the early 1980s, are also enriched in other metals (Halbach et al., 1982; Hein et al., 2013). Some of these metals (e.g., copper, nickel and manganese) offer an additional source of raw materials beyond terrestrial deposits for the development of renewable energy applications and green technologies. FeMn crusts precipitate in cold water at high pressure and are typically found within OMZs in areas with low organic carbon content, and low sedimentation rates (Hein et al.,

2013; Usui et al., 2017; Mizell et al., 2020; Benites et al., 2023). These crusts are found at depths of 400-7,000 m on seamounts, ridges and plateaus, with a higher density in the Pacific compared to the Atlantic and Indian oceans (Hein et al., 2013).

Marine phosphorites occur in the Pacific and Atlantic oceans along the western continental margins at depths above 2,500 m in upwelling areas, on seamounts and lagoon deposits (Hein et al., 2016). Some occurrences of these phosphorous-rich rocks are primarily of interest to the mining industry because they can be a source of macronutrients for fertilizers used in agriculture and (USGS), and some phosphorites may also be of interest as a source of rare earth elements as a secondary ore (Hein et al. 2016).

Extraction of these mineral-rich geological features is likely to come at a cost to deep-ocean biodiversity and the health of the global ocean (Levin et al., 2016). FeMn crusts and phosphorite rocks are inherently interwoven with the life of deep-ocean fauna as they cover miles of the seafloor where animals live and where biogeochemical processes fundamental to the overall balance of ocean ecosystems occur (Jones et al., 2018). However, the relationship between macrofauna communities and mineral-rich hard substrates, beyond the fact that they provide a source of attachment or physical habitat, is still not well understood (Schlacher et al., 2014).

Biodiversity and species abundance in the deep ocean are responsible for key ecological functions, such as nutrient cycling, bioturbation, connectivity, primary and secondary production, respiration, habitat, and food supply (Le et al., 2017). These ecological functions translate into provisioning services (such as fisheries, pharmaceuticals, industrial agents and biomaterials); regulating services (such as climate regulation, biological control, waste absorption); and cultural services (such as educational, aesthetic, existence and stewardship; Le et al., 2017). The loss of biodiversity leads to a decline in these important functions and services on which we rely

(Danovaro et al., 2008). Furthermore, the biodiversity in the deep ocean is a crucial component of the resilience of these ecosystems contributing to their ability to withstand the effects of anthropogenic disturbance (Oliver et al., 2015).

Deep water fishing, climate change and deep-seabed mining are the main potential stressors to deep-ocean ecosystems (Ramirez-Llodra et al., 2011). For example, according to Levin et al. (2016), mining of FeMn crusts and phosphorite rocks will remove currently living structure-forming organisms that provide habitat and food for other smaller fauna (Buhl-Mortensen et al., 2010), resulting in the loss of heterogeneity and therefore driving a decline in biodiversity. Other potential effects discussed are 1) flattening of seamount surfaces, 2) more soft sediment, 3) the creation of sediment plumes that can temporarily bury fauna and negatively impact larval settlement, 4) increase of metal concentrations in the water that could potentially bioaccumulate in the tissues of animals and cause toxicity (Levin et al., 2016). Moreover, the consequences of climate change, including oxygen loss, have the potential to amplify the adverse impacts stemming from mining operations (Le et al., 2017). The consensus of the scientific community is that prudence and caution must be exercised in approach to these activities (Levin et al., 2016; Jones et al., 2018; Montserrat et al., 2019), which baseline studies such as this can help define.

Oxygen Minimum Zone of the Southern California Borderland

The Southern California Borderland (SCB) offers a unique environment to study the relationship between mineral-rich hardgrounds and the benthic fauna that live on them. A variety of geological features (e.g. banks, ridges, knolls, escarpments and seamounts) and environmental conditions (low oxygen, various depths, varying food supply, temperature ranges) add to the heterogeneity of the region and make it suitable habitat for many marine species that inhabit hard substrates. The SCB exhibits characteristics that allow for a well-formed OMZ at bathyal depths

(400-1,100 m in the case of this study) because it is located on the eastern boundary of the Pacific Ocean Basin, where upwelling acts as one of the drivers of oxygen depletion (Gooday et al., 2010). Equatorward winds blowing along the coast in the SCB underpin the upwelling of nutrients from depths of 200 m; these nutrients support primary productivity (Checkley & Barth, 2009). More productivity in shallow waters leads to large amounts of organic matter sinking to deeper depths where bacteria use oxygen to decompose organic particles, further driving oxygen depletion (Levin, 2003).

Ocean deoxygenation is a phenomenon characterized by the reduction of dissolved oxygen content in the ocean due to human activities, primarily the addition of nutrients and global warming (Breitburg et al., 2018; Oschlies et al., 2018). Schmidtko et al. (2017) revealed that the entire ocean has lost 2% of its oxygen over the past 50 years (~0.072 μmol/kg per year) and predict that dissolved oxygen will continue to decline (up to 7%) in the next eighty years. This overall loss of oxygen has caused the expansion of oxygen minimum zones (OMZs), leading to changes in the physical and chemical dynamics of the ocean (Stramma et al., 2010). OMZs are defined as regions where oxygen concentrations are <0.5 ml/l or <22 mM (Levin, 2003). The expansion of these zones can reduce or increase the habitat of marine species, which may trigger a variety of biological responses within and among different species of marine animals (Stramma et al., 2010).

Moreover, as the atmosphere has warmed due to the burning of fossil fuels, the ocean has taken up massive amounts of heat, which has had severe consequences on the physics and biogeochemistry of the ocean (Keeling et al., 2010). Stratification of the water column results from increased heat transfer from the atmosphere into the surface layers of the ocean. Stratification may offset the effect of strong alongshore winds and thus, weaken vertical mixing processes that transport oxygenated waters from the surface of the ocean to its depths (Keeling et al., 2010).

Another effect of climate change is the reduction of the ocean's capacity to hold dissolved gas. As the ocean's temperatures increase, dissolved oxygen concentrations decrease because oxygen is less soluble in warm water (Garcon et al., 2019). For these reasons, a continuous increase in the ocean's uptake of heat can exacerbate oxygen depletion in the global ocean and particularly in the SCB (Howard et al., 2020).

Species composition and abundance have been shown to respond to OMZs. For example, macrofauna densities are lowest in the core of the OMZ (Levin, 2003), and macrofauna diversity decreases with declining oxygen concentrations (Gooday et al., 2010; Levin et al., 2002; Levin et al., 1991). In this study, oxygen concentrations were obtained to evaluate the potential relationship of low oxygen in OMZs to the distribution of marine organisms on mineral-rich substrates in the deep ocean.

Deep-Ocean Faunal Studies and Their Relevance

Since the *Challenger* expedition, much interest has sprung within the oceanographic community to study the ocean, especially at its depths. During the past three decades, technological advancements have allowed scientists to study the diversity, ecology and surrounding environment of deep-ocean macrofauna using multicores (De Smet et al., 2017), submersibles (Dong et al., 2021; Li, 2017) and ROVs (Schlacher et al., 2014). Various studies have explored the relationship between benthic faunal communities and the substrate on which they live (Gage & Tyler, 1991; Gooday et al., 2010; Vanreusel et al., 2010; Schlacher et al., 2014; Simon-Lledó et al., 2019; Pereira et al., 2022;). However, most studies that examine this relationship have focused on chemosynthetic ecosystems (Baco & Smith, 2003; Levin et al., 2015, 2017; Bourque et al., 2017; Pereira et al., 2021, 2022), and deep-ocean sediments (Wei et al., 2012; Baldrighi et al., 2014; Leduc et al., 2015; De Smet et al., 2017; Dong et al., 2021). Those studies undertaken on non-

reducing hard substrates have mainly examined the characteristics of the megafauna community (Clark, 2011; Grigg et al., 2013; Amon et al., 2016; De Smet et al., 2021; Vlach 2022). Other studies consider the megafauna to be the hard substrate that provides shelter and food to smaller animals affecting their biodiversity (Buhl-Mortensen et al., 2010). Only a few studies consider the macrofaunal assemblages on mineral-rich abyssal plain nodules, and they largely focus on foraminifera (Mullineaux, 1987, 1989). The one study of macrofauna on FeMn crusts was only qualitative (Toscano & Raspini, 2005). Therefore, the SCB analysis is the first to examine the macrofaunal relationship with mineral-rich hard substrates in a quantitative analysis of density, diversity and community composition in the region.

These data contribute to the development of management and conservation plans that maintain a safe development standard for waters off the coast of California. Studying healthy ecosystems such as the SCB also offers opportunities for comparative studies against areas currently under consideration for mining activities. Regions such as the Mid-Pacific ocean basins hosting FeMn crust, as well as areas in Mexico, Namibia, South Africa, and New Zealand with phosphorites are currently being considered for their economic potential, causing a need to understand the biodiversity of these locales (Levin et al., 2016). Safeguarding and studying analogous ecosystems in regions not currently targeted by mining enterprises, such as the SCB, will contribute to the overarching objective of maintaining equilibrium in the ocean and ensuring ecosystem services and functions continue to contribute to humanity. This is of particular importance to the people of California, who are spiritually, culturally and economically connected to the deep ocean (CA AB1832, 2022).

Research Objectives.

The objective of this study is to understand the relationship of macrofaunal (> 300 μm) assemblages to mineral-rich substrates in the SCB off the Pacific coast of the United States, and to other environmental factors. For substrates collected during two oceanographic expeditions (NA124 cruise in 2020 and FK210726 cruise in 2021), I characterize the macrofaunal (> 300 μm) density, diversity and community composition (hereafter community structure) of the mineral-rich and other hard substrates of the SCB. To do this I evaluate the relationship between community structure and geological, hydrological and biological features. Specifically, I examine faunal association with a) various substrate types (mainly ferromanganese crusts, and phosphorite, basalt and sedimentary rocks); b) various sites in the SCB; c) different environmental variables (oxygen, depth, temperature and proximity to shore); and d) megafauna presence (Table 1). The quantitative measurements used in this study to analyze the differences in macrofaunal community structure across various substrate types, locations, and environmental variables are density, diversity (H', J', rarefaction diversity and species richness) and community composition, which refers to the identification and relative abundance of species and higher taxa in a community. These data will provide baseline information that can inform decision-making processes and support conservation management strategies for biodiversity in Southern California and in the deep ocean.

Table 1. Hypotheses relating to the research objectives and questions.

Objectives	Research Questions	Hypotheses
Analyze the macrofaunal (> 300 μm) community structure (density, diversity and community composition) characteristics of the mineral-rich hard substrates of the SCB.	What is the density, diversity, and species composition of macrofaunal assemblages of hardgrounds in the SCB? And how does it compare to other hardground ecosystems?	H1: Macrofaunal assemblages will exhibit lower densities compared to chemosynthetic ecosystems. The diversity of the assemblages will be higher than at chemosynthetic ecosystems because they harbor more specialized fauna.
Examine the correlation of various substrate types (mainly ferromanganese crusts, phosphorite and basalt rocks) with the community structure of macrofaunal assemblages.	Do the macrofauna communities of ferromanganese crusts and phosphorite exhibit unique biological characteristics?	H1: The density, diversity and community composition of macrofauna are significantly different across various mineral-rich hard substrates.
Quantify the differences in the community structure of macrofaunal assemblages at various sites in the SCB.	Should conservation management strategies of the SCB be developed for specific sites depending on their abundance and uniqueness of the biodiversity?	H1: The density, diversity and community composition of macrofauna across sites are significantly different to one another.
Evaluate the effects of different environmental variables (oxygen, depth and proximity to shore) on the community structure of macrofaunal assemblages.	Will future environmental changes (e.g. deoxygenation and changes in food availability) have an effect on the biodiversity of macrofaunal assemblages?	H1: Macrofaunal assemblages within the OMZ will exhibit lower densities and diversity compared to those in more oxygenated areas. H2: Macrofauna communities in deeper waters are significantly less dense but more diverse than at shallower depths. H3: Macrofauna communities closer to shore will have significantly higher densities and differences in their community composition compared to those off-shore.
Determine whether the densities and diversities of macrofauna change as a function of megafauna presence.	Does the presence of larger fauna enhance the biodiversity of smaller animals?	H1: The presence of megafauna enhances the density and diversity of macrofaunal assemblages due to the provision of shelter and food.

STUDY AREA

The samples used for the analysis of macrofauna in this study came from 14 sites in the Southern California Borderland (Figure 1). This area is located on the California continental margin where tectonic and volcanic activity has formed numerous geological features, including banks, ridges, knolls, escarpments and seamounts, that add to the heterogeneity of the region and make it a suitable place to study the benthic communities of macrofauna living on hard substrates. The area has unique hydrological characteristics that include a variety of depths, oxygen concentrations (Figure 2A) and temperature variations (Figure 2B).

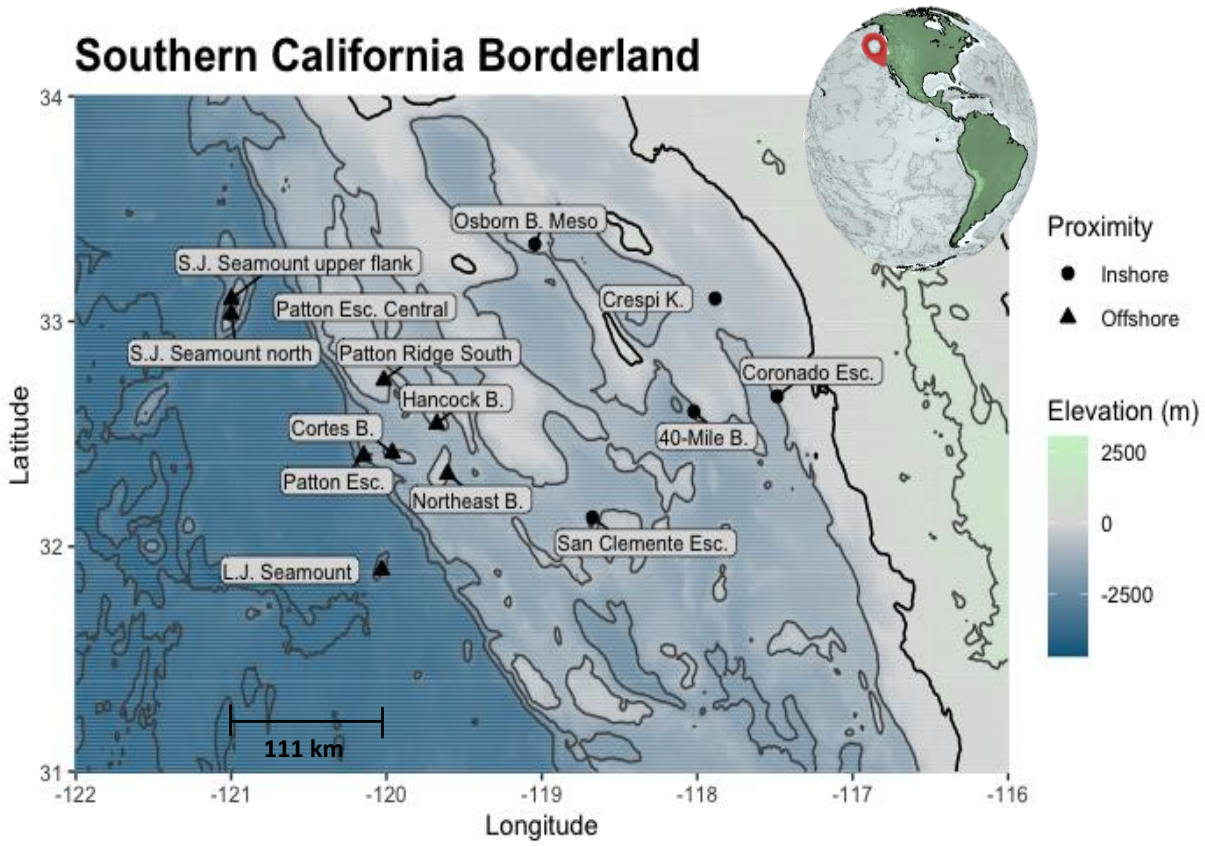

Figure 1. Map of the Southern California Borderland and the locations visited during the expedition aboard *E/V Nautilus* in 2020 and *R/V Falkor* in 2021. Eight sites (Patton Esc. = Patton Escarpment, S.J. Seamount Upper Flank = San Juan Seamount Upper Flank, Northeast B. = Northeast Bank, Cortes B. = Cortes Bank, Patton Ridge South, 40-Mile B. = 40-Mile Bank, San Clemente Esc. = San Clemente Escarpment, Osborn B. Meso = Osborn Bank Mesophotic Zone) were visited on the Nautilus cruise (NA 124) and 7 sites (Hancock B. = Hancock Bank, S.J. Seamount North = San Juan Seamount North, Patton Esc. = Patton Escarpment, L.J. Seamount = Little Joe Seamount, Crespi K. = Crespi Knoll, Coronado Esc. = Coronado Escarpment) visited on the Falkor cruise (FK210726). Inshore sites are situated within a proximity of 100 km from the shoreline.

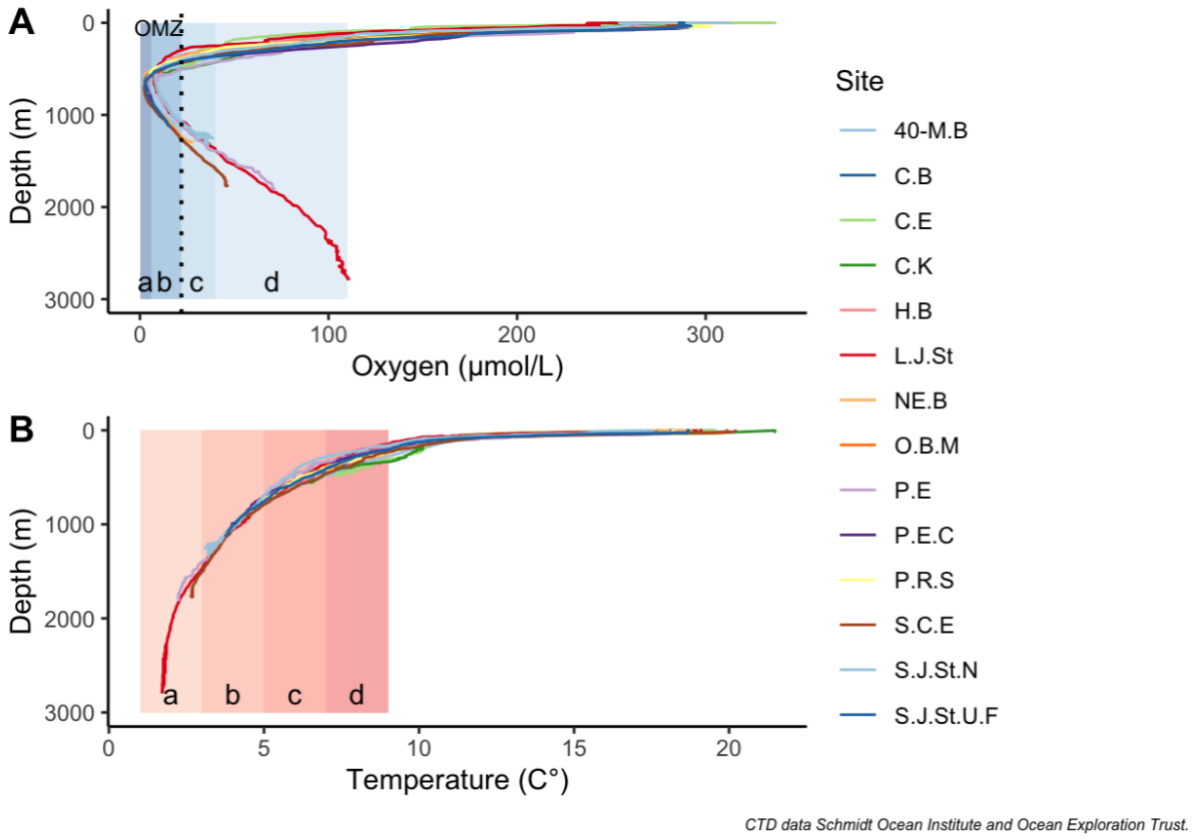

Figure 2. CTD casts for all sites. Letters a, b, c, and d reflect the different oxygen and temperature categories used in this study. A) Oxygen profile of the sites visited in the SCB. Oxygen categories: a) 0-6 µmol/L, b) 6-22 µmol/L, c) 22-40 µmol/L, d) 40-110 µmol/L). The dotted line reflects the highest oxygen limit of the OMZ (22 µmol/L), this feature occurs within 400 and 1100 m at the SCB. Categories a and b are within the OMZ. B) Temperature profile of the sites visited in the SCB. Temperature categories: a)1-3 C°, b)3-5 C°, c)5-7 C°, d)7-9 C°. Site initials: 40-M.B = 40-Mile Bank, C.B = Coronado Bank, C.E = Coronado Escarpment, C.K = Crespi Knoll, H.B = Hancock Bank, L.J.St = Little Joe Seamount, NE.B = Northeast Bank, O.B.M = Osborn Bank Mesophotic Zone, P.E = Patton Escarpment, P.E.C = Patton Escarpment Central, P.R.S = Patton Ridge South, S.C.E = San Clemente Escarpment, S.J.St.N = San Juan Seamount North, S.J.St.U.F = San Juan Seamount Upper Flank.

MATERIALS AND METHODS

Biological and Environmental Data Collection

The collection of samples for this study took place during two separate expeditions. The first expedition took place aboard the exploration vessel E/V *Nautilus*, from October 28 to November 6 of 2020. The second expedition took place aboard the vessel R/V *Falkor*, from July 26 to August 6 of 2021. Each vessel travelled to different locations (Table 2) within the Southern California Borderland to collect rocks of different mineral types (Table 3) along with the community of animals living on them. Samples from Lasuen Knoll and the DDT barrel sites were not used in this study and therefore, they do not appear in the figures and tables herein. These were not considered because chemosynthetic systems (Lasuen Knoll) and soft sediment basins (DDT site) are not under consideration in this thesis. The collection of rocks was carried out using two remotely operated vehicles (ROV), *Hercules* (onboard E/V *Nautilus*) and *SuBastian* (onboard R/V *Falkor*). *Hercules* is equipped with two manipulator arms, one high-definition video camera, LED lights. *SuBastian* is equipped with two manipulators, two high-resolution video cameras, and LED lights. Both ROVs carry a variety of sensors, such as a Conductivity-Temperature-Depth sensor or CTD, an oxygen sensor, and a temperature probe. These sensors are used to measure pressure, depth, water temperature, oxygen concentration, and salinity. These characteristics enable these robots to collect physical samples, such as biological collections, and sediment and water samples.

Table 2. Sites visited aboard E/V Nautilus (NA124) and R/V Falkor (FK210726) with the dive number, date sampled, site name, depth range (from the start to the end of the dive) and physical coordinates at the start of the dive.

Cruise number	***Dive***	***Date***	***Site/Location***	***Depth range (m)***	***Lat***	***Long***
NA124	H1840	29-Oct-20	Patton Escarpment Central	476 – 1054	33.06	-120.12
	H1841	30-Oct-20	San Juan Seamount upper flank	605 – 113	33.03	-121
	H1842	31-Oct-20	Northeast Bank	503 – 1319	32.31	-119.59
	H1843	1-Nov-20	Cortes Bank	439 – 575	32.41	-119.29
	H1844	2-Nov-20	Patton Ridge South	567 – 772	32.73	-120.01
	H1845	3-Nov-20	40-Mile Bank	594 – 1114	32.60	-118.02
	H1846	4-Nov-20	San Clemente Escarpment	842 – 1778	32.67	-118.13
	H1847	5-Nov-20	Osborn Bank Mesophotic Zone	106 – 459	33.34	-119.04
FK210726	S0440	26-Jul-21	Hancock Bank	319 – 579	32.54	-119.67
	S0443	28-Jul-21	San Juan Seamount North	689 – 1442	33.03	-120.99
	S0444	29-Jul-21	Patton Escarpment	1358 – 1797	32.40	-120.14
	S0445	30-Jul-21	Little Joe Seamount	2362 – 2772	31.89	-120.03
	S0448	1-Aug-21	Crespi Knoll	430 – 550	33.10	-117.88
	S0452	5-Aug-21	Coronado Escarpment	376 – 477	32.66	-117.48

Sampling and At-Sea Processing

For this study, a total of 82 rocks were collected, 37 of which were ferromanganese crusts, 19 were phosphorite rocks, 19 were basalt rocks, and 7 were sedimentary rocks. Rock types and numbers of rocks collected per site are summarized in Table 3. The ROV collected rocks with the manipulator arm and attempted to keep each rock in its in-situ orientation and jostle it as little as possible to preserve fauna settled on the substrate. Each rock was placed into its own isolated biobox compartment on the ROV to avoid cross-contamination or loss of fauna during transport. Upon collection of the rocks, the CTD attached to the ROV obtained measurements of temperature,

pressure (depth) and oxygen concentrations for each of the locations where the rocks were found. Table A1 presents environmental data recorded at the time of rock collection. The rock substrates were processed quantitatively for their associated biological community. Once the rocks arrived in the wet lab, they were kept in a refrigerator until processing. Every rock was photographed with a scale and label. All the visible biology was removed using forceps and kept in crystalizing dishes with seawater. The residual water contained in each biobox pertaining to each rock was washed through a 0.042 mm and 0.3 mm mesh to collect meiofauna and macrofauna, respectively. The macrofauna from each rock was preserved in ethanol and the meiofauna in formalin. Only macrofauna are discussed in this thesis. Then, the rocks were wrapped in a monolayer of aluminum foil, which was later weighed to obtain surface area in cm^2. Furthermore, the rocks were left overnight in seawater buckets at room temperature to allow the remaining fauna to crawl away or fall out of the rock's crevices. Finally, each bucket was washed again to recover the fauna. Once all the metazoans were removed from the rocks, the geologist onboard processed them following the methods below to identify the rock and mineral type.

Table 3. Number of rocks collected aboard the E/V *Nautilus* and their specific substrate type. The average temperature was calculated using the temperature measured at the exact location where each rock was found. The depth and oxygen ranges depict the values measured where the first and last rocks were collected. For a full list of the substrate type per rock, FeMn crust thickness and surface area per rock, see Table A2.

Cruise	***Site and dive number***	***Depth range (m)***	***Average temperature (°C)***	***Oxygen range (µmol/ L)***	***Rock type***			
					Basalt	***Phosphorite***	***FeMn crusts***	***Sedimen-tary***
NA124	*Patton Escarpment Central (HD1840)*	587-820	*5.34*	*2.61-5.14*	*1*	*1*		*3*
	San Juan Seamount upper flank (HD1841)	691-1129	4.39	2.79-14.04			5	
	Northeast Bank (HD1842)	553-1132	5.15	2.68-15.95	2		3	
	Cortes Bank (HD1843)	437-529	6.41	4.14-8.31		5		
	Patton Ridge South (HD1844)	562-726	5.40	2.55-3.96		5		
	40-Mile Bank (HD1845)	658-1036	4.76	2.11-14.6			2	3
	San Clemente Escarpment (HD1846)	1189-1718	3.03	15.27-37.46	1		4	
	Osborn Bank Mesophotic Zone (HD1847)	231-396	7.83	19.71-54.79	4			
FK210726	*Hancock Bank (S0440)*	319-594	6.54	9 – 36.48	6	1	1	
	San Juan Seamount North (S0443)	1138-1442	3.29	26.7 – 36.48			8	
	Patton Escarpment (S0444)	1463-1797	2.60	46.89 – 70.9			6	
	Little Joe Seamount (S0445)	2368-2688	1.81	100.17 – 108.14			8	
	Crespi Knoll (S0448)	443-525	7.08	12.99 – 33.11	5			1
	Coronado Escarpment (S0452)	443-467	7.57	24.16 – 28.28		7		

Substrate Identification by U.S Geological Survey

Dr. Kira Mizell, of the U.S. Geological Survey, identified the rocks collected from the Southern California Borderland. Rock samples were cut along their longest axis using a diamond blade, and the cut face was described in detail regarding apparent mineral type, stratigraphy, texture, and size. FeMn crusts are identifiable by color and morphology; they are black precipitates occurring on hard substrate of a different rock type (often basalt or other volcanic rock). Phosphorite are typically smooth, shiny, and dense; however, in some cases, it was difficult to tell if a sample was carbonate or phosphorite. To confirm mineral type when ambiguous, representative slabs were cut from each sample for crushing and powdering. Powdered sample was then analyzed by x-ray diffraction (XRD) to determine the presence of carbonate fluorapatite (phosphorite), calcite (carbonate or limestone), clay minerals (mudstone), or volcanic minerals (e.g. feldspar). XRD data were produced by a Panalytical X'Pert3 x-ray diffractometer with CuKα radiation and graphite monochromator. The first and primary measurement for all samples was collected every 0.02 °2 theta between 4 ° and 70 °2 theta at 40 kV and 45 mA. Diffraction peaks from the digital scan data were identified using Phillips X'Pert High Score software, and mineral patterns were matched to patterns from the ICDD PDF4+ database.

Lab Processing and Data Synthesis

At Scripps Institution of Oceanography, the surface area of the rocks was obtained by weighing 10 pieces of aluminum foil of 25 cm^2 using a top-loading balance to calculate the weight of 1 cm^2. Later, each piece of aluminum foil corresponding to each rock was weighed and the number obtained was divided by the weight of a 1 cm^2 piece of aluminum foil (0.0064 g) to obtain the surface area of each piece. The surface area of each rock was used to calculate the densities of organisms per 200 cm^2.

The macrofauna preserved in ethanol at sea, was re-sieved in distilled water using a 0.3 mm mesh. Then, the contents were poured into a petri-dish with freshwater for sorting under a dissecting microscope at 12x magnification. Organisms were divided into 5 glass vials, depending on their taxonomic classification. The vials were labelled with the following Phylum: Mollusca, Annelida, Echinodermata, Arthropoda and other (for all other specimens). Once all samples were sorted, each vial was emptied in a petri-dish to identify the organisms to the lowest taxonomic level possible and count the total number of animals. A total of 140 individuals were paired to a specific genus and 59 were given a species name, the rest were identified to their lowest taxonomic level possible and designated as morphospecies. Finally, the counts of animals that were removed at sea for genetic or isotopic analyses were added to the dataset. The counts of the megafauna present on the rocks were added by looking at the shipboard photographs of each rock. Megafaunal specimens were retrieved by Greg Rouse and Paul Jensen; some specimens were sent to the Benthic Invertebrate Collection at Scripps Institution of Oceanography and others were kept in the Jensen Lab for further analysis. Identifications were acquired from these two sources. Voucher specimens of macrofaunal morphospecies are being deposited to the Scripps Institution of Oceanography Benthic Invertebrate Collection (SIO-BIC).

Statistical Analyses

Univariate analysis

Density

Procedures from Levin et al. (2015) were followed to standardize the densities of the macrofauna community to 200 cm^2. This involved dividing the number of animals in each sample by the surface area of the rock (in cm^2) and multiplying by 200. The dataset used to calculate densities included encrusting bryozoans and hydrozoans, which were not identified to species level, since species identification is not required to assess density. Total densities per sample were tested for normality using Shapiro-Wilk test. A square-root transformation was applied to density to generate a normal distribution. Then, Bartlett's test was used to assess if the variances were homogeneous. To determine if there were any statistically significant differences in densities between depth ranges and between various oxygen concentrations, a one-way analysis of variance (ANOVA) test was used followed by a Post Hoc Tukey test (Tukey's Honest Significant Difference test) for pairwise comparisons in ANOVA. As not all environmental variables showed homogeneity of variance, Kruskal-Wallis tests followed by Dunn's tests using Benjamini-Hochberg adjustment (Benjamini & Hochberg, 1995) were performed when comparing densities across substrate types, sites and various temperature categories. Mann-Whitney U test was used to compare the means between inshore and offshore sites and also to compare the means between rocks with and without megafauna. These tests were performed in R software using the packages vegan and car, and plots were done with ggplot2 package.

Diversity

The following diversity metrics were performed to provide a robust analysis:

Rarefaction curves show in graphical representation the expected species richness as a function of sample size. The x-axis of a rarefaction curve represents the number of individuals and the y-axis represents the expected number of species. The formula uses the expected number of species as follows:

$$E(S_n) = \sum_{i=1}^{S} 1 - \frac{\binom{N-N_i}{n}}{\binom{N}{n}}$$

where S is the total number of species in the sample, N the total number of individuals and N_i is the total number of individuals of species *i* in the sample and n is the sample size that is used for the rarefaction (Zou et al., 2023).

ES (n): Shows the expected number of species given a certain sample size, i.e., number of individuals (n).

Shannon-Weiner diversity index (H'): Considers the number of species in a sample and incorporates the distribution of species among individuals or their relative abundance (evenness = J'). The equation is as follows:

$$Shannon\ Index\ (H) = -\sum_{i=1}^{S} p_i\ ln\ p_i$$

where *p* is the proportion of individuals of one species found in the sample (n) divided by the total number of individuals in the sample (N), S is the number of species (Gardener, 2014). Here, Shannon index was calculated using loge and log10. Species richness is the number of species present in a sample. It can be heavily influenced by the number of individuals in the sample.

Count data excluding encrusting bryozoans and hydrozoans (not identified at the species level) were stored in R using the *phyloseq* package and were extracted each time before calculating metrics or creating plots. Rarefaction curves were created using the "rarecurve" function from *vegan* and subsequently using *ggplot2* for plotting. $ES_{(20)}$ was calculated using a personalized

function in R. Shannon-Weiner diversity index ($H'_{[loge]}$, $H'_{[log10]}$), Pielou's evenness (J'), and species richness (S) were calculated using functions "diversity", "evenness", and "Estimate", respectively, from the *vegan* package in R. $ES_{(20)}$ values and Shannon-Weiner diversity index (H') were tested for normality using Shapiro-Wilk test and then, Bartlett's test was used to assess if the variances were homogeneous. To determine if there were any statistically significant differences between $ES_{(20)}$ values and Shannon-Weiner diversity index (H') across substrate, site, oxygen, depth and temperature, a Kruskal-Wallis test followed by Dunn's tests using Benjamini-Hochberg adjustment was performed due to variance homoscedasticity. Independent two-sample t-tests were used to compare $ES_{(20)}$ values and Shannon-Weiner diversity index (H') between inshore and offshore sites and between rocks with and without megafauna.

Multivariate analysis

A multivariate analysis was performed to provide a measure of the dissimilarity of macrofauna community composition between samples across different environmental variables. Counts excluding encrusting bryozoans and hydrozoans (not identified to species level) were transformed to densities per 200 cm^2 and 4^{th} root transformed before performing a multi-dimensional scaling analysis of Bray-Curtis dissimilarities using *Primer*. In addition, permutational multivariate analysis of variance (PERMANOVA) and ANOSIM were used to test for significance of environment categories (depth, oxygen, temperature) and substrate, proximity to shore and megafauna presence in explaining dissimilarity of community composition across samples and SIMPER test was used to examine which taxa are creating those dissimilarities. A distance based linear model was performed using PRIMER to test for the relationship between the environmental variables and the macrofauna community composition. The variables that significantly explained the variation of the benthic macrofauna community composition were

plotted in a distance-based redundancy analysis (partial dbRDA) ordination diagram for visualization.

RESULTS

Ecology of the SCB Hardground Macrofauna Community

In this study, a total of 3,555 (11.08 ± 0.87 individuals /200 cm^2) macrofauna individuals were counted and identified from 82 hard substrates (including ferromanganese crust, phosphorite, basalt and sedimentary rocks) from the deep ocean (231 m to 2688 m). The total number of macrofauna individuals is 3,012 (9.57 ± 0.81 individuals /200 cm^2) when excluding all species of encrusting bryozoans and hydrozoans, which were not identified at the species level. The 10 species of branching bryozoan colonies that were identified at the species level have been included in both counts. Overall, density was mainly dominated by the phyla Annelida (1009 individuals, ~33%) and Echinodermata (832 individuals, ~27%). The other 2/5 of the individuals consisted of Arthropoda (601 individuals, ~19%), Mollusca (268 individuals, ~8%), and Porifera (190 individuals, ~6%). Less abundant phyla (<4% of the total) were Bryozoa (considering only branching colonies), Cnidaria, Hemichordata, Platyhelminthes, Brachiopoda, and Chordata (Figure 3A). Information on the total number of individuals per rock and the densities per 200 cm^2 are given in Table A3.

In terms of species representation, these animals cover a total of 417 different taxa ($H'_{(loge)}$ = 2.22 ± 0.07) excluding encrusting bryozoans and hydrozoans. The phylum Annelida had the most species (170 species, ~40% of species), dominating more so than for density. Arthropoda had the next most species (88 species, ~21% of species). The other 2/5 of the species consisted of Mollusca (63 species, 15% of species), Porifera (44 species, ~10% of species), and Echinodermata (32 species, ~7% of species). Less dominant phyla (~5% of the total) included Bryozoa (considering only branching colonies); Cnidaria; Hemichordata; Chordata; Brachiopoda; and Platyhelminthes (Figure 3B). For photos of some of the specimens collected, see Figures 4 and 5.

Macrofaunal diversity measured as Shannon Weiner diversity on SCB rocks increases with increasing density (R = 0.36, p = 0.0008). At around 10 individuals per 200 cm^2, diversity stops increasing and remains relatively constant or shows little variation (Figure 6). In addition, ¾ of the rocks with the highest densities (>25 individuals per cm^2) displayed a lower diversity than the mean ($H'_{(loge)}$ = 2.22 ± 0.07) (Figure 6). Diversity metrics for each rock, including species richness, Shannon Weiner index (H'), evenness (J'), and rarefaction $ES_{(20)}$, are provided in Table A4.

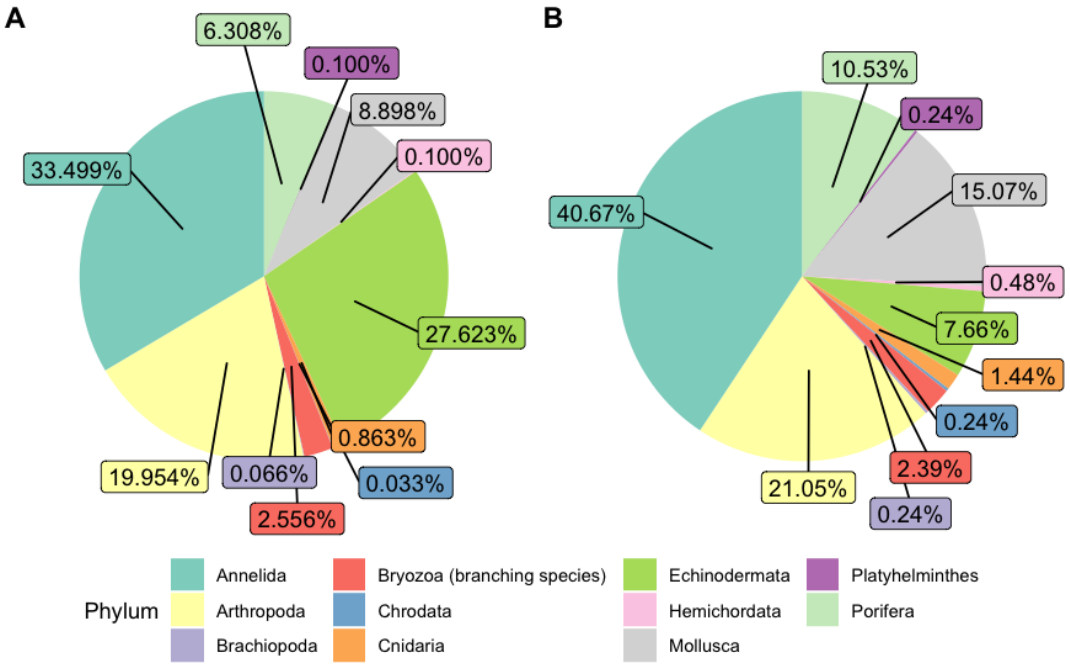

Figure 3. A) Phyletic composition of the macrofaunal community in the SCB based on numbers of individuals. (B) Phyletic composition of the macrofaunal community in the SCB based on numbers of species. These figures do not include encrusting bryozoan colonies (455 individuals) and hydrozoans (88 individuals) since they were not identified to species level and therefore a proper comparison of individuals to species is not possible.

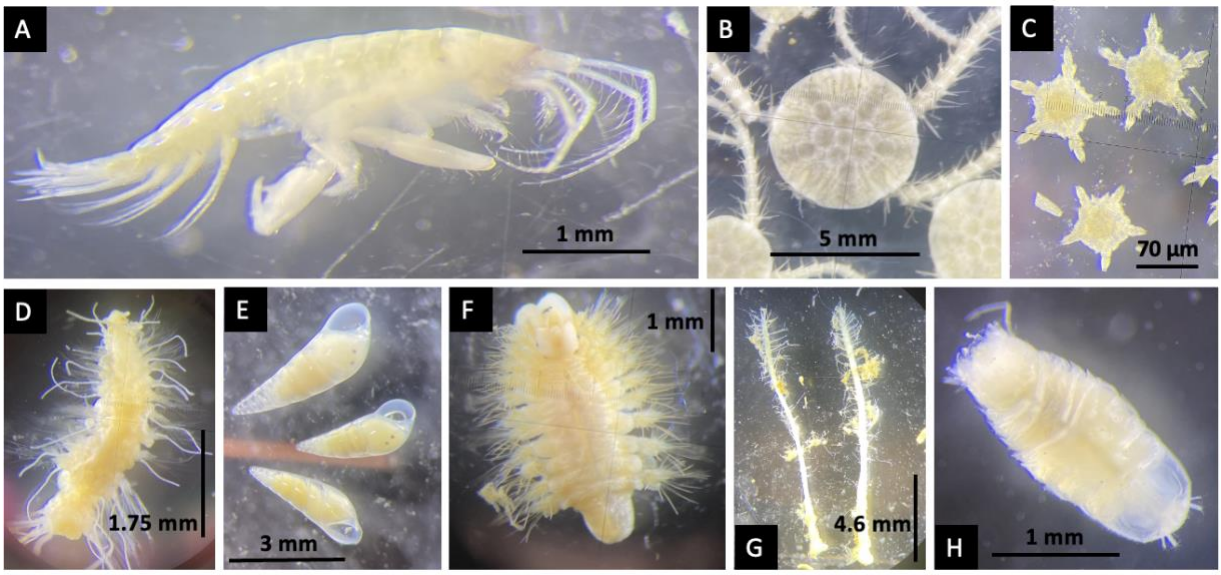

Figure 4. Specimens collected from the SCB. A) Photidae sp. 1 from San Juan Seamount North (SCB-095), B) *Amphipholis pugetana*? (juvenile) from Crespi Knoll (SCB-224), C) Ophiuroidea sp. 5 (postlarvae) from Coronado Escarpment (SCB-329), D) *Amphiduros* sp.1 from Crespi Knoll (SCB-224), E) *Vitreolina yod* from Osborn Bank Mesophotic Zone (HD1847-R5), F) *Harmothoe* nr. *multisetosa* from Crespi Knoll (SCB-218), G) *Asbestopluma* sp. 1 from Coronado Escarpment (SCB-330), H) *Munnopsorus* sp. 1 from Little Joe Seamount (SCB-151). Information on the substrate type, depth, oxygen concentrations, and temperature where these animals were found are in Table A1 and Table A2.

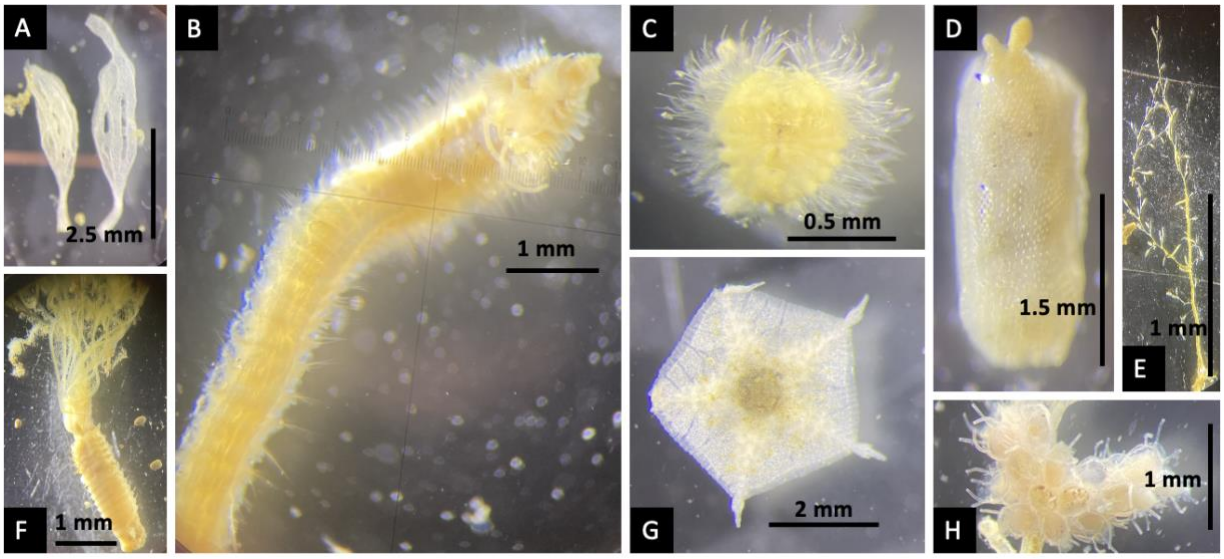

Figure 5. Specimens collected from the SCB. A) Porifera sp. 15 from Patton Ridge South (HD1844-R3), B) *Prionospio ehlersi* from Coronado Escarpment (SCB-330), C) *Chloeia* sp from Hancock Bank (SCB-026), D) *Psolus* sp. Coronado Escarpment (SCB-333), E) Hydrozoa sp. 3 from Coronado Escarpment (SCB-331), F) *Pseudopotamilla* sp. From Coronado Escarpment (SCB-332), G) *Astrophiura marionae* Patton Escarpment (SCB-127), H) encrusting bryozoa from San Juan Seamount Upper Flank (HD1841-R1). Information on the substrate type, depth, oxygen concentrations, and temperature where these animals were found can be reviewed in Table A1 and Table A2.

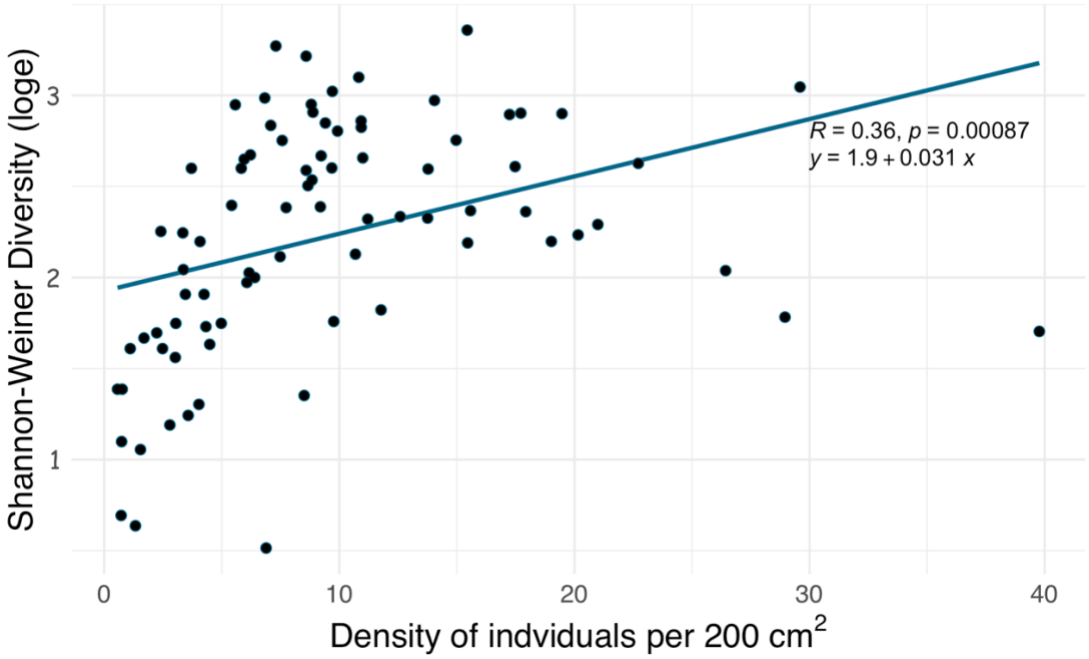

Figure 6. Regression line of density vs. diversity of the macrofauna communities on each rock.

Overall the five most abundant taxa in the entire study (~21% of the total individuals) were: Ophiuroidea sp. 5 (postlarvae) (304 individuals, ~10%), *Ophiocten* cf. *centobi* (160 individuals, ~5%), *Protocirrineris* nr. *socialis* (137 individuals, ~4%), A*strophiura marionae* (105 individuals, ~3%), and Porifera sp. 5 (71 individuals, ~2%). The top five taxa that occurred on the most number of rocks (highest frequency of occurrence) were: Ophiuroidea sp. 5 (postlarvae), Ophiuroidea sp. 7 *(*postlarvae*), Sphaerosyllis* nr. *ranunculus*, *Ophiocten* cf. *centobi* and *Munnopsurus* sp. 1 (Table 4). Twenty-five species (6%) account for over half (52.4%) of the animals collected. However, 235 of the 417 species collected (56.35%) were represented by only 1 or 2 individuals (38.6% were singletons) thus most of the diversity in the system lies with rare species. Over half of the species were found on only 1 rock (213 species) suggesting that much of the diversity probably remains undiscovered. The third most abundant taxon, *Protocirrineris* nr. *socialis* was found on only one rock. Only 4 species occurred on 30% of the rocks or more (>25 rocks). The information

above refers to the data without bryozoans and hydrozoans, which were not identified to species level. Taxonomy of each of the macrofauna species collected is given in Supplemental Table 1, and a list of all specimens collected including number of individuals counted per rock are given in Supplemental Table 2.

Table 4. Top 10 taxa based on total number of individuals and frequency of occurrence (number of rocks the taxa were present on). This table does not include bryozoans and hydrozoans, which were not identified to species level.

Top 10 taxa based on most number of individuals	**Total number of individuals**	**Percent of total**	**Top 10 taxa by frequency of occurrence**	**Frequency of occurrence**
Ophiuroidea sp.5 (postlarvae)	304	~10%	Ophiuroidea sp. 5 (postlarvae)	42
Ophiocten cf *centobi*	160	~5%	Ophiuroidea sp. 7 (postlarvae)	27
Protocirrineris nr. *socialis*	137	~4%	*Sphaerosyllis* nr. *ranunculus*	26
Astrophiura marionae	105	~3%	*Ophiocten* cf. *centobi*	25
Porifera sp. 5	71	~2%	*Munnopsurus* sp. 1	23
Ophiuroidea sp. 7 (postlarvae)	69	~2%	*Pseudotanais* sp.1	21
Spirorbis? Sp. 1	61	~2%	*Amphipholis pugetana*? (juvenile)	19
Sphaerosyllis nr. *ranunculus*	61	~2%	*Astrophiura marionae*	18
Amphipholis pugetana? (juvenile)	56	~1%	*Spirorbis?* Sp. 1	18
Munnopsurus sp. 1	52	~1%	Bryozoa sp. 5	17

Macrofaunal density varied significantly across sites (Chi-square = 50.795, p = 2.177e-06, df = 13). The highest average macrofaunal densities were found on Cortes Bank (20.46 ± 0.94 ind. /200 cm^2), Crespi Knoll (17.43 ± 4.90 ind. /200 cm^2), Osborn Bank Mesophotic Zone (16.45 ± 1.26 ind. /200 cm^2), Hancock Bank (16.42 ± 2.05 ind. /200 cm^2), and Coronado Escarpment (14.86 ± 2.19 ind. /200 cm^2). The sites with the lowest densities were Patton Escarpment (2.97 ± 1.07 ind.

/200 cm^2) and Little Joe Seamount (2.54 ± 0.82 ind. /200 cm^2) (Figure 7A). The largest differences in density across sites were between the shallowest and most hypoxic sites, such as Cortes Bank (depth range: 437-529 m, O_2 range: 4.14-8.31 µmol/L) and the deepest and most oxygenated sites, such as Little Joe Seamount (depth range: 2368-2688 m, O_2 range: 100.17 – 108.14 µmol/L) (Z = 4.48, p = 0.0003); and Cortes Bank and Patton Escarpment (depth range: 1463-1797 m, O_2 range: 46.89 – 70.9 µmol/L) (Z = 4.12, p = 0.0006) (Table A5).

Macrofauna diversity differed significantly between deep and oxygenated sites versus shallow and hypoxic sites (chi-square = 46.008, p = 1.419e-05, df = 13) (Table 5). Notable distinctions include Patton Escarpment vs. Patton Ridge South (z = 4.19, p = 0.0012), Patton Escarpment vs. Cortes Bank (z = 4.16, p = 0.0007), and Little Joe Seamount vs. Cortes Bank (z = 3.59, p = 0.0036) (Figure 7B; Table A6). While Cortes Bank exhibits the highest Shannon diversity index (H' = 2.93), Patton Ridge South has the highest expected number of species ($ES_{(20)}$ = 14.56). Patton Escarpment shows the lowest diversity in both indices (H' = 1.18, $ES_{(20)}$ = 4.33) but demonstrates high evenness (J' = 0.92), comparable to sites with greater diversity. Little Joe Seamount, despite a lower Shannon index (H' = 1.71), maintains high evenness (J' = 0.98) (Table 5).

Rarefaction richness (Figure 7C) peaked at San Juan Seamount Upper Flank, Little Joe Seamount, and 40-Mile Bank, while being lowest at Crespi Knoll, San Juan Seamount North, and San Clemente Escarpment. At Crespi Knoll, 5 out of 55 species constitute 64% of the total individuals, with *Protocirrineris* nr. *socialis* being the most abundant (137 individuals, ~38% of the total). In San Juan Seamount North, 53% of individuals are represented by 4 species, including Stenothoidae sp.3 (44 individuals, ~19% of the total), Photidae sp.1 (29 individuals, ~12% of the total), Serpulidae spp. (28 individuals, ~12% of the total), and Ophiuroidea sp.5 (21 individuals, ~9% of the total). Hancock Bank (35 species or 42% of species present), Coronado Escarpment

(27 species or 41% of species present), Osborn Bank Mesophotic Zone (26 species or 45% of species present), Little Joe Seamount (22 species or 56% of species present), and San Juan Seamount North (21 species or 44% of species present) boast the highest number of unique species. Dissimilarities in community composition were significant across sites (ANOSIM, Global R = 0.567, p = 0.001) (Figure 7D).

Figure 7. A) Average ± one standard error density of macrofauna per 200 cm^2, B) Shannon Weiner diversity index with standard error, C) rarefaction curve for macrofauna diversity and D) multi-dimensional scaling analysis of macrofauna community composition across different sites. Site initials: 40-M.B = 40-Mile Bank, C.B = Coronado Bank, C.E = Coronado Escarpment, C.K = Crespi Knoll, H.B = Hancock Bank, L.J.St = Little Joe Seamount, Ne.B = Northeast Bank, O.B.M = Osborn Bank Mesophotic Zone, P.E = Patton Escarpment, P.E.C = Patton Escarpment Central, P.R.S = Patton Ridge South, S.C.E = San Clemente Escarpment, S.J.S.N = San Juan Seamount North, S.J.St.U.F = San Juan Seamount Upper Flank.

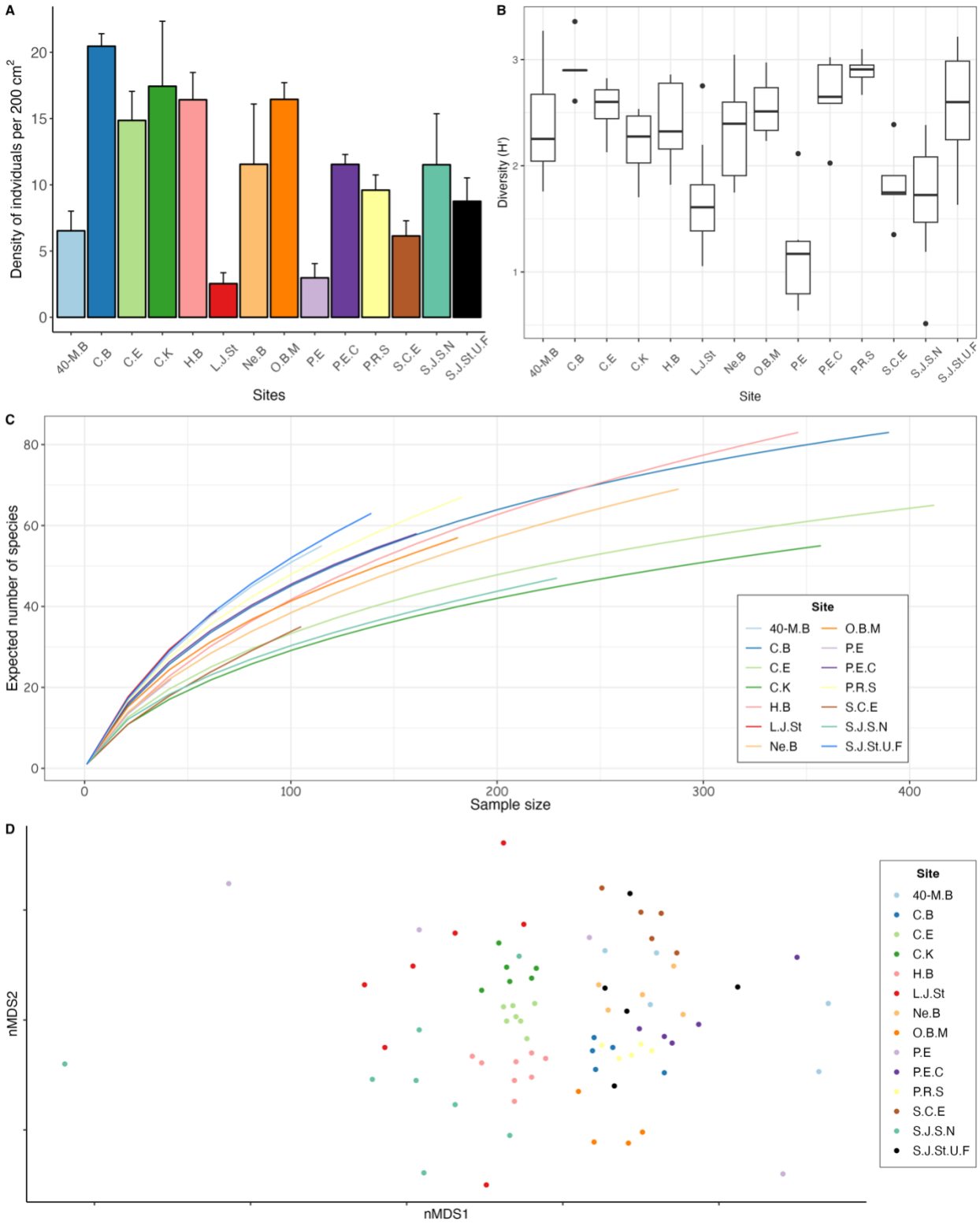
A
Density of individuals per 200 cm²
Sites
40-M.B
C.B
C.E
C.K
H.B
L.J.St
Ne.B
O.B.M
P.E
P.E.C
P.R.S
S.C.E
S.J.S.N
S.J.St.U.F
B
Diversity (H')
Site
C
Expected number of species
Sample size
Site
D
nMDS2
nMDS1
Site

Table 5. Macrofauna average species richness (S), diversity (H'), evenness (J'), and $ES_{(20)}$ for each site per rock. Chi-square and p-values are given for Kruskal-Wallis test.

Site	*Depth range (m)*	*Oxygen range (µmol/L)*	*Species richness (S)*	*Shannon Index (H'_{loge})*	*Shannon Index (H'_{log10})*	*Evenness (J')*	*Rarefaction $ES_{(20)}$*
Patton Escarpment Central	587-820	*2.61-5.14*	18.20 ± 2.85	2.65 ± 0.18	1.15 ± 0.08	0.94 ± 0.02	13.28 ± 1.57
San Juan Seamount Upper Flank	691-1129	2.79-14.04	17.40 ± 4.48	2.65 ± 0.28	1.10 ± 0.12	0.94 ± 0.01	11.96 ± 1.79
Northeast Bank	553-1132	2.68-15.95	18.00 ± 7.85	2.34 ± 0.24	1.02 ± 0.10	0.91 ± 0.04	10.61 ± 1.33
Cortes Bank	437-529	4.14-8.31	28.60 ± 5.60	2.93 ± 0.12	1.27 ± 0.05	0.90 ± 0.03	13.52 ± 0.63
Patton Ridge South	562-726	2.55-3.96	21.80 ± 1.59	2.89 ± 0.07	1.26 ± 0.03	0.94 ± 0.01	14.56 ± 0.50
40-Mile Bank	658-1036	2.11-14.6	14.60 ± 4.08	2.40 ± 0.26	1.04 ± 0.11	0.94 ± 0.01	11.34 ± 1.80
San Clemente Escarpment	1189-1718	15.27-37.46	10.00 ± 2.34	1.82 ± 0.17	0.79 ± 0.07	0.84 ± 0.07	7.81 ± 0.88
Osborn Bank Mesophotic Zone	231-396	19.71-54.79	19.50 ± 2.54	2.56 ± 0.16	1.11 ± 0.07	0.87 ± 0.02	11.72 ± 0.86
Hancock Bank	319-594	9 – 36.48	17.75 ± 2.05	2.40 ± 0.14	1.04 ± 0.06	0.84 ± 0.02	10.97 ± 0.68
San Juan Seamount North	1138-1442	26.7 – 36.48	9.50 ± 1.69	1.68 ± 0.22	0.73 ± 0.09	0.77 ± 0.07	7.51 ± 1.09
Patton Escarpment	1463-1797	46.89 – 70.9	4.33 ± 1.22	1.18 ± 0.22	0.51 ± 0.09	0.92 ± 0.03	4.33 ± 1.23
Little Joe Seamount	2368-2688	100.17 – 108.14	6.63 ± 1.61	1.71 ± 0.19	0.74 ± 0.08	0.98 ± 0.01	6.48 ± 1.48
Crespi Knoll	443-525	12.99 – 33.11	15.50 ± 2.61	2.21 ± 0.13	0.96 ± 0.06	0.84 ± 0.07	10.11 ± 0.97
Coronado Escarpment	443-467	24.16 – 28.28	20.57 ± 1.30	2.55 ± 0.10	1.11 ± 0.04	0.85 ± 0.02	11.16 ± 0.57

Table 6. Macrofauna average species richness (S), diversity (H'), evenness (J'), and $ES_{(20)}$ for each site per rock. Chi-square and p-values are given for Kruskal-Wallis test, Continued.

Site	*Depth range (m)*	*Oxygen range (µmol/L)*	*Species richness (S)*	*Shannon Index (H'_{loge})*	*Shannon Index (H'_{log10})*	*Evenness (J')*	*Rarefaction $ES_{(20)}$*
Chi-squared	-	-	44.11	46	46	39.72	42.19
df	-	-	13	13	13	13	13
p-value	-	-	2.93e-05	1.41e-05	1.41e-05	0.00015	6.08e-05

Macrofauna Community Differences by Substrate Type

Density

The highest average macrofaunal densities were found on basalt (15.62 ± 1.83 ind. /200 cm^2) and phosphorite (14.72 ± 1.28 ind. /200 cm^2) rocks (Chi-squared = 30.116, p = 1.305e-06, df = 3). These two substrates had approximately 50% more animals than ferromanganese crusts (7.13 ± 1.25 ind. /200 cm^2) and sedimentary rocks (9.78 ± 0.64 ind. /200 cm^2) (FeMn crusts vs basalt: z = 4.48, p = 0.00001; phosphorite vs FeMn crusts: z = -4.49, p = 0.00001) (Figure 9A). Macrofauna do not exhibit significantly different densities on phosphorite compared to basalt and sedimentary rocks, and on FeMn crusts compared to sedimentary rocks (Table A7).

Diversity

Macrofaunal diversity was highest on phosphorite and lowest on FeMn crust as indicated by species richness, H', and $ES_{(20)}$ calculated per rock (Table 6 and Figure 9C). Macrofaunal diversity on FeMn crust was significantly lower than on phosphorite, basalt and sedimentary rocks, and significantly higher on phosphorite compared to basalt rocks (H': FeMn crusts vs basalt : z = 2.82, p = 0.004; FeMn crusts vs phosphorite: z = -5.31, p = 0.0001; FeMn crusts vs sedimentary rocks:

z = -3.06, p = 0.003; phosphorite vs basalt: z = -2.16, p = 0.02) (Table A8). Although all substrates exhibited similar evenness, sedimentary rocks and FeMn crusts had the highest values (Table 6).

FeMn crusts had the greatest number of unique taxa (95 out of 200), followed by basalt, phosphorite and sedimentary rocks (78 out of 178, 72 out of 177 and 22 out of 89, respectively) (Figure 8). FeMn crusts are most similar to basalt rocks, followed by phosphorite and sedimentary rocks (25, 24, and 5 taxa in common, respectively). Phosphorite rocks have the most taxa in common with FeMn crust (Figure 8). When rock assemblages are pooled by substrate type, FeMn crusts and sedimentary rocks exhibit the highest diversity (Figure 9D).

Table 7. Average macrofauna species richness (S), diversity (H'), evenness (J'), and $ES_{(20)}$ for each substrate type, using rocks as replicates and results from the Kruskal-Wallis test. The different letters in parenthesis next to each value represent the substrates that are statistically different from one another in terms of each diversity metric.

Substrate	*Species richness (S)*	*Shannon Index (H'_{loge})*	*Shannon Index (H'_{log10})*	*Evenness (J')*	*$ES_{(20)}$*
FeMn crust	10.08 ± 1.48 (a)	1.80 ± 0.10 (a)	0.785 ± 0.04 (a)	0.89 ± 0.02 (a)	7.65 ± 0.62 (a)
Phosphorite	23.26 ± 1.67 (b)	2.75 ± 0.06 (b)	1.19 ± 0.02 (b)	0.88 ± 0.01 (a)	12.74 ± 0.43 (b)
Basalt	16.68 ± 1.24 (b)	2.37 ± 0.07 (c)	1.03 ± 0.03 (c)	0.86 ± 0.02 (a)	11.15 ± 0.53 (b)
Sedimentary	17.57 ± 3.08 (b)	2.60 ± 0.20 (bc)	1.13 ± 0.08 (bc)	0.94 ± 0.01 (a)	12.78 ± 1.44 (b)
Chi-squared	34.91	32.43	32.43	8.95	28.49
df	3	3	3	3	3
p-value	1.27e-07	4.233e-07	4.233e-07	0.0299	2.86e-06

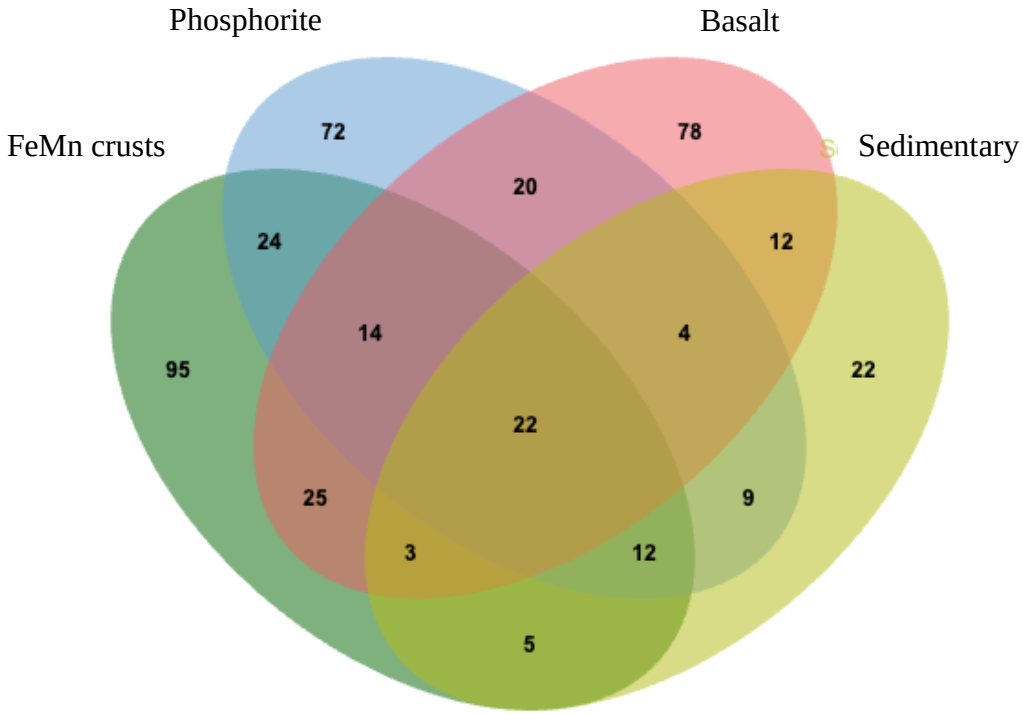

Figure 8. Venn diagram showing numbers of overlapping invertebrate taxa among macrofaunal communities on different substrate types.

Community composition

In terms of phyletic composition, the macrofaunal communities on FeMn crusts, phosphorite and basalt rocks were similar to one another. The dominant phyla across all substrates were Annelida and Echinodermata with the highest percentage of Annelida (~35%) on sedimentary rocks, and an equal amount of Annelida (~27%) and Echinodermata (~27%) on phosphorite rocks (Figure 9B). FeMn crusts and basalts had a similar percentage of Annelida present (~23 and ~25, respectively).

Benthic macrofauna community composition differed across substrate type (PERMANOVA: $F = 1.65$, $p = 0.001$) between FeMn crust and sedimentary rocks (t: 1.19, p: 0.043), phosphorite and basalt rocks (t: 1.61, p: 0.001), and phosphorite and sedimentary rocks (t: 1.53, p: 0.001) (Table

A9). Community composition also varies within a substrate – particularly among FeMn crusts (SIMPER, Average similarity = 5.39%) (Figure 9E). The taxa that occurred on the most number of FeMn crusts were: *Ophiocten* cf. *centobi*, *Pseudotanais* sp. 1, *Ophioleuce* cf. *gracilis*, and Ophiuroidea sp. 5 (postlarvae) (present on 12, 9, 9, and 8 out of 37 rocks, respectively). For a list of the 135 taxa that occurred only one time on any FeMn crust, see Table A10. Of the 95 unique taxa on FeMn crusts, 31 taxa are annelids, 17 taxa are arthropods, 1 taxon is a branching bryozoan, 1 taxon is a chordate, 2 taxa are cnidarians, 9 taxa are echinoderms, 22 taxa are mollusks, and 12 taxa are sponges (Table A11). Of the 72 unique taxa on phosphorite rocks, 39 taxa are annelids, 13 taxa are arthropods, 3 taxa are branching bryozoans, 1 taxon is cnidarians, 5 taxa are echinoderms, 6 taxa are mollusks, and 4 taxa are sponges (Table A12). The six most important taxa contributing to the dissimilarity between FeMn crusts and sedimentary rocks (SIMPER, Average dissimilarity = 94.08%) were: *Spirorbis*? Sp. 1, *Ophiocten* cf. *centobi*, Sabellidae sp.1, Ophiuroidea sp. 11, *Pseudotanais* sp. 1, *and* Ophiuroidea sp. 5 (postlarvae), which were less abundant on FeMn crusts. The six most important taxa contributing to the dissimilarity between phosphorite and basalt rocks (SIMPER, Average dissimilarity = 86.47%) were: Ophiuroidea sp. 5 (postlarvae), *Sphaerosyllis* nr. *ranunculus*, *Amphipholis pugetana*? (juvenile), *Munnopsorus* sp. 1, Ophiuroidea sp. 7 (postlarvae), *Ophiocten* cf. *centobi*, which were nearly absent on phosphorite rocks. The six most important taxa contributing to the dissimilarity between phosphorite and sedimentary rocks (SIMPER, Average dissimilarity = 88.14%) were: Ophiuroidea sp.5, *Spirorbis*? sp. 1, *Ophiocten* cf. *centobi*, *Sphaerosyllis* nr. *ranunculus*, *Amphipholis pugetana*? (juvenile), Ophiuroidea sp. 7 (postlarvae), which were nearly absent on sedimentary rocks. See Table 7 for a list of the top 10 taxa found at each substrate.

Table 8. Top 10 taxa found at each substrate type with number of individuals.

FeMn crust species	**#**	**Phosphorite rock species**	**#**	**Basalt rock species**	**#**	**Sedimentary rock species**	**#**
Ophiocten cf. *centobi*	72	Ophiuroidea sp. 5 (postlarvae)	160	*Protocirrineris* nr. *socialis*	137	*Spirorbis?* sp. 1	12
Porifera sp. 5	57	*Astrophiura marionae*	66	Ophiuroidea sp. 5 (postlarvae)	92	*Ophiocten* cf. *centobi*	12
Ophiuroidea sp. 5 (postlarvae)	48	*Sphaerosyllis* nr. *ranunculus*	42	*Ophiocten* cf. *centobi*	36	*Sphaerosyllis* nr. *ranunculus*	7
Stenothoidae sp. 3	44	*Ophiocten* cf. *centobi*	40	Placopecten sp. 1	29	Sabellidae sp. 1	6
Spirorbis? sp. 1	40	*Amphipholis pugetana*? (juvenile)	35	*Ophryotrocha* spp.	26	*Rhachotropis inflata*	6
Photidae sp. 1	29	Ophiuroidea sp. 7 (postlarvae)	33	*Astrophiura marionae*	25	Stegocephalidae sp. 3	5
Serpulidae spp. (juvenile)	28	*Munnopsurus* sp. 1	32	Ophiuroidea sp. 7 (postlarvae)	21	*Pseudotanais* sp. 1	5
Ophioleuce cf. *gracilis*	26	*Metopa* nr. *dawsoni*	28	*Amphipholis pugetana*? (juvenile)	18	Ampharetidae sp. 2	4
Sabellidae sp. 1	16	Stenothoe sp. 1	25	*Psolus* sp.	17	Cirratulidae sp. 1	4
Gyptis sp. 1	15	*Pseudotanais* sp. 1	25	Bivalvia sp. 3 (juvenile)	17	Ophiuroidea sp. 11	4

Figure 9. A) Average ± one standard error density of macrofauna per 200 cm^2, B) community composition of macrofauna by phyla, C) Shannon Weiner diversity index with standard error, D) rarefaction curve (ES) for macrofauna diversity, and E) multi-dimensional scaling analysis of macrofauna community composition across different substrate types.

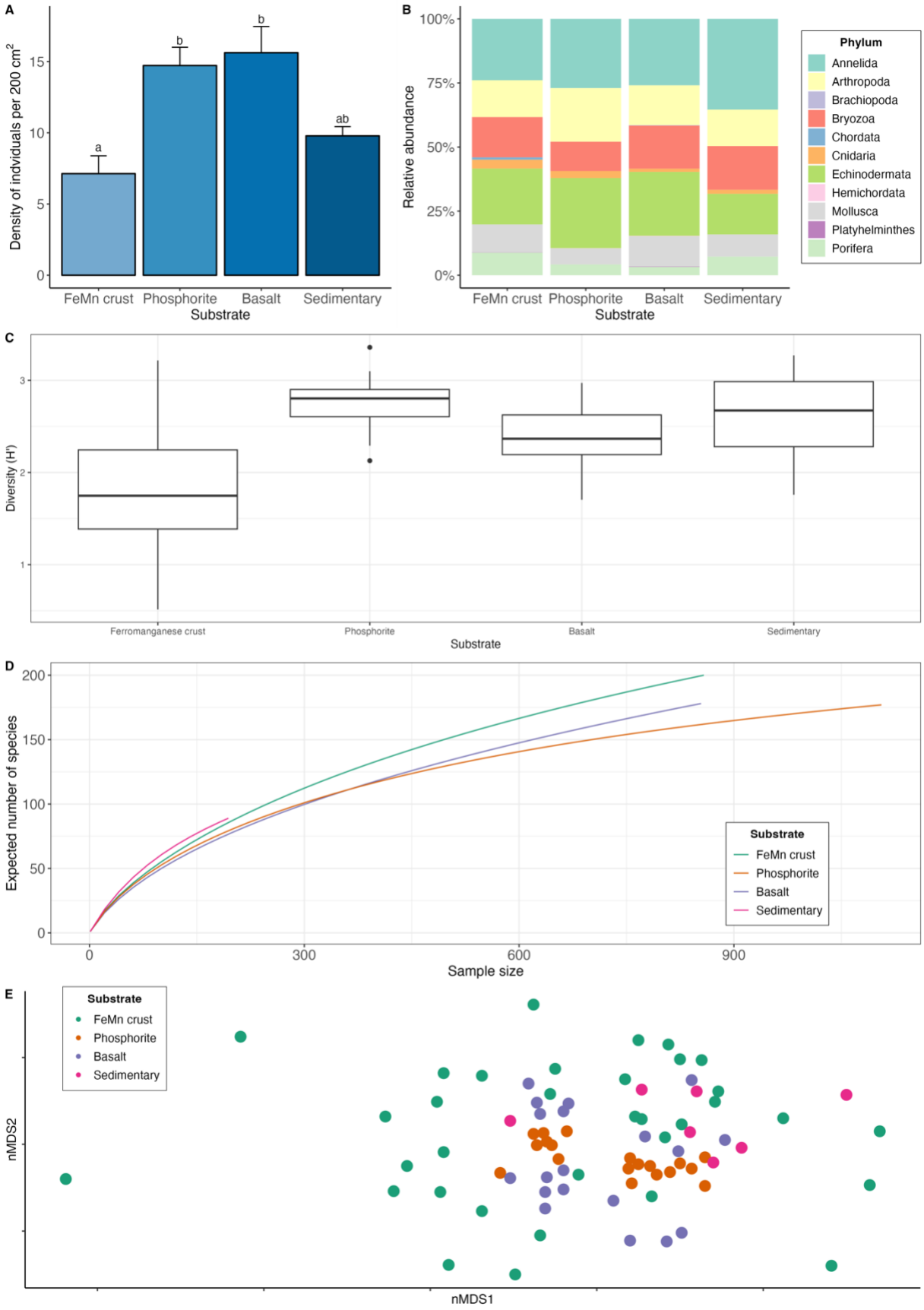
A
Density of indviduals per 200 cm2
a
b
b
ab
FeMn crust
Phosphorite
Basalt
Sedimentary
Substrate
B
Relative abundance
100%
75%
50%
25%
0%
Phylum
Annelida
Arthropoda
Brachiopoda
Bryozoa
Chordata
Cnidaria
Echinodermata
Hemichordata
Mollusca
Platyhelminthes
Porifera
C
Diversity (H')
Ferromanganese crust
Phosphorite
Basalt
Sedimentary
Substrate
D
Expected number of species
Sample size
Substrate
FeMn crust
Phosphorite
Basalt
Sedimentary
E
nMDS2
nMDS1

Macrofauna Community Differences: Relationships of Oxygen, Depth and Temperature to Macrofauna at Different Substrate Types

Multicollinearity of environmental variables

Oxygen, depth and temperature exhibited multicollinearity. A high positive correlation was found between depth and oxygen ($r = 0.82$, $p = 1.6e\text{-}34$), and depth and temperature exhibit a high negative correlation ($r = -0.92$, $p = 2.43e\text{-}34$) (Figure A1). This complicates the interpretation of relationships with the macrofauna community, as changes in one variable may be confounded by the influence of others. Therefore, the following results are presented for each substrate to test the effects of each variable among comparable samples.

Density

Densities on FeMn crust decrease with increasing oxygen (Figure 10A), however on phosphorite, basalt and sedimentary rocks (which were found at shallower depths), densities increase with increasing oxygen (Figure 10B and 10C). Across all substrates, macrofaunal densities decrease with increasing depth (Figure 10D, 10E, 10F) and decreasing temperature (Figure 10G, 10H, 10I).

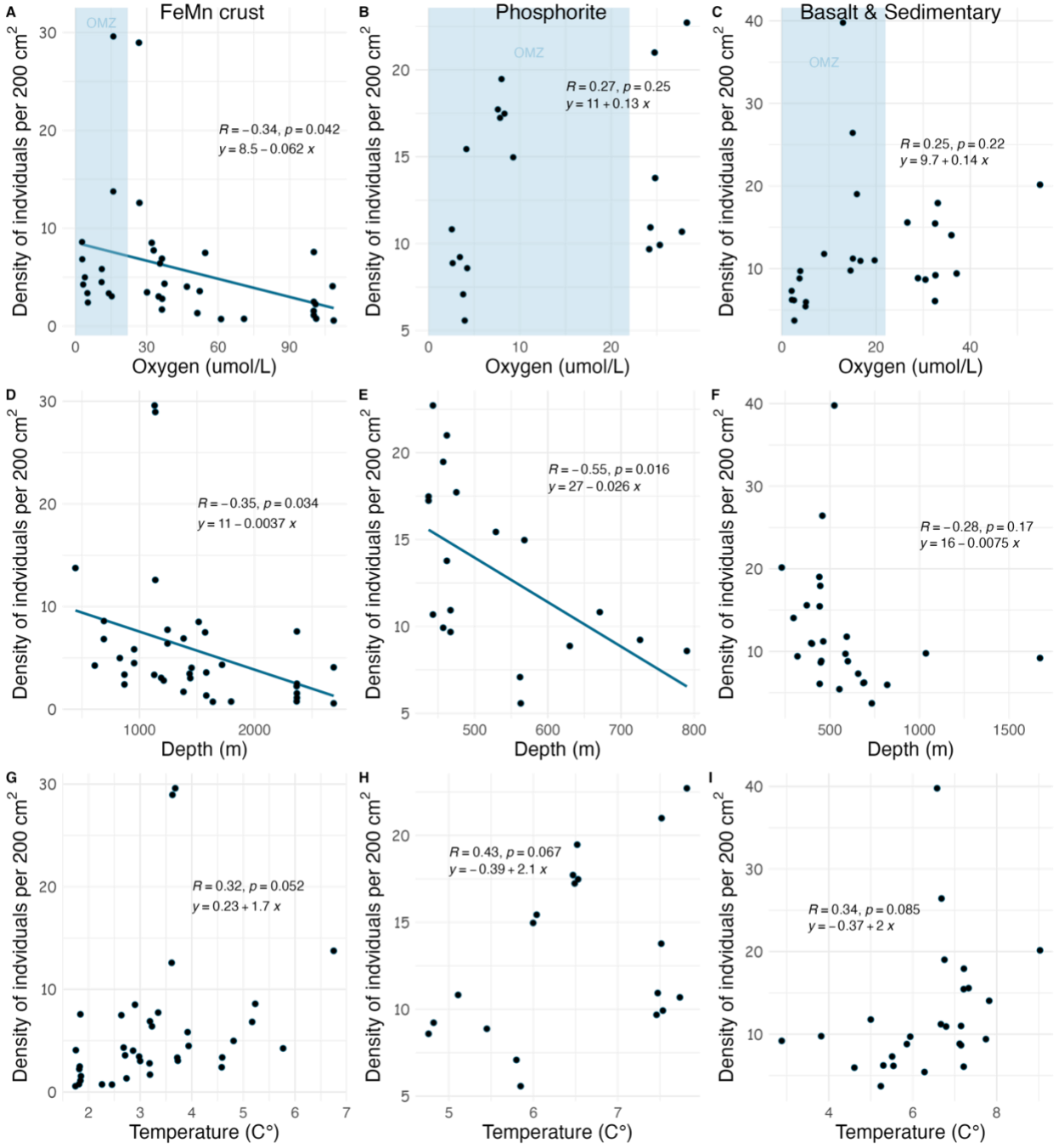

Figure 10. Relationship between macrofaunal density and environmental variables (oxygen, depth and temperature) by substrate type (FeMn crust: A, D, G; phosphorite: B, E, H; basalt and sedimentary: C, F, I). The highlighted areas in the top row represent the oxygen minimum zone.

Diversity

Across all substrate types, macrofaunal diversity decreases with increasing oxygen (Figures 11A, 11B, 11C). Macrofaunal diversity on FeMn crust, basalt and sedimentary rocks decreases with increasing depth (Figure 11D and 11F), however on phosphorites, it increases with depth (Figure 11E). The relationship between temperature and diversity is opposite to depth due to the negative correlation between these environmental variables (Figures 11G, 11H, 11I).

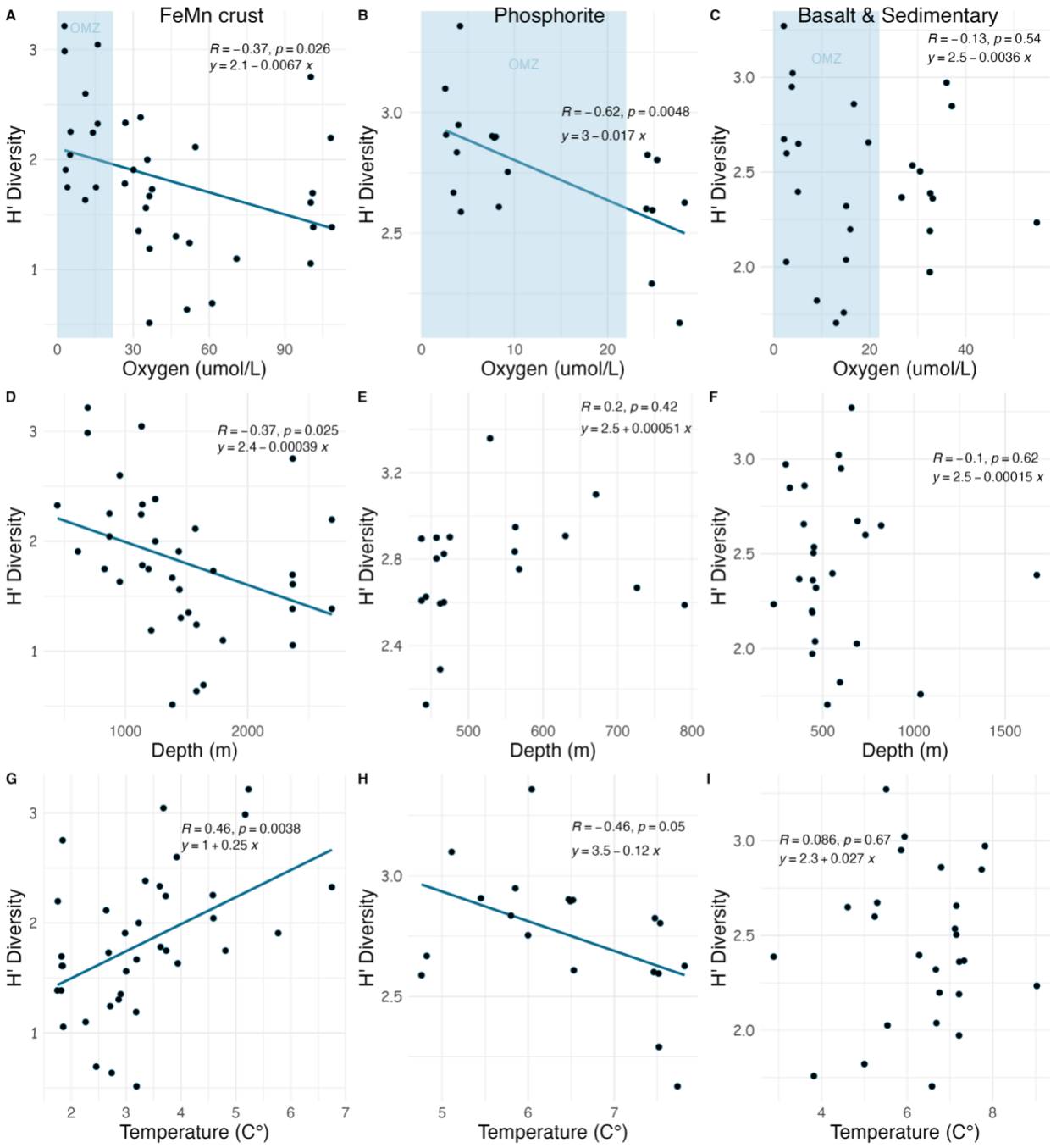

Figure 11. Relationship between macrofaunal diversity and environmental variables (oxygen, depth and temperature) by substrate type (FeMn crust: A, D, G; phosphorite: B, E, H; basalt and sedimentary: C, F, I). The highlighted areas in the top row represent the oxygen minimum zone.

Community composition

The variation in benthic macroinvertebrate community composition can be partially explained by oxygen, depth and temperature (model AICc: 681.67). Of all the variance in community composition observed, DISTLM analysis revealed that 12.56% can be explained by depth, temperature and oxygen. These three variables significantly explained the variation in macrofaunal community composition (depth: $F = 4.44$, $p = 0.001$; temperature: $F = 4.93$, $p = 0.001$; oxygen: $F = 3.91$, $p = 0.001$). Of the total macrofaunal variance explained by these variables, depth is the most influential at 47.97%, followed by temperature and oxygen at 35.07% and 16.95%, respectively. Temperature accounts for the variation of basalt rocks, whereas depth explains more of the variation in composition seen on FeMn crusts (Figure 12).

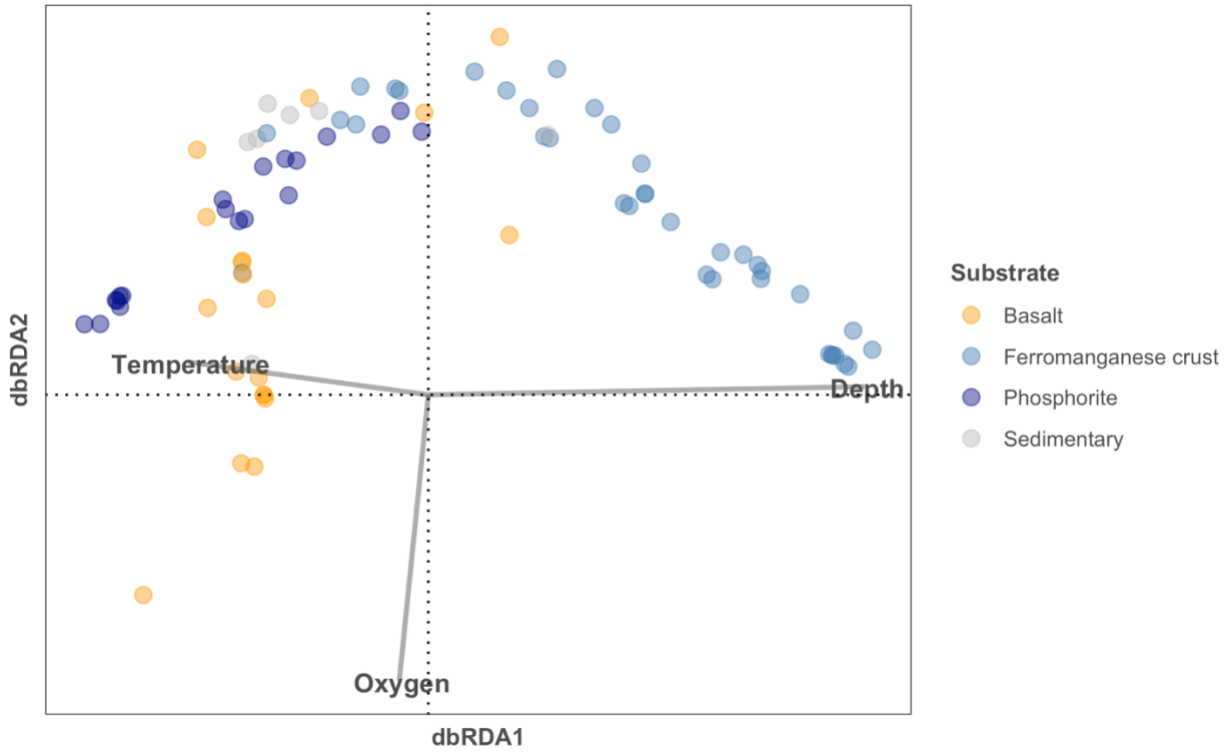

Figure 12. dbRDA diagram performed on the macrofaunal community composition data with the environmental variables that significantly explain the variation in grey lines. The horizontal axis shows 6% of the total variation between samples and the vertical axis shows 4.4%.

Macrofauna Community Differences: Relationships of Oxygen and Depth to Macrofauna across all samples

Density

Across rocks of all substrates, the highest average macrofaunal densities were found at low oxygen concentrations from 6 to 22 μmol/L (17.07 ± 2.07 ind. /200 cm^2), 22 to 40 μmol/L (12.09 ± 1.4 ind. /200 cm^2), and 0 to 6 μmol/L (9.51 ± 0.83 ind. /200 cm^2), whereas the lowest densities were present at higher oxygen concentrations from 40 to 110 μmol/L (3.89 ± 1.3 ind. /200 cm^2) (F = 16, p = 3.37e-08, df = 3) (Figure A2a and Table A13). Overall, the highest macrofaunal densities were present on rocks at depths between 0-500 m (16.09 ± 1.06 ind. /200 cm^2) and the lowest were found between 1500-2700 m (3.51 ± 0.76 ind. /200 cm^2) (F = 20.98, p = 4.59e-10, df = 3) (Figure A2b and Table A15). Macrofaunal densities within the OMZ and outside the OMZ did not differ when compared across similar depths (rocks above 800 m: t = -0.02, p = 0.98, df = 40.73; rocks below 800 m: t = -1.14, p = 0.27, df = 15.05) (Figure A3). The rock with the highest density observed (299 individuals, 39.77 ind. /200 cm^2) was a basalt found within the OMZ at 12.99 μmol/L in Crespi Knoll at a relatively shallow depth of 525 m.

Diversity

Across all substrate types, species richness, H' and $ES_{(20)}$ indicate that diversity was significantly lower at oxygen concentrations of 40 to 110 μmol/L than at oxygen concentrations of 6 to 22 μmol/L and 0 to 6 μmol/L (H': 0 to 6 μmol/L vs 40 to 110 μmol/L : z = 5.16, p = 0.0000; 6 to 22 μmol/L vs 40 to 110 μmol/L: z = -3.48, p = 0.0007) (Table A14 and Table A17). As indicated by species richness, H', and $ES_{(20)}$, the highest macrofaunal diversity was found at intermediate depths of 500 to 800 m deep, followed by the shallowest depths 0 to 500 m deep (Chi-square =36.79, p = 5.092 e-08, df = 3) (Table A18). Diversity was lowest at depths of 800 to 1500

m and 1500 to 2700 m (0-500 m vs 1500-2700 m: Z = 4.39, p = 0.0000; 500-800 m vs 1500-2700 m: Z = -5.19, p = 0.0000; 0-500 m vs 800-1500 m Z = 3.12, p = 0.0013; 500-800 m vs 800-1500 m: Z = 4.03, p = 0.0001) (Table A16). As indicated by species richness, H', and $ES_{(20)}$, diversity was significantly higher within the OMZ compared to outside of the OMZ for samples below 800 m. However, for samples above 800 m, diversity was not significantly higher within the OMZ compared to outside of the OMZ (Table A19).

Covariate effects of depth driving relationships between oxygen and macrofaunal density and diversity

The relationship between oxygen and density may depend on the depth category (ANCOVA: F = 4.2, p = 0.008, df = 3) (Figure A4). From 0 to 500 m, 800 to 1500 m and 1500 to 2700 m, density decreases with increasing oxygen, however between ~500 to 800 m (within the OMZ core) density increases with increasing oxygen. This relationship of oxygen and diversity may depend on the depth categories (ANCOVA: F = 4.94, p = 0.0034, df = 3). Diversity decreases with increasing oxygen at all depth categories except between 800 and 1500 where it increases with rising oxygen concentrations (Figure A4). The influence of depth on density is independent of the oxygen categories (ANCOVA: F = 0.83, p = 0.477, df = 3).

Macrofauna Community Differences by Proximity to Shore

A list of sites designated as inshore and offshore can be found in Table A20. Inshore sites are located within 100 km from the shoreline. Macrofaunal densities on rocks from inshore sites (12.51 ± 1.52 ind. /200 cm^2) did not differ from those at offshore sites (10.38 ± 1.05 ind. /200 cm^2) (W = 601, p-value = 0.16) (Figure A5). The same was true for community composition (ANOSIM, Global R = 0.049, p = 0.13). When rock assemblages are pooled by offshore vs inshore,

macrofauna from rocks at offshore sites have a higher rarefaction diversity (Figure A5). However, macrofaunal species richness (S), Shannon diversity index (H'_{loge}), and $ES_{(20)}$ did not exhibit significant differences between rocks from inshore vs offshore sites (Table A21).

Megafaunal influence on Macrofauna Communities

A list of rocks with megafauna is shown in Table A22. When all rocks are considered, those that harboured megafauna had significantly higher macrofaunal densities (14.53 ± 1.98 ind. /200 cm^2) than those without megafauna (9.97 ± 0.92 ind. /200 cm^2) (W=417, p = 0.02), and no difference in macrofauna diversity was apparent (Figure A 12.3 A&B). However, rocks collected with megafauna were significantly shallower in average depth (761.5 ± 118.7 m) than those collected without megafauna (1032.32 ± 83 m) (W = 416, p = 0.02). If only the rock samples from above 500 m are considered, the rocks with megafauna did not harbour significantly higher macrofaunal densities (16.51 ± 1.58 ind. /200 cm^2) than those without megafauna (15.63 ± 1.63 ind. /200 cm^2) (W = 110, p = 0.44), nor did they differ in terms of diversity (Table A24). Although species richness was higher in rocks with megafauna compared to those with no megafauna, the difference in species richness, H', and $ES_{(20)}$, of rocks below 500 m, was not statistically significant (Figure A6). Notably, community composition was similar on rocks with and without megafauna (ANOSIM, Global R = -0.055, p = 0.83).

DISCUSSION

Density, Diversity and Community Composition of the SCB: Comparisons With Other Studies

Only a limited number of studies provide quantitative data for macrofauna on hard substrates in the deep ocean. The overall macrofaunal densities from this study in the SCB (11.08 ± 0.87 ind. /200 cm^2) are similar to those found by (Levin et al., 2017) at inactive sites near methane seeps on the Oregon margin (average of 11.8 ± 7.85 ind. /200 cm^2) and smaller than those found by Pereira et al. (2021) and (2022) at transition sites (sites with lesser seepage activity) near methane seeps on the Costa Rica margin (average of 57 ± 26 ind. /200 cm^2) (Supplemental Table 3). In contrast, densities from the SCB were about 2% that of macrofauna on carbonates at active methane seeps off Costa Rica (610 ± 123 ind. /200 cm^2) (Pereira et al., 2022); 24% of densities on carbonates at active methane seeps on the Oregon margin (45.61 ± 22.85 ind. /200 cm^2) (Levin et al., 2017); 5% that of macrofauna on whale skeletons from Southern California (average of 223 ind. /200 cm^2) (Baco & Smith, 2003); and 11% that of macrofauna on wood from an active methane seep in Costa Rica (100 ± 23 ind. /200 cm^2) (Pereira et al., 2022) (Supplemental Table 3). In terms of diversity, the macrofauna on rocks from the SCB have a higher average Shannon index compared to the average diversity at hardgrounds from active sites at methane seeps documented by (Levin et al., 2015, 2017) (Supplemental Table 3). High macrofaunal densities in methane seeps are a result of bacterial production stimulated by the availability of methane. Bacteria provide a food source for small heterotrophic animals and therefore support high densities of animals (Levin et al., 2015).

Macrofaunal community composition of hard substrates at methane seeps is also affected by bacteria, for example, these communities are dominated by specific groups, such as annelids and gastropods (Levin et al., 2015). Therefore, these reducing hard substrates could be harbouring

more specialized fauna compared to non-reducing hard substrates, which have similar proportions of annelids, gastropods, arthropods, and cnidarians as seen in this study and in inactive carbonates from (Leduc et al., 2015; Levin et al., 2015). The number of macrofaunal species found per phylum in this study was similar to that found by Leduc et al. (2015) in sediments surrounding phosphorite deposits, with arthropods and annelids being the most diverse groups overall.

Most deep-sea paradigms, such as those involving depth gradients, have evolved based on the study of sediment ecosystems. This study offers an opportunity to examine these paradigms for hard substrates. Researchers initially proposed the concept of peak diversity occurring at mid to lower bathyal depths (1500 to 2000 m), establishing the unimodal hypothesis for deep-sea diversity (Rex, 1981). However, the SCB hardground macrofauna does not exhibit the typical unimodal diversity pattern observed in sediments (Rex, 1981). In the SCB, diversity at shallower depths (500 to 1000 m) was highly variable, low at intermediate depths (1250 to 1600 m) and high at deeper depths (Figure 13). Consequently, in alignment with other studies, it becomes evident that the presumed universal applicability of the unimodal hypothesis may not hold true across all deep-sea ecosystems (Levin et al., 2001). The SCB study also contributes to a growing understanding of the high heterogeneity and complexity of continental margins, and the deep sea in general (Levin and Sibuet, 2012; Danovaro et al., 2014). The original paradigm of homogeneous, desert-like sediment covered ecosystem has been replaced by one of heterogeneous substrates, topographic features and environmental conditions supporting diverse biota. The SCB escarpments, seamounts, knolls, and ridges comprised of ferromanganese crusts, phosphorites, basalts and sedimentary rocks spanning a range of depths, temperatures and oxygen regimes reflect this heterogeneity.

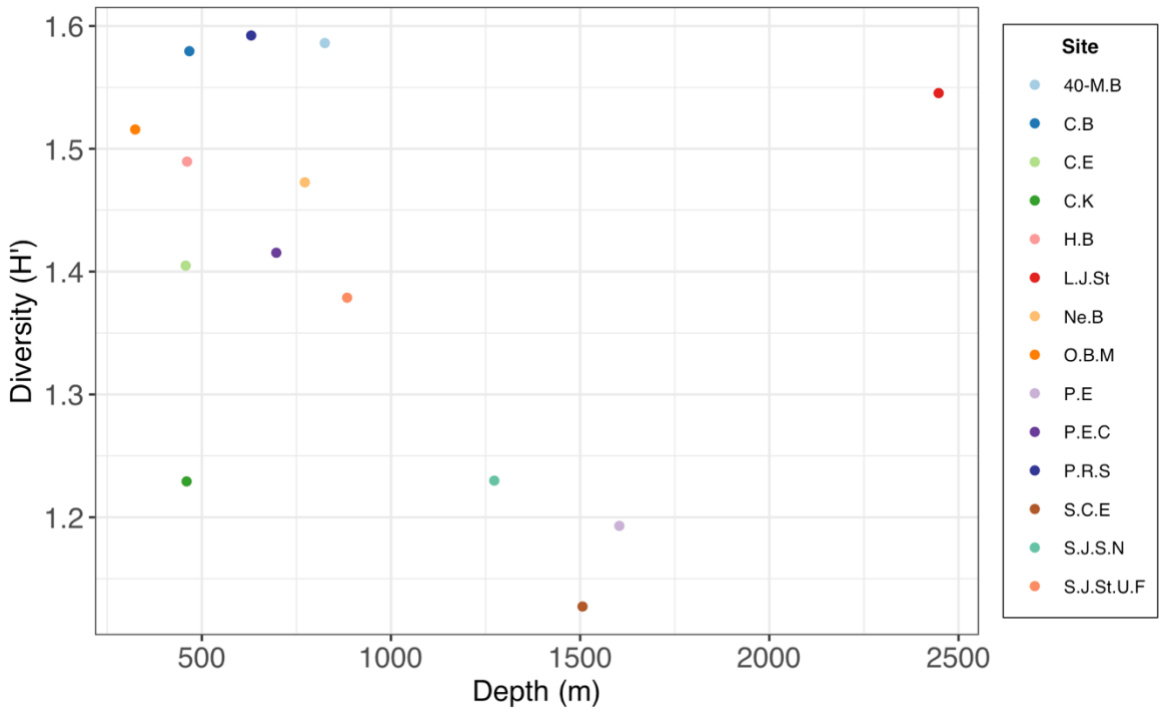

Figure 13. Scatterplot of diversity (H') pooled per site and average depth per site.

As observed in deep-sea ecosystems (Bax, 2011), the SCB appears to be dominated by rare species that appear as one or two individuals in the whole study. Such species (singletons or doubletons) accounted for 56.35% of all individuals sampled. This finding suggests that macrofauna in mineral-rich hard substrates may resemble macrofauna of deep-sea sediments in being comprised largely of rare species (Carney, 1997). This trend has also been observed for other substrates considered for deep-sea mining in the Clarion Clipperton Zone located in the Pacific (Christodoulou et al., 2019; Macheriotou et al., 2020), and it raises concerns about the potential loss of unique biodiversity associated with the exploitation of deep-sea ecosystems.

Macrofauna Community: Relationship to Substrate Type and Environmental Variables

In line with previous studies on FeMn crusts on seamounts, our results from the SCB revealed lower fauna abundance on FeMn crusts compared to non-FeMn substrates (Grigg et al., 2013; Schlacher et al., 2014). In the SCB, phosphorite rocks had 50% more macrofauna than FeMn crusts on average. Only phosphorite rocks were retrieved from Coronado Escarpment, Cortes Bank and Patton Ridge South at depths <700 m. Among the surveyed sites, Little Joe Seamount exhibited the lowest macrofaunal density and the highest diversity when pooled by site (Figure 7A and 7C). Vlach (2022) reported the same pattern for megafauna, which exhibited the lowest density and highest diversity at Little Joe Seamount in the SCB.

Results presented here show that the community composition of macrofaunal assemblages on FeMn crusts in the SCB have a higher number of unique taxa and their rarefaction diversity is higher compared to non-FeMn substrates. In contrast, (Schlacher et al., 2014; Corrêa et al., 2022) found no differences in the number of unique taxa nor did they find significant variation in diversity according to rarefaction curves between macrofauna of FeMn crusts and non-FeMn substrates of a Hawaiian Seamount Chain in the Central North Pacific. However, Vlach (2022) reported that megafaunal communities on FeMn crust exhibit higher rarefaction diversity compared to phosphorite and other rock types in the SCB. Corrêa et al. (2022) also noted distinct biological communities on FeMn crusts compared to non-FeMn substrates at the Rio Grande Rise, a seamount region in the Southwest Atlantic.

The different microbial communities associated with FeMn crusts at different depths could promote high diversity among microbial grazing macrofauna communities. Kato et al. (2018) showed that FeMn crusts from water depths of 1,150 to 5,520 m on a seamount of the northwestern Pacific have distinct microbial communities across depths. Although Bergo et al. (2021) showed

that FeMn substrates of the Rio Grande Rise show no difference in their microbial community compared to other substrates in the same region, sampling depth was also correlated with differences in microbial community structure. The same SCB FeMn encrusted rocks studied for macrofauna exhibit high microbial diversity and a distinct microbial community compared to phosphorite, basalt and sedimentary rocks, which all appear at varying depths (J. Gutleben personal communication, 2023). These microbial findings suggest that water depth and substrate type might be influencing the uniformity of the microbial community and may be contributing to variations in the macrofauna community that rely on these microbes as a food source.

Variation in macrofauna community composition among metal-rich hard substrates may be influenced by the faunas' tolerance to metal concentrations, impacting their settlement (Schlacher et al., 2014). For instance, although it is unclear which aspect of the rocks is supporting the macrofaunal communities, Verlaan (1992) observed higher foraminifera densities on ferromanganese crusts compared to basalt rocks. On the other hand, studies like Veillette et al. (2007) found no clear relationship between the geochemical composition of FeMn crusts and associated fauna. These conflicting results suggest the need for more comprehensive research for conclusive insights (Clark, 2011; Schlacher et al., 2014).

The chemical composition of FeMn crusts varies with depth, distance from shore, surface productivity, and distance from the Oxygen Minimum Zone (OMZ) (Usui et al., 2017; Mizell et al., 2020; Benites et al., 2023). Benites et al. (2023) identified higher concentrations of certain metals, such as Mn, Co, V, As, Mo, Tl, U, Zn, and Sb in FeMn crusts collected at depths exceeding 2000 m in the Southwest Atlantic Ocean. Given the diverse depth range of FeMn crusts in this study, it suggests potential variations in metal concentrations among rocks. If geochemistry influences faunal distribution based on metal tolerance, it could contribute to the observed

community composition differences among FeMn crusts (Figure 8E) compared to phosphorites found at similar depths. For example, in the north of France, a study found that polluted soil containing high concentrations of heavy metals, such as zinc, exhibited significantly lower densities of macrofauna compared to non-polluted soil (Nahmani & Lavelle, 2002).

The relationship between substrate type and macrofaunal density, diversity and composition may be best explained by environmental factors occurring where each of the substrate types were collected, rather than by substrate type alone. Oxygen, depth and temperature were found to be significantly correlated in the SCB study, and the relationship between oxygen and density and diversity of the macrofauna assemblages is influenced by the depth categories as per a covariate statistical test. Most FeMn crusts were collected from deeper waters (>600 m) and a broad depth range, in contrast all phosphorite rocks, and most of the basalt and sedimentary rocks were collected from shallower waters and a smaller depth range (<800 m) (Figure 14). FeMn crusts were the only substrate collected from the most oxygenated waters (>90 μmol/L) at the deepest depths (>2,200 m). Most phosphorite rocks (12 out of 19) were found within the OMZ above 800 m deep (Figure 14).

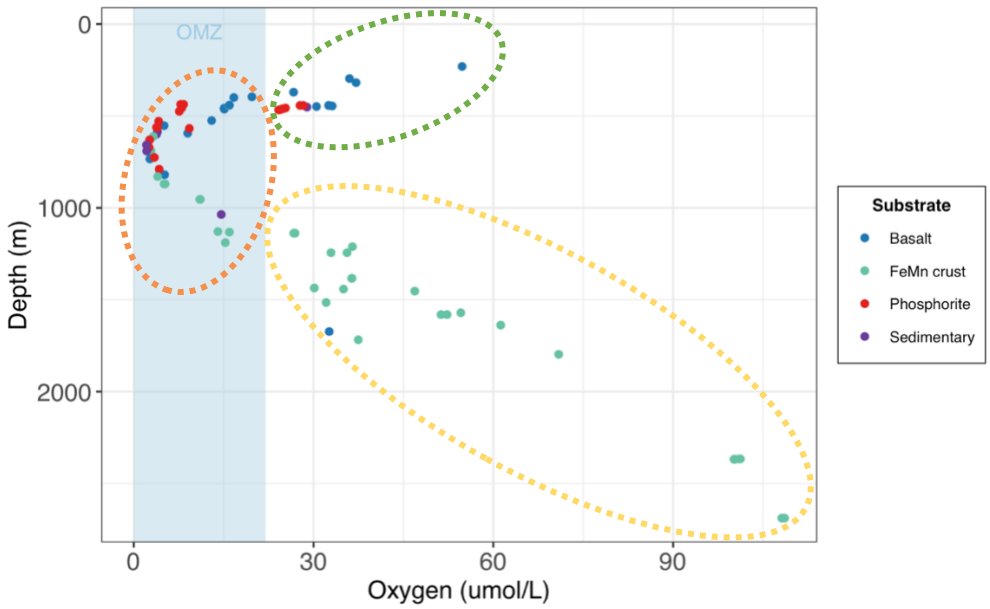

Figure 14. Scatterplot of rock samples as a function of oxygen and depth at collection site, colored by substrate type. Ellipses represent the OMZ categories (green = above OMZ, orange = within OMZ and yellow = below OMZ).

Across all substrates, density decreased with water depth in the SCB. This trend has been observed in other deep-ocean studies from sediments (Levin et al., 2000; Wei et al., 2012; Baldrighi et al., 2014) possibly as a result of decreasing food availability with depth (Ramirez-Llodra et al., 2010). Density of macrofaunal assemblages on FeMn crust was significantly correlated and negatively correlated with oxygen and depth. Macrofaunal densities on FeMn crust were lowest at depths >2000 m and highest within the OMZ (400 – 1100 m), and at higher temperatures (more than 5°C; Figure 9). Ma et al. (2021), showed that decomposition of organic matter within the OMZ happens at a slower rate. Thus, more food may arrive at the seafloor within the OMZ, which could explain the pattern of high density on FeMn crusts, phosphorite, basalt and sedimentary rocks in this zone.

On a per rock basis, FeMn crusts have lower diversity than the other substrates (Table 6). However, when data are pooled by substrate, FeMn crusts exhibit the highest diversity as shown

by rarefaction diversity (Figure 8 and 9E). This is likely due to the greater depth range they were collected from (Figure 9E). This mirrors the high diversity recently reported for polymetallic nodule zone in the Clarion Clipperton Zone (Rabone et al., 2023).

Schlacher et al., (2014), found that faunal assemblages on Pacific seamounts may vary from one site to another within a single seamount (separated by 1-2 km), from seamount to seamount, and due to depth variations. The dissimilarity of macrofauna among FeMn crusts sampled in this study may thus be explained by the different sites and depth ranges where the crusts were found (ranging from 600 m to 2700 m). To illustrate, FeMn crusts exhibited high dissimilarity in community composition at different sites on San Juan Seamount. Since all FeMn crusts were found at depths of >600 m and most of them were at >1000 m (Figure 12), the high diversity could be linked to low dominance due to diminishing supply of organic matter with depth (Wei & Rowe, 2019; Levin et al., 2001). Levin et al. (2000), also found highest rarefaction richness for pooled samples at depths >600 m deep for deep-ocean sediments. In alignment with Schlacher et al. (2014), the primary contributors to community differences among benthic assemblages on FeMn crusts and other substrates in this study were diverse, spanning annelids, arthropods, cnidarians, echinoderms, molluscs and sponges (Figure 9B).

Oxygen showed a significant negative correlation with diversity on phosphorite rocks (Figure 11). Instead of the commonly reported lowest species richness within OMZs (Levin et al., 2001), diversity of phosphorite rocks was highest within the OMZ, and as oxygen increased, diversity decreased. When considering individual rocks, average diversity metrics were highest for phosphorites compared to all other substrates analyzed in this study (Table 6). Leduc et al. (2015), found that macro-infaunal diversity in a phosphorite nodule ecosystem in the regions where the nodules were sitting, is correlated with topographic heterogeneity and variability. All

the phosphorite rocks from this study were characterized by uneven surfaces, including depressions, crevices, and holes, which could explain the high macrofaunal diversity on these rocks (Figure 15). The other substrates studied tended to be smoother and flatter without as many depressions and crevices.

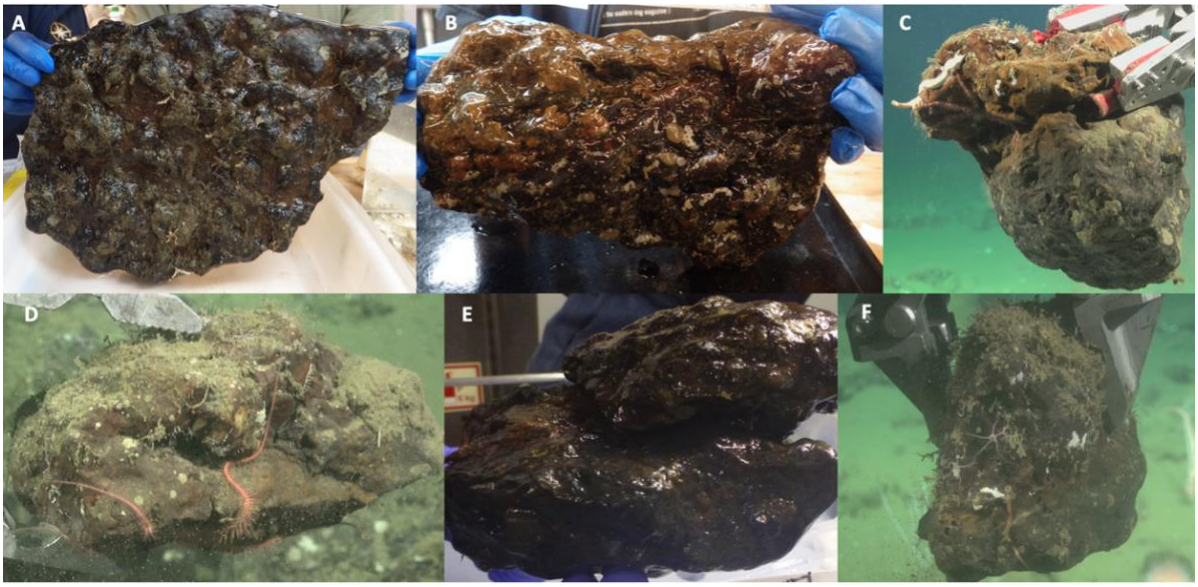

Figure 15. Photos of a few phosphorite rocks taken upon recovery. The rock IDs are as follows: A) HD1843-R3, B) HD1844-R7, C) SCB-329, D) SCB-342, E SCB-333, F) SCB-343.

Edge Effects

The most abundant groups on phosphorite rocks were annelids and echinoderms (~27%), followed by arthropods (~20). Five of the 10 most abundant taxa on phosphorites were echinoderm species, including Ophiuroidea sp.5 (postlarvae) and *Astrophiura marionae*, *Ophiocten* cf. *centobi*, *Amphipholis pugetana*? (juvenile), and Ophiuroidea sp.7 (postlarvae). The most abundant annelid was *Sphaerosyllis* nr. *ranunculus* and the other most abundant species were isopods, amphipods and tanaids (Table 7). Ophiuroids were the most abundant on phosphorite rocks at shallower depths (0-500 m), at the lower transition zone of the OMZ where oxygen concentrations ranged from 6-22 and 22-40 μmol/L and start to decrease. According to Levin (2003) and Gooday et al. (2010),

large abundances of ophiuroids are common at these zones because of more food availability. Earlier studies in Central and Southern California also found high densities of ophiuroids at oxygen concentrations of 22.3 μmol/L and 17 μmol/L (Smith & Hamilton, 1983; Thompson et al., 1985). A similar trend was observed for the megafauna of the SCB (Vlach, 2022).

Megafauna Influence on Macrofauna

It is well known that larger animals can serve as biological structures that enhance the complexity and heterogeneity of macrofaunal habitat, thus allowing more individuals and species to thrive in their presence (Buhl-Mortensen et al., 2010). Megafauna, such as sponges, corals, annelids, sea cucumbers and sea pens, were found on the rocks across all the different substrates (Table A23). These groups of animals can provide available habitat (on and within), protection from predators and food for smaller taxa, which explains higher abundance of macrofauna when megafauna are present (Buhl-Mortensen et al., 2010). However, in this study, macrofaunal densities were possibly significantly higher on rocks with megafauna due to the depth factor, since rocks with megafauna were collected from significantly shallower depths compared to those without megafauna. When only rocks with and without megafauna from above 500 m were compared, the rocks did not exhibit significantly higher macrofaunal densities or diversity with the presence of megafauna. Similarly, the comparison of sites inshore versus offshore showed no significant relationship with the macrofauna density and diversity (Figure A5 and Table A21).

CONNECTIONS TO CONSERVATION AND RECOMMENDATIONS

California state waters, within the territorial sea (0 to 3 nautical miles from shore), have been protected from mining under the California Seabed Mining Prevention Act published last year on September 20th, 2022 (CA AB1832, 2022). However, the bill does not protect the sites of interest in this study, which are beyond 3 nautical miles from shore (Figure 3). Therefore, the surrounding waters and deep-ocean ecosystems of the SCB would be susceptible to disturbance from mining, should commercial interest be developed; however, at present, there are none and metal grades suggest it is not likely soon (e.g. Conrad et al. 2017). However, the baseline research presented here can help us understand other regions where FeMn crust and phosphorite rocks are present and which are being considered for exploitation. Lighter protections, mainly against harmful commercial fishing gear, have been implemented by NOAA Fisheries on San Juan Seamount, 40-Mile Bank, and Northeast Bank due to their classification as Habitat Areas of Particular Concern (HAPC; PCGFMP, 2020; NOAA, 2021). HAPCs are conservation priority areas considered for their rarity, ecosystem function importance and sensitivity to human activities (NOAA, 2021).

Based on the findings of the study, certain sites emerge as potentially important for conservation efforts, should interest in exploiting minerals or other extractive activities ever occur. Cortes Bank, Patton Ridge South and Coronado Escarpment, from which only phosphorite rocks were collected, stand out as a conservation priority due to their notable combination of high macrofaunal density and diversity compared to other sites in the SCB (Table 6 and Figure 9A). Although, some areas of Patton Ridge South and Cortes Bank are designated as HAPCs (Vlach, 2022), no restrictions currently exist at these sites against mining activities (Gurish). Additionally, differences in the community composition of FeMn crusts at San Juan Seamount Upper Flank, San

Juan Seamount North, Patton Escarpment and Little Joe Seamount emphasize the ecological significance of these substrates and sites (Figure 7D). These sites showcase a diverse array of species from one rock to another (Figure 7C), contributing to overall biodiversity and ecosystem stability. Failing to implement measures of protection for these locations could lead to a decline in biodiversity, posing a threat to the essential ecosystem services and functions of the deep ocean (Danovaro et al., 2008; Montserrat et al., 2019). Moreover, recognizing the distinctiveness of each site, conservation strategies should be tailored to address the specific ecological dynamics and potential threats faced by individual locations, ensuring the long-term sustainability of these valuable marine ecosystems.

Each site in the SCB exhibited a distinct array of species when compared to one another. Coronado Escarpment, Hancock Bank, Little Joe Seamount, Osborn Bank Mesophotic Zone, and San Juan Seamount stood out, each hosting over 40% of its species as unique occurrences found at no other site. The examination of all FeMn crusts revealed that they host a high level of diversity when pooled and 47% of the species examined were exclusive to this substrate. Similarly, phosphorite rocks exhibited notable diversity on an individual rock basis and 40% of the species found were exclusive to this substrate. This study shows that FeMn crusts and phosphorite rocks fulfill the criteria of being unique and diverse to meet the standards for designating ecologically or biologically significant areas (EBSAs; CBD, 2008). This classification is integral to the conservation strategy aimed at establishing marine protected areas, as outlined by the United Nations Convention on Biological Diversity (CBD; Le et al., 2017). Furthermore, diversity was strongly influenced by depth and it will be important to include protected areas at various depths in the SCB to cover a wide range of unique habitats and species.

SUMMARY AND CONCLUSIONS

1. In comparison with deep-ocean sediments and chemosynthetic ecosystems, the macrofauna communities on mineral-rich hard substrates in the SCB are poorly understood and often less mentioned in conservation efforts. Non-reducing hard substrates harbor lower densities of macrofauna but a higher diversity than chemosynthetic ecosystems at methane seeps. Protecting them from the cumulative effects of fishing, pollution, mining, climate change and other anthropogenic stressors may be a conservation priority.
2. The macrofaunal diversity observed among FeMn crusts in this study suggests that the distinct environmental conditions at the different study sites (Figure 12)—including varying temperatures, pressure, oxygen levels, and food supply—could contribute to the high macrofaunal diversity observed on this substrate. Understanding the effects of substrate will be moderated by the different depth distributions and locations where they appear. The heterogeneity of the SCB is likely a key factor contributing to the significant differences in density, diversity and community composition of the macrofauna communities among sites, substrate type and depth zones.
3. The high diversity of macrofauna on FeMn crusts and phosphorites in the SCB makes them a potential target for conservation efforts for sites such as San Juan Seamount upper flank, San Clemente Escarpment, San Juan Seamount North, Patton Escarpment, little Joe Seamount, Cortes Bank, Patton Ridge South, and Coronado Escarpment.
4. The SCB hard substrates at bathyal depths resemble deep-sea sediments in having high diversity comprised of rare species.
5. These findings suggest that a complicated relationship exists between water depth, substrate type and macrofauna communities. Some potential factors influencing this

relationship could be the microbial community, which grazing macrofauna rely on as a food source or food availability from the water column. On FeMn crusts specifically, high microbial diversity, which can be influenced by depth, depth-related oceanographic factors (e.g. oxygen, temperature, water mass, current regime) and substrate characteristics (density, rugosity, oxidative environment), could explain the high macrofaunal diversity observed because the microbes are a food source to some invertebrate fauna.

6. There is a significant relationship between macrofaunal density and diversity on FeMn crusts and oxygen concentrations, which may be due to the large oxygen range of FeMn crusts. Conversely, this is potentially a depth effect. From 500 to 2,700 m, depth associated changes in food supply, water mass, or current regime are also potential determinants of macrofauna abundance patterns rather than oxygen availability alone.
7. Disparity in surface features may contribute to differences in macrofaunal diversity across the studied substrates. The phosphorite rocks were characterized by holes, crevices and depressions, which could account for the observed high macrofaunal diversity on a per rock basis, when compared to the other smoother substrates in this study.
8. The low oxygen concentrations of the OMZ did not inhibit macrofauna diversity and abundance on the substrates of study. However, the potential threat posed by deoxygenation remains significant. The oxygen conditions in the OMZ in the SCB were not as severe as observed in other low-oxygen environments, indicating a relatively favorable oxygen availability and organism adaptation that supports species existence. Additionally, the presence of hard substrates may offer animals increased exposure to water flow, potentially enhancing their ability to tolerate low oxygen conditions compared to their counterparts in sediments, where oxygen depletion occurs rapidly with depth.

Ongoing monitoring of oxygen levels in the SCB will be crucial for comprehending the implications of climate change and deoxygenation on a global scale.

9. This study offers biological and environmental insights for organizations tasked with formulating regulations and safeguarding the integrity of ecosystems where marine minerals of economic interest occur.

APPENDICES

Substrate, biological and environmental information for each sample collected form the SCB.

Table A1. Environmental data collected per rock sample, including depth, temperature and oxygen concentrations. Sample, dive, rock number and site are provided for context.

Sample	*Dive*	*Rock*	*Site*	*Depth (m)*	*Temperature (℃)*	*Oxygen (μmol/L)*
HD1840-R2	HD1840	2	Patton Escarpment Central	820	4.61	5.14
HD1840-R3	HD1840	3	Patton Escarpment Central	790	4.76	4.23
HD1840-R4	HD1840	4	Patton Escarpment Central	687	5.54	2.61
HD1840-R5	HD1840	5	Patton Escarpment Central	600	5.86	3.78
HD1840-R6	HD1840	6	Patton Escarpment Central	587	5.94	3.94
HD1841-R1	HD1841	1	San Juan Seamount Upper Flank	1129	3.72	14.04
HD1841-R3	HD1841	3	San Juan Seamount Upper Flank	954	3.94	11.01
HD1841-R4	HD1841	4	San Juan Seamount Upper Flank	954	3.92	11.1
HD1841-R5	HD1841	5	San Juan Seamount Upper Flank	692	5.23	2.79
HD1841-R6	HD1841	6	San Juan Seamount Upper Flank	691	5.17	2.87
HD1842-R1	HD1842	1	Northeast Bank	1132	3.68	15.95
HD1842-R2	HD1842	2	Northeast Bank	830	4.81	3.98
HD1842-R3	HD1842	3	Northeast Bank	734	5.24	2.68
HD1842-R4	HD1842	4	Northeast Bank	612	5.77	3.26
HD1842-R5	HD1842	5	Northeast Bank	553	6.28	5.05
HD1843-R1	HD1843	1	Cortes Bank	529	6.04	4.14
HD1843-R3	HD1843	3	Cortes Bank	475	6.47	7.59
HD1843-R4	HD1843	4	Cortes Bank	457	6.52	7.99
HD1843-R5	HD1843	5	Cortes Bank	437	6.53	8.31
HD1843-R6	HD1843	6	Cortes Bank	437	6.49	7.83
HD1844-R2	HD1844	2	Patton Ridge South	726	4.82	3.43
HD1844-R3	HD1844	3	Patton Ridge South	671	5.11	2.55
HD1844-R4	HD1844	4	Patton Ridge South	630	5.45	2.64
HD1844-R6	HD1844	6	Patton Ridge South	562	5.8	3.79
HD1844-R7	HD1844	7	Patton Ridge South	563	5.85	3.96
HD1845-R1	HD1845	1	40-Mile Bank	1036	3.82	14.6

Table A1. Environmental data collected per rock sample, including depth, temperature and oxygen concentrations. Sample, dive, rock number and site are provided for context, Continued.

Sample	*Dive*	*Rock*	*Site*	*Depth (m)*	*Temperature (℃)*	*Oxygen (μmol/L)*
HD1845-R2	HD1845	2	40-Mile Bank	870	4.58	5.22
HD1845-R3	HD1845	3	40-Mile Bank	870	4.59	5.04
HD1845-R5	HD1845	5	40-Mile Bank	691	5.3	2.15
HD1845-R6	HD1845	6	40-Mile Bank	658	5.51	2.11
HD1846-R1	HD1846	1	San Clemente Escarpment	1718	2.68	37.46
HD1846-R2	HD1846	2	San Clemente Escarpment	1673	2.88	32.61
HD1846-R3	HD1846	3	San Clemente Escarpment	1515	2.9	32.1
HD1846-R4	HD1846	4	San Clemente Escarpment	1436	2.98	30.12
HD1846-R6	HD1846	6	San Clemente Escarpment	1189	3.73	15.27
HD1847-R2	HD1847	2	Osborn Bank Meso	396	7.15	19.71
HD1847-R3	HD1847	3	Osborn Bank Meso	371	7.33	26.66
HD1847-R5	HD1847	5	Osborn Bank Meso	297	7.82	36
HD1847-R7	HD1847	7	Osborn Bank Meso	231	9.03	54.79
SCB-006	S0440	1	Hancock Bank	594	5	9
SCB-007	S0440	2	Hancock Bank	568	5.998	9.27
SCB-010	S0440	3	Hancock Bank	463	6.67	15.1
SCB-011	S0440	4	Hancock Bank	458	6.685	15.06
SCB-015	S0440	5	Hancock Bank	444	6.75	15.92
SCB-016	S0440	6	Hancock Bank	441	6.755	15.95
SCB-019	S0440	7	Hancock Bank	400	6.794	16.7
SCB-026	S0440	8	Hancock Bank	319	7.742	37.1
SCB-075	S0443	1	San Juan Seamount North	1442	3	35
SCB-076	S0443	2	San Juan Seamount North	1384	3.19	36.38
SCB-077	S0443	3	San Juan Seamount North	1383	3.19	36.38
SCB-085	S0443	4	San Juan Seamount North	1244	3.229	35.58
SCB-087	S0443	5	San Juan Seamount North	1244	3.349	32.91
SCB-090	S0443	6	San Juan Seamount North	1211	3.182	36.48
SCB-095	S0443	7	San Juan Seamount North	1138	3.626	26.7
SCB-096	S0443	8	San Juan Seamount North	1138	3.611	26.91
SCB-099	S0444	1	Patton Escarpment	1797	2.261	70.9
SCB-107	S0444	3	Patton Escarpment	1638	2.454	61.23
SCB-116	S0444	4	Patton Escarpment	1581	2.736	51.27
SCB-117	S0444	5	Patton Escarpment	1581	2.709	52.27
SCB-119	S0444	6	Patton Escarpment	1571	2.636	54.57
SCB-127	S0444	8	Patton Escarpment	1453	2.863	46.89

Table A1. Environmental data collected per rock sample, including depth, temperature and oxygen concentrations. Sample, dive, rock number and site are provided for context, Continued.

Sample	*Dive*	*Rock*	*Site*	*Depth (m)*	*Temperature (℃)*	*Oxygen (μmol/L)*
SCB-134	S0445	1	Little Joe Seamount	2688	1.754	108.14
SCB-135	S0445	2	Little Joe Seamount	2688	1.746	108.6
SCB-145	S0445	3	Little Joe Seamount	2366	1.815	101.24
SCB-146	S0445	4	Little Joe Seamount	2366	1.821	100.97
SCB-151	S0445	5	Little Joe Seamount	2368	1.829	100.22
SCB-152	S0445	6	Little Joe Seamount	2368	1.842	100.24
SCB-154	S0445	7	Little Joe Seamount	2368	1.843	100.22
SCB-155	S0445	8	Little Joe Seamount	2368	1.853	100.17
SCB-208	S0448	1	Crespi Knoll	525	6.58	12.99
SCB-218	S0448	3	Crespi Knoll	452	7.117	28.9
SCB-223	S0448	4	Crespi Knoll	446	7.218	33.11
SCB-224	S0448	5	Crespi Knoll	449	7.15	30.49
SCB-227	S0448	6	Crespi Knoll	443	7.213	32.54
SCB-229	S0448	7	Crespi Knoll	443	7.213	32.51
SCB-329	S0452	1	Coronado Escarpment	467	7.459	24.16
SCB-330	S0452	2	Coronado Escarpment	467	7.473	24.29
SCB-331	S0452	3	Coronado Escarpment	462	7.515	24.81
SCB-332	S0452	4	Coronado Escarpment	462	7.519	24.75
SCB-333	S0452	5	Coronado Escarpment	457	7.534	25.32
SCB-342	S0452	6	Coronado Escarpment	443	7.818	28.28
SCB-343	S0452	7	Coronado Escarpment	443	7.735	27.74

Table A2. Substrate type, ferromanganese crust thickness, and surface area of the each rock collected. Sample number, dive number, rock number and site are provided for context.

Sample	*Dive*	*Rock*	*Site*	*Substrate type*	*FeMn crust thickness*	*Surface Area (cm^2)*
HD1840-R2	HD1840	2	Patton Escarpment Central	Basalt	-	671.97
HD1840-R3	HD1840	3	Patton Escarpment Central	Phosphorite	-	1466.76
HD1840-R4	HD1840	4	Patton Escarpment Central	Sedimentary	-	356.94
HD1840-R5	HD1840	5	Patton Escarpment Central	Sedimentary	-	794.8
HD1840-R6	HD1840	6	Patton Escarpment Central	Sedimentary	-	700.87
HD1841-R1	HD1841	1	San Juan Seamount Upper Flank	Ferromanganese crust	16 mm	777.46
HD1841-R3	HD1841	3	San Juan Seamount Upper Flank	Ferromanganese crust	<1mm (patina)	534.68
HD1841-R4	HD1841	4	San Juan Seamount Upper Flank	Ferromanganese crust	2 mm	926.3
HD1841-R5	HD1841	5	San Juan Seamount Upper Flank	Ferromanganese crust	<1mm (patina)	1210.98
HD1841-R6	HD1841	6	San Juan Seamount Upper Flank	Ferromanganese crust	<1mm (patina)	1317.92
HD1842-R1	HD1842	1	Northeast Bank	Ferromanganese crust	0.5 mm	1588.15
HD1842-R2	HD1842	2	Northeast Bank	Ferromanganese crust	<1mm (patina)	401.73
HD1842-R3	HD1842	3	Northeast Bank	Basalt		862.72
HD1842-R4	HD1842	4	Northeast Bank	Ferromanganese crust	<1mm (patina)	565.03
HD1842-R5	HD1842	5	Northeast Bank	Basalt	-	553.47
HD1843-R1	HD1843	1	Cortes Bank	Phosphorite	-	1437.86
HD1843-R3	HD1843	3	Cortes Bank	Phosphorite	-	1963.87
HD1843-R4	HD1843	4	Cortes Bank	Phosphorite	-	380.06
HD1843-R5	HD1843	5	Cortes Bank	Phosphorite	-	423.41
HD1843-R6	HD1843	6	Cortes Bank	Phosphorite	-	417.63
HD1844-R2	HD1844	2	Patton Ridge South	Phosphorite	-	671.97
HD1844-R3	HD1844	3	Patton Ridge South	Phosphorite	-	942.2
HD1844-R4	HD1844	4	Patton Ridge South	Phosphorite	-	765.9
HD1844-R6	HD1844	6	Patton Ridge South	Phosphorite	-	1101.16
HD1844-R7	HD1844	7	Patton Ridge South	Phosphorite	-	1004.34
HD1845-R1	HD1845	1	40-Mile Bank	Sedimentary	-	348.27
HD1845-R2	HD1845	2	40-Mile Bank	Ferromanganese crust	5 mm	1328.03

Table A2. Substrate type, ferromanganese crust thickness, and surface area of the each rock collected. Sample number, dive number, rock number and site are provided for context, Continued.

Sample	*Dive*	*Rock*	*Site*	*Substrate type*	*FeMn crust thickness*	*Surface Area (cm^2)*
HD1845-R3	HD1845	3	40-Mile Bank	Ferromanganese crust	2 mm	534.68
HD1845-R5	HD1845	5	40-Mile Bank	Sedimentary	-	868.5
HD1845-R6	HD1845	6	40-Mile Bank	Sedimentary	-	1260.12
HD1846-R1	HD1846	1	San Clemente Escarpment	Ferromanganese crust	<1mm (patina)	647.4
HD1846-R2	HD1846	2	San Clemente Escarpment	Basalt	-	848.27
HD1846-R3	HD1846	3	San Clemente Escarpment	Ferromanganese crust	0.5 mm	776.01
HD1846-R4	HD1846	4	San Clemente Escarpment	Ferromanganese crust	<1mm (patina)	695.09
HD1846-R6	HD1846	6	San Clemente Escarpment	Ferromanganese crust	1 mm	459.54
HD1847-R2	HD1847	2	Osborn Bank Meso	Basalt	-	745.66
HD1847-R3	HD1847	3	Osborn Bank Meso	Basalt	-	436.42
HD1847-R5	HD1847	5	Osborn Bank Meso	Basalt	-	868.5
HD1847-R7	HD1847	7	Osborn Bank Meso	Basalt	-	446.53
SCB-006	S0440	1	Hancock Bank	Basalt	-	526.56
SCB-007	S0440	2	Hancock Bank	Phosphorite	-	775
SCB-010	S0440	3	Hancock Bank	Basalt	-	767.18
SCB-011	S0440	4	Hancock Bank	Basalt	-	385.93
SCB-015	S0440	5	Hancock Bank	Ferromanganese crust	<1mm (patina)	523.43
SCB-016	S0440	6	Hancock Bank	Basalt	-	273.43
SCB-019	S0440	7	Hancock Bank	Basalt	-	1025
SCB-019	S0440	7	Hancock Bank	Basalt	-	1025
SCB-026	S0440	8	Hancock Bank	Basalt	-	978.12
SCB-075	S0443	1	San Juan Seamount North	Ferromanganese crust	~27 mm	396.87
SCB-076	S0443	2	San Juan Seamount North	Ferromanganese crust	5-15 mm	696.87
SCB-077	S0443	3	San Juan Seamount North	Ferromanganese crust	~27 mm	945.31
SCB-085	S0443	4	San Juan Seamount North	Ferromanganese crust	~5 mm	781.25
SCB-087	S0443	5	San Juan Seamount North	Ferromanganese crust	~1 mm	620.31
SCB-090	S0443	6	San Juan Seamount North	Ferromanganese crust	~2 mm	1504.68
SCB-095	S0443	7	San Juan Seamount North	Ferromanganese crust	~3 mm	870.31

Table A2. Substrate type, ferromanganese crust thickness, and surface area of the each rock collected. Sample number, dive number, rock number and site are provided for context, Continued.

Sample	*Dive*	*Rock*	*Site*	*Substrate type*	*FeMn crust thickness*	*Surface Area (cm^2)*
SCB-096	S0443	8	San Juan Seamount North	Ferromanganese crust	<1 mm (patina)	571.87
SCB-099	S0444	1	Patton Escarpment	Ferromanganese crust	~2 mm	810.93
SCB-107	S0444	3	Patton Escarpment	Ferromanganese crust	75 mm diameter FeMn cobble	554.68
SCB-116	S0444	4	Patton Escarpment	Ferromanganese crust	~1 mm	451.56
SCB-117	S0444	5	Patton Escarpment	Ferromanganese crust	~1 mm	335.93
SCB-119	S0444	6	Patton Escarpment	Ferromanganese crust	~5 mm	507.81
SCB-127	S0444	8	Patton Escarpment	Ferromanganese crust	~40 mm	446.87
SCB-134	S0445	1	Little Joe Seamount	Ferromanganese crust	~13 mm	490.62
SCB-135	S0445	2	Little Joe Seamount	Ferromanganese crust	~5 mm	1410.93
SCB-135	S0445	2	Little Joe Seamount	Ferromanganese crust	~5 mm	1410.93
SCB-145	S0445	3	Little Joe Seamount	Ferromanganese crust	~3 mm	1046.87
SCB-146	S0445	4	Little Joe Seamount	Ferromanganese crust	~30 mm	895.31
SCB-151	S0445	5	Little Joe Seamount	Ferromanganese crust	~53 mm diameter FeMn cobble	403.125
SCB-152	S0445	6	Little Joe Seamount	Ferromanganese crust	~10 mm	581.25
SCB-154	S0445	7	Little Joe Seamount	Ferromanganese crust	~3 mm	903.125
SCB-155	S0445	8	Little Joe Seamount	Ferromanganese crust	~3 mm	648.4375
SCB-208	S0448	1	Crespi Knoll	Basalt	-	1151.5625
SCB-218	S0448	3	Crespi Knoll	Sedimentary	-	610.9375
SCB-223	S0448	4	Crespi Knoll	Basalt	-	401.5625
SCB-224	S0448	5	Crespi Knoll	Basalt	-	807.81
SCB-227	S0448	6	Crespi Knoll	Basalt	-	323.43
SCB-229	S0448	7	Crespi Knoll	Basalt	-	362.5
SCB-329	S0452	1	Coronado Escarpment	Phosphorite	-	1301.56
SCB-330	S0452	2	Coronado Escarpment	Phosphorite	-	1060.93

Table A2. Substrate type, ferromanganese crust thickness, and surface area of the each rock collected. Sample number, dive number, rock number and site are provided for context, Continued.

Sample	***Dive***	***Rock***	***Site***	***Substrate type***	***FeMn crust thickness***	***Surface Area (cm^2)***
SCB-331	S0452	3	Coronado Escarpment	Phosphorite	-	1146.87
SCB-332	S0452	4	Coronado Escarpment	Phosphorite	-	590.625
SCB-333	S0452	5	Coronado Escarpment	Phosphorite	-	987.5
SCB-342	S0452	6	Coronado Escarpment	Phosphorite	-	651.562
SCB-343	S0452	7	Coronado Escarpment	Phosphorite	-	917.187

Table A3. Macrofaunal density per rock, macrofaunal density per 200 cm^2, surface area of each rock collected. Sample number, dive number, rock number and site are provided for context.

Sample	*Dive*	*Rock*	*Site*	*Macrofauna density*	*Macrofauna density /200 cm^2*	*Surface Area (cm^2)*
HD1840-R2	HD1840	2	Patton Escarpment Central	48	14.28	671.97
HD1840-R3	HD1840	3	Patton Escarpment Central	73	9.95	1466.76
HD1840-R4	HD1840	4	Patton Escarpment Central	20	11.20	356.94
HD1840-R5	HD1840	5	Patton Escarpment Central	42	10.56	794.8
HD1840-R6	HD1840	6	Patton Escarpment Central	41	11.69	700.87
HD1841-R1	HD1841	1	San Juan Seamount Upper Flank	13	3.34	777.46
HD1841-R3	HD1841	3	San Juan Seamount Upper Flank	22	8.22	534.68
HD1841-R4	HD1841	4	San Juan Seamount Upper Flank	35	7.55	926.3
HD1841-R5	HD1841	5	San Juan Seamount Upper Flank	85	14.03	1210.98
HD1841-R6	HD1841	6	San Juan Seamount Upper Flank	70	10.62	1317.92
HD1842-R1	HD1842	1	Northeast Bank	236	29.72	1588.15
HD1842-R2	HD1842	2	Northeast Bank	15	7.467	401.73
HD1842-R3	HD1842	3	Northeast Bank	27	6.25	862.72
HD1842-R4	HD1842	4	Northeast Bank	20	7.07	565.03
HD1842-R5	HD1842	5	Northeast Bank	20	7.22	553.47
HD1843-R1	HD1843	1	Cortes Bank	141	19.61	1437.86
HD1843-R3	HD1843	3	Cortes Bank	196	19.96	1963.87
HD1843-R4	HD1843	4	Cortes Bank	46	24.20	380.06
HD1843-R5	HD1843	5	Cortes Bank	41	19.36	423.41
HD1843-R6	HD1843	6	Cortes Bank	40	19.15	417.63
HD1844-R2	HD1844	2	Patton Ridge South	33	9.82	671.97
HD1844-R3	HD1844	3	Patton Ridge South	61	12.94	942.2
HD1844-R4	HD1844	4	Patton Ridge South	39	10.18	765.9
HD1844-R6	HD1844	6	Patton Ridge South	51	9.26	1101.16
HD1844-R7	HD1844	7	Patton Ridge South	29	5.77	1004.34
HD1845-R1	HD1845	1	40-Mile Bank	19	10.91	348.27
HD1845-R2	HD1845	2	40-Mile Bank	18	2.71	1328.03
HD1845-R3	HD1845	3	40-Mile Bank	10	3.74	534.68
HD1845-R5	HD1845	5	40-Mile Bank	34	7.82	868.5

Table A3. Macrofaunal density per rock, macrofaunal density per 200 cm^2, surface area of each rock collected. Sample number, dive number, rock number and site are provided for context, Continued.

Sample	*Dive*	*Rock*	*Site*	*Macrofauna density*	*Macrofauna density /200 cm^2*	*Surface Area (cm^2)*
HD1845-R6	HD1845	6	40-Mile Bank	47	7.45	1260.12
HD1846-R1	HD1846	1	San Clemente Escarpment	14	4.32	647.4
HD1846-R1	HD1846	1	San Clemente Escarpment	14	4.32	647.4
HD1846-R2	HD1846	2	San Clemente Escarpment	39	9.19	848.27
HD1846-R3	HD1846	3	San Clemente Escarpment	33	8.50	776.01
HD1846-R4	HD1846	4	San Clemente Escarpment	12	3.45	695.09
HD1846-R6	HD1846	6	San Clemente Escarpment	12	5.22	459.54
HD1847-R2	HD1847	2	Osborn Bank Meso	58	15.55	745.66
HD1847-R3	HD1847	3	Osborn Bank Meso	34	15.58	436.42
HD1847-R5	HD1847	5	Osborn Bank Meso	63	14.50	868.5
HD1847-R7	HD1847	7	Osborn Bank Meso	45	20.15	446.53
SCB-006	S0440	1	Hancock Bank	39	14.81	526.56
SCB-007	S0440	2	Hancock Bank	60	15.48	775
SCB-010	S0440	3	Hancock Bank	45	11.73	767.18
SCB-011	S0440	4	Hancock Bank	51	26.42	385.93
SCB-015	S0440	5	Hancock Bank	46	17.57	523.43
SCB-016	S0440	6	Hancock Bank	32	23.40	273.43
SCB-019	S0440	7	Hancock Bank	61	11.90	1025
SCB-026	S0440	8	Hancock Bank	49	10.01	978.12
SCB-075	S0443	1	San Juan Seamount North	6	3.02	396.87
SCB-076	S0443	2	San Juan Seamount North	24	6.88	696.87
SCB-077	S0443	3	San Juan Seamount North	8	1.69	945.312
SCB-085	S0443	4	San Juan Seamount North	29	7.42	781.25
SCB-087	S0443	5	San Juan Seamount North	38	12.25	620.312
SCB-090	S0443	6	San Juan Seamount North	35	4.65	1504.68
SCB-095	S0443	7	San Juan Seamount North	138	31.71	870.31
SCB-096	S0443	8	San Juan Seamount North	70	24.48	571.875

Table A3. Macrofaunal density per rock, macrofaunal density per 200 cm^2, surface area of each rock collected. Sample number, dive number, rock number and site are provided for context, Continued.

Sample	*Dive*	*Rock*	*Site*	*Macrofauna density*	*Macrofauna density /200 cm^2*	*Surface Area (cm^2)*
SCB-099	S0444	1	Patton Escarpment	3	0.73	810.93
SCB-107	S0444	3	Patton Escarpment	2	0.72	554.68
SCB-116	S0444	4	Patton Escarpment	3	1.32	451.56
SCB-117	S0444	5	Patton Escarpment	6	3.57	335.93
SCB-119	S0444	6	Patton Escarpment	19	7.48	507.81
SCB-127	S0444	8	Patton Escarpment	9	4.02	446.87
SCB-134	S0445	1	Little Joe Seamount	10	4.07	490.62
SCB-135	S0445	2	Little Joe Seamount	4	0.56	1410.93
SCB-145	S0445	3	Little Joe Seamount	4	0.76	1046.87
SCB-146	S0445	4	Little Joe Seamount	10	2.23	895.31
SCB-151	S0445	5	Little Joe Seamount	5	2.48	403.12
SCB-152	S0445	6	Little Joe Seamount	22	7.56	581.25
SCB-154	S0445	7	Little Joe Seamount	5	1.10	903.12
SCB-155	S0445	8	Little Joe Seamount	5	1.54	648.43
SCB-208	S0448	1	Crespi Knoll	229	39.77	1151.56
SCB-218	S0448	3	Crespi Knoll	27	8.83	610.93
SCB-223	S0448	4	Crespi Knoll	38	18.92	401.56
SCB-224	S0448	5	Crespi Knoll	39	9.65	807.81
SCB-227	S0448	6	Crespi Knoll	31	19.16	323.43
SCB-229	S0448	7	Crespi Knoll	15	8.27	362.5
SCB-329	S0452	1	Coronado Escarpment	66	10.14	1301.56
SCB-330	S0452	2	Coronado Escarpment	61	11.49	1060.93
SCB-331	S0452	3	Coronado Escarpment	79	13.77	1146.87
SCB-332	S0452	4	Coronado Escarpment	66	22.34	590.62
SCB-333	S0452	5	Coronado Escarpment	51	10.32	987.5
SCB-342	S0452	6	Coronado Escarpment	78	23.94	651.56
SCB-343	S0452	7	Coronado Escarpment	55	11.99	917.18

Table A4. Diversity metrics per rock sample.

Sample	*Dive*	*Rock*	*Species richness*	$H'_{(loge)}$	$H'_{(log10)}$	*J'*	$ES_{(5)}$	$ES_{(10)}$	$ES_{(20)}$
HD1840-R2	HD1840	2	16	2.65	1.15	0.96	4.67	8.72	16.00
HD1840-R3	HD1840	3	21	2.59	1.12	0.85	4.14	7.04	11.36
HD1840-R4	HD1840	4	8	2.03	0.88	0.97	4.56	8.00	8.00
HD1840-R5	HD1840	5	23	2.95	1.28	0.94	4.64	8.59	15.29
HD1840-R6	HD1840	6	23	3.02	1.31	0.96	4.74	8.89	15.77
HD1841-R1	HD1841	1	10	2.25	0.98	0.98	4.62	8.27	10.00
HD1841-R3	HD1841	3	6	1.63	0.71	0.91	3.70	5.49	6.00
HD1841-R4	HD1841	4	16	2.60	1.13	0.94	4.50	8.00	13.20
HD1841-R5	HD1841	5	30	3.22	1.40	0.95	4.71	8.85	16.04
HD1841-R6	HD1841	6	25	2.99	1.30	0.93	4.61	8.42	14.54
HD1842-R1	HD1842	1	49	3.05	1.32	0.78	4.29	7.40	12.03
HD1842-R2	HD1842	2	7	1.75	0.76	0.90	3.98	7.00	7.00
HD1842-R3	HD1842	3	14	2.60	1.13	0.98	4.83	9.25	14.00
HD1842-R4	HD1842	4	8	1.91	0.83	0.92	4.11	6.99	8.00
HD1842-R5	HD1842	5	12	2.40	1.04	0.96	4.64	8.55	12.00
HD1843-R1	HD1843	1	40	3.36	1.46	0.91	4.65	8.54	14.76
HD1843-R3	HD1843	3	44	2.90	1.26	0.77	4.02	6.94	11.85
HD1843-R4	HD1843	4	22	2.90	1.26	0.94	4.61	8.40	14.43
HD1843-R5	HD1843	5	16	2.61	1.13	0.94	4.46	7.77	12.12
HD1843-R6	HD1843	6	21	2.89	1.26	0.95	4.65	8.51	14.42
HD1844-R2	HD1844	2	17	2.67	1.16	0.94	4.51	8.05	13.30
HD1844-R3	HD1844	3	27	3.10	1.35	0.94	4.66	8.59	14.81
HD1844-R4	HD1844	4	22	2.91	1.26	0.94	4.63	8.51	14.84
HD1844-R6	HD1844	6	22	2.83	1.23	0.92	4.53	8.11	13.69
HD1844-R7	HD1844	7	21	2.95	1.28	0.97	4.77	9.00	16.17
HD1845-R1	HD1845	1	7	1.76	0.76	0.90	3.74	5.54	7.00
HD1845-R2	HD1845	2	11	2.25	0.98	0.94	4.40	7.74	11.00
HD1845-R3	HD1845	3	8	2.04	0.89	0.98	4.72	8.00	8.00
HD1845-R5	HD1845	5	18	2.67	1.16	0.92	4.50	8.14	14.24
HD1845-R6	HD1845	6	29	3.27	1.42	0.97	4.80	9.12	16.45
HD1846-R1	HD1846	1	7	1.73	0.75	0.89	3.74	5.78	7.00
HD1846-R2	HD1846	2	19	2.39	1.04	0.81	3.96	6.62	11.10
HD1846-R3	HD1846	3	10	1.35	0.59	0.59	2.63	4.16	6.95
HD1846-R4	HD1846	4	8	1.91	0.83	0.92	4.11	6.99	8.00
HD1846-R6	HD1846	6	6	1.75	0.76	0.98	4.52	6.00	6.00
HD1847-R2	HD1847	2	21	2.66	1.15	0.87	4.25	7.47	12.81
HD1847-R3	HD1847	3	15	2.37	1.03	0.87	4.14	6.92	10.88

Table A4. Diversity metrics per rock sample, Continued.

Sample	*Dive*	*Rock*	*Species richness*	$H'_{(loge)}$	$H'_{(log10)}$	*J'*	$ES_{(5)}$	$ES_{(10)}$	$ES_{(20)}$
HD1847-R5	*HD1847*	*5*	*26*	*2.97*	*1.29*	*0.91*	*4.54*	*8.14*	*13.48*
HD1847-R7	HD1847	7	16	2.23	0.97	0.81	3.84	6.23	9.73
SCB-006	S0440	1	11	1.82	0.79	0.76	3.39	5.44	8.56
SCB-007	S0440	2	25	2.75	1.20	0.86	4.26	7.39	12.31
SCB-010	S0440	3	16	2.32	1.01	0.84	3.99	6.53	10.16
SCB-011	S0440	4	13	2.04	0.88	0.79	3.65	5.68	8.46
SCB-015	S0440	5	17	2.33	1.01	0.82	3.89	6.68	11.41
SCB-016	S0440	6	12	2.20	0.95	0.88	4.07	6.67	10.28
SCB-019	S0440	7	24	2.86	1.24	0.90	4.45	7.87	13.01
SCB-026	S0440	8	24	2.85	1.24	0.90	4.42	7.90	13.58
SCB-075	S0443	1	5	1.56	0.68	0.97	4.33	5.00	5.00
SCB-076	S0443	2	4	0.51	0.22	0.37	1.63	2.25	3.50
SCB-077	S0443	3	6	1.67	0.72	0.93	4.11	6.00	6.00
SCB-085	S0443	4	11	2.00	0.87	0.83	3.75	6.15	9.70
SCB-087	S0443	5	14	2.38	1.04	0.90	4.28	7.39	12.29
SCB-090	S0443	6	6	1.19	0.52	0.66	2.64	4.03	6.00
SCB-095	S0443	7	14	1.78	0.77	0.68	3.23	4.68	6.73
SCB-096	S0443	8	16	2.33	1.01	0.84	4.02	6.72	10.90
SCB-099	S0444	1	3	1.10	0.48	1.00	3.00	3.00	3.00
SCB-107	S0444	3	2	0.69	0.30	1.00	2.00	2.00	2.00
SCB-116	S0444	4	2	0.64	0.28	0.92	2.00	2.00	2.00
SCB-117	S0444	5	4	1.24	0.54	0.90	3.50	4.00	4.00
SCB-119	S0444	6	10	2.11	0.92	0.92	4.16	6.80	10.00
SCB-127	S0444	8	5	1.30	0.57	0.81	3.22	5.00	5.00
SCB-134	S0445	1	9	2.20	0.95	1.00	5.00	9.00	9.00
SCB-135	S0445	2	4	1.39	0.60	1.00	4.00	4.00	4.00
SCB-145	S0445	3	4	1.39	0.60	1.00	4.00	4.00	4.00
SCB-146	S0445	4	6	1.70	0.74	0.95	3.97	6.00	6.00
SCB-151	S0445	5	5	1.61	0.70	1.00	5.00	5.00	5.00
SCB-152	S0445	6	17	2.75	1.20	0.97	4.75	8.91	15.81
SCB-154	S0445	7	5	1.61	0.70	1.00	5.00	5.00	5.00
SCB-155	S0445	8	3	1.05	0.46	0.96	3.00	3.00	3.00
SCB-208	S0448	1	27	1.70	0.74	0.52	2.81	4.29	6.63
SCB-218	S0448	3	15	2.54	1.10	0.94	4.46	7.86	12.77
SCB-223	S0448	4	14	2.36	1.03	0.89	4.18	6.98	10.84
SCB-224	S0448	5	17	2.50	1.09	0.88	4.23	7.30	12.06

Table A4. Diversity metrics per rock sample, Continued.

Sample	*Dive*	*Rock*	*Species richness*	$H'_{(loge)}$	$H'_{(log10)}$	J'	$ES_{(5)}$	$ES_{(10)}$	$ES_{(20)}$
SCB-227	S0448	6	12	2.19	0.95	0.88	4.07	6.66	10.37
SCB-229	S0448	7	8	1.97	0.86	0.95	4.33	7.46	8.00
SCB-329	S0452	1	20	2.60	1.13	0.87	4.24	7.19	11.31
SCB-330	S0452	2	24	2.82	1.23	0.89	4.41	7.75	12.82
SCB-331	S0452	3	24	2.60	1.13	0.82	4.07	6.88	11.09
SCB-332	S0452	4	16	2.29	0.99	0.83	3.96	6.32	9.37
SCB-333	S0452	5	21	2.80	1.22	0.92	4.48	7.97	13.17
SCB-342	S0452	6	23	2.63	1.14	0.84	4.16	7.00	11.13
SCB-343	S0452	7	16	2.13	0.92	0.77	3.66	5.88	9.23

Results from statistics performed on the densities and diversity (H') of macrofaunal communities across sites.

Table A5. Z-statistic and associated p-values for pairwise comparisons (Benjamini-Hochberg) between macrofaunal density of sites. Asterisks (*) indicate statistical significance at a 2.5% level. The first line shows the z-statistic and the second shows the p-value.

Site	*40-M.B*	*Cortes Bank*	*Coronado Escarpment*	*Crespi Knoll*	*Hancock Bank*	*Little Joe Seamount*	*Northeast Bank*
Cortes Bank	-2.93						
	0.0127*						
Coronado Escarpment	-2.17	1.00					
	0.05	0.25					
Crespi Knoll	-1.91	1.15	0.20				
	0.08	0.21	0.45				
Hancock Bank	-2.54	0.72	-0.34	-0.53			
	0.03	0.30	0.42	0.35			
Little Joe Seamount	1.23	4.48	3.81	3.44	4.29		
	0.19	0.0003*	0.0013*	0.0033*	0.0004*		
Northeast Bank	-0.61	2.32	1.51	1.28	1.86	-1.90	
	0.33	0.05	0.13	0.18	0.08	0.08	
Osborn Bank Meso	-2.40	0.37	-0.54	-0.70	-0.27	-3.77	-1.82
	0.04	0.41	0.35	0.31	0.43	0.0012*	0.08
Patton Escarpment	1.06	4.12	3.44	3.12	3.86	-0.11	1.69
	0.24	0.0006*	0.0030*	0.0084*	0.0013*	0.47	0.10
Patton Escarpment Central	-1.51	1.42	0.54	0.33	0.86	-2.91	-0.90
	0.13	0.15	0.35	0.42	0.26	0.0128*	0.26
Patton Ridge South	-0.89	2.04	1.21	0.98	1.55	-2.21	-0.28
	0.27	0.07	0.19	0.25	0.12	0.05	0.43
San Clemente Escarpment	0.12	3.05	2.30	2.04	2.67	-1.09	0.73
	0.47	0.0093*	0.04	0.07	0.0245*	0.23	0.30
San Juan Seamount North	-0.80	2.46	1.58	1.30	1.98	-2.31	-0.12
	0.28	0.04	0.12	0.18	0.07	0.05	0.47
San Juan Seamount Upper Flank	-0.64	2.30	1.49	1.25	1.83	-1.93	-0.03
	0.33	0.04	0.13	0.19	0.08	0.08	0.49

Table A5. Z-statistic and associated p-values for pairwise comparisons (Benjamini-Hochberg) between macrofaunal density of sites. Asterisks (*) indicate statistical significance at a 2.5% level. The first line shows the z-statistic and the second shows the p-value, Continued.

Site	*Osborn Bank Meso*	*Patton Escarpment*	*Patton Escarpment Central*	*Patton Ridge South*	*San Clemente Escarpment*	*San Juan Seamount North*
Patton Escarpment	3.49					
	0.0032*					
Patton Escarpment Central	0.97	-2.64				
	0.25	0.03				
Patton Ridge South	1.56	-1.99	0.62			
	0.13	0.07	0.33			
San Clemente Escarpment	2.51	-0.93	1.63	1.01		
	0.03	0.26	0.11	0.25		
San Juan Seamount North	1.89	-2.03	0.88	0.19	-0.93	
	0.08	0.07	0.27	0.45	0.26	
San Juan Seamount Upper Flank	1.80	-1.72	0.88	0.25	-0.76	0.09
	0.09	0.10	0.26	0.43	0.30	0.47

Table A6. Z-statistic and associated p-values for pairwise comparisons (Benjamini-Hochberg) between macrofaunal diversity (H') of sites. Asterisks (*) indicate statistical significance at a 2.5% level. The first line shows the z-statistic and the second shows the p-value.

Site	*40-Mile Bank*	*Coronado Escarpment*	*Cortes Bank*	*Crespi Knoll*	*Hancock Bank*	*Little Joe Seamount*	*Northeast Bank*
Coronado Escarpment	-0.39						
	0.40						
Cortes Bank	-1.51	-1.24					
	0.14	0.20					
Crespi Knoll	0.68	1.15	2.26				
	0.33	0.22	0.05				
Hancock Bank	0.03	0.48	1.71	-0.73			
	0.50	0.39	0.10	0.32			
Little Joe Seamount	1.92	2.56	3.60	1.26	2.15		
	0.08	0.03	0.0036*	0.20	0.05		
Northeast Bank	0.11	0.52	1.63	-0.56	0.09	-1.79	
	0.49	0.38	0.12	0.38	0.48	0.09	
Osborn Bank	-0.45	-0.11	0.98	-1.11	-0.52	-2.28	-0.56
	0.39	0.49	0.26	0.23	0.39	0.05	0.38
Patton Ridge South	-1.54	-1.27	-0.03	-2.29	-1.74	-3.63	-1.65
	0.13	0.20	0.49	0.05	0.10	0.0043*	0.11
Patton Escarpment	2.59	3.23	4.17	2.94	2.87	0.87	2.47
	0.03	0.0071*	0.0007*	0.07	0.0145*	0.28	0.03
Patton Escarpment Central	-0.73	-0.40	0.78	-1.44	-0.84	-2.73	-0.84
	0.32	0.41	0.30	0.15	0.29	0.0206*	0.29
San Clemente Escarpment	1.51	2.02	3.02	0.89	1.64	-0.25	1.39
	0.14	0.07	0.0115*	0.28	0.11	0.45	0.16
San Juan Seamount North	1.84	2.47	3.52	1.18	2.06	-0.09	1.71
	0.09	0.03	0.0033*	0.22	0.06	0.49	0.11
San Juan Seamount Upper Flank	-0.39	-0.02	1.13	-1.08	-0.46	-2.35	-0.50
	0.40	0.49	0.22	0.23	0.39	0.04	0.39

Table A6. Z-statistic and associated p-values for pairwise comparisons (Benjamini-Hochberg) between macrofaunal diversity (H') of sites. Asterisks (*) indicate statistical significance at a 2.5% level. The first line shows the z-statistic and the second shows the p-value, Continued.

Site	*Osborn Bank*	*Patton Ridge South*	*Patton Escarpment*	*Patton Escarpment Central*	*San Clemente Escarpment*	*San Juan Seamount North*
Coronado Escarpment						
Cortes Bank						
Crespi Knoll						
Hancock Bank						
Little Joe Seamount						
Northeast Bank						
Osborn Bank						
Patton Ridge South	-1.00					
	0.25					
Patton Escarpment	2.89	4.20				
	0.0144*	0.0012*				
Patton Escarpment Central	-0.24	0.81	-3.35			
	0.45	0.30	0.0053*			
San Clemente Escarpment	1.87	3.05	-1.01	2.24		
	0.08	0.0117*	0.25	0.05		
San Juan Seamount North	2.20	3.54	-0.96	2.65	0.16	
	0.05	0.0036*	0.26	0.0247*	0.48	
San Juan Seamount Upper Flank	0.09	1.16	-2.99	0.35	-1.89	-2.26
	0.48	0.22	0.0116*	0.42	0.08	0.05

Results from statistics performed on the densities, diversity (H') and community composition of macrofaunal communities across substrate types.

Table A7. *Z-statistic and associated p-values for pairwise comparisons (Benjamini-Hochberg) between macrofaunal density of substrates –FeMn crust, phosphorite, basalt, and sedimentary rocks. Asterisks (*) indicate statistical significance at a 2.5% level.*

Substrate type	***Basalt***	***FeMn crust***	***Phosphorite***
FeMn crust	Z: 4.48		
	p: 0.0001*		
Phosphorite	Z: -0.013	Z: -4.49	
	p: 0.49	p: 0.0001*	
Sedimentary	Z: 1.32	Z: -1.64	Z: 1.33
	p: 0.11	p: 0.09	p: 0.13

Table A8. Z-statistic and associated p-values for pairwise comparisons (Benjamini-Hochberg) between diversity (H') of substrates –FeMn crust, phosphorite, basalt, and sedimentary rocks. Asterisks (*) indicate statistical significance at a 2.5% level.

Substrate type	***Basalt***	***FeMn crust***	***Phosphorite***
FeMn crust	Z: 2.82		
	p: 0.0047*		
Phosphorite	Z: -2.16	Z: -5.31	
	p: 0.0227*	p: 0.0000*	
Sedimentary	Z: -1.04	Z: -3.06	Z: 0.54
	p: 0.17	p: 0.0033*	p: 0.29

Table A9. T-statistic and p-value of pairwise test from PERMANOVA for macrofaunal community composition between substrate type.

Substrate type	***FeMn crust***	***Basalt***	***Sedimentary***
Basalt	t: 0.89, p: 0.82	-	-
Sedimentary	t: 1.19, p: 0.043	t: 1.19, p: 0.111	-
Phosphorite	t: 1.05, p: 0.27	t: 1.61, p: 0.001	t: 1.53, p: 0.001

Specific species found on FeMn crusts and phosphorite rocks.

Table A10. All 200 species on FeMn crusts and their frequency of occurrence (number of times they were found at any particular rock).

Taxa	***Frequency of occurrence***
Ophiocten cf. *centobi*	12
Pseudotanais sp. 1	9
Ophioleuce cf. *gracilis*	9
Ophiuroidea sp. 5 (postlarvae)	8
Spirorbis? sp. 1	7
Chloeia spp.	6
Munnopsurus sp. 1	6
Ophiuroidea sp. 7 (postlarvae)	6
Porifera sp. 5	6
Serpulidae spp. (juvenile)	5
Munnidae sp. 1	5
Bryozoa sp. 5	5
Actiniaria	5
Astrophiura marionae	5
Ophiuroidea sp. 13	5
Ophiuroidea sp. 6 (postlarvae)	5
Tellinidae sp. 1	5
Maldanidae sp. 1	4
Flabelligeridae sp. 1	4
Acari sp. 4	4
Stenothoidae sp. 3	4
Paramunnidae sp. 1	4
Bryozoa sp. 8	4
Ophiuroidea sp. 11	4
Gastropoda sp. 11	4
Porifera sp. 15	4
Porifera sp. 29	4
Syllidae sp. 6 (juvenile)	3
Sabellidae sp. 1	3
Spio? Spp.	3
Aphelochaeta spp. (juvenile)	3
Acari sp. 1	3

Table A10. All 200 species on FeMn crusts and their frequency of occurrence (number of times they were found at any particular rock), Continued.

Taxa	***Frequency of occurrence***
Acari sp. 3	3
Paraleptognathia bisetulosa	3
Ophiuroidea sp. 1 (juvenile)	3
Aplacophora sp. 2	3
Gastropoda sp. 22	3
Monoplacophora sp. 2	3
Porifera sp. 20	3
Porifera sp. 30	3
Ophryotrocha spp.	2
Lepidonotus sp. 1	2
Polynoidae sp. 4	2
Polynoidae sp. 5 (juvenile)	2
Eusyllis sp. 1	2
Salmacina tribranchiata sp. *1*	2
Laonice sp. 1 (juvenile)	2
Oedicerotidae sp. 1	2
Gnathia sp. 1	2
Munnopsidae sp. 1	2
Nannoniscidae sp. 1	2
Tridentellidae sp. 1 (juvenile)	2
Unid. Isopoda sp. 1	2
Araphura sp.1	2
Bryozoa sp. 13	2
Aplacophora sp. 1	2
Aplacophora sp. 3	2
Bivalvia sp. 4 (juvenile)	2
Gastropoda sp. 3	2
Limpet sp. 1	2
Scaphopoda sp. 1	2
Demospongiae sp. 1	2
Demospongiae sp. 2	2
Porifera sp. 10	2
Porifera sp. 27	2
Notomastus sp. 1	1

Table A10. All 200 species on FeMn crusts and their frequency of occurrence (number of times they were found at any particular rock), Continued.

Taxa	***Frequency of occurrence***
Clymenella californica	1
Maldanidae sp. 3	1
Lumbrineris nr. *inflata*	1
Lumbrineris nr. *latreillei*	1
Lumbrineridae sp. 2	1
Chrysopetalidae? sp. 1	1
Gyptis sp. 1	1
Podarkeopsis perkinsi	1
Hesionidae sp. 1 (juvenile)	1
Nereididae sp.	1
Eulalia (Sige) nr. *bifoliata*	1
Phyllodocidae (fragment)	1
Phyllodocidae sp. 1	1
Harmothoe nr. *imbricata*	1
Lepidasthenia sp. 1	1
Malmgreniella nr. *baschi*	1
Polynoidae sp. 1	1
Polynoidae sp. 3	1
Sphaerodoridae sp. 3	1
Sphaerodoridae sp.	1
Dioplosyllis nr. *Tridentata*	1
Dioplosyllis sp. 1	1
Dioplosyllis sp. 3	1
Eusyllinae sp. 1	1
Exogone "parexogone"? sp. 1	1
Sphaerosyllis nr. *ranunculus*	1
Exogoninae sp. 1	1
Syllidae sp. 2 (juvenile)	1
Syllidae sp. 3	1
Protis? sp. 1	1
Serpulidae sp. 3	1
Serpulidae sp. 4	1
Serpulidae sp. 5	1
Serpulidae sp. 6 (juvenile)	1
Polydoridae sp. 1	1

Table A10. All 200 species on FeMn crusts and their frequency of occurrence (number of times they were found at any particular rock), Continued.

Taxa	***Frequency of occurrence***
Laonice nr. *nuchula*	1
Paraprionospio? (juvenile)	1
Spionidae (fragments)	1
Ampharetidae sp. 1 (juvenile)	1
Chaetozone sp. 1	1
Cirratulidae sp. 3	1
Cirratulidae? (fragments)	1
Pherusa sp. 1	1
Trophoniella? sp. 1	1
Flabelligeridae fragment	1
Pista nr. *Elongata*	1
Terebellidae sp. 4	1
Terebellidae spp. (juvenile)	1
Trichobranchidae sp. 1 (juvenile)	1
Polychaeta fragment	1
Acari sp. 2	1
Acari sp. 5	1
Caprellidae sp. 1	1
Dulichiidae sp. 1	1
Rhachotropis inflata	1
Paradaliscidae sp. 1	1
Rhynohalicella hadona	1
Photidae sp. 1	1
Stegocephalidae sp.2	1
Stegocephalidaes p. 4 (juvenile)	1
Metopa nr. *dawsoni*	1
Stenothoe frecanda	1
Galatheidae sp. 1	1
Metopa nr. *dawsoni*	1
Stenothoe frecanda	1
Galatheidae sp. 1	1
Munididae sp. 1	1
Munnidae sp. 3	1

Table A10. All 200 species on FeMn crusts and their frequency of occurrence (number of times they were found at any particular rock), Continued.

Taxa	***Frequency of occurrence***
Penaeidae sp. 1	1
Unid. shrimp larvae sp. 1	1
Cirolanidae sp. 1	1
Desmosoma sp. 1	1
Haploniscidae sp. 1	1
Haploniscidae sp. 2	1
Pleurogonium sp. 1	1
Tridentella glutocantha	1
Unid. Isopoda sp. 2 (juvenile)	1
Anarthruridae sp. 1	1
Araphura sp. 2	1
Cirripedia sp. 1	1
Bryozoa sp. 6	1
Bryozoa sp. 9	1
Megalodicopia sp.	1
Actiniaria?	1
Dendrophylliidae sp. 1	1
Ypsilothuria sp. 1	1
Amphipholis pugetana? (juvenile)	1
Ophiacantha (Ophiotreta) sp?	1
Ophiacantha normani	1
Ophiuroidea sp. 12	1
Ophiuroidea sp. 14	1
Ophiuroidea sp. 15	1
Ophiuroidea sp. 3 (juvenile)	1
Ophiuroidea sp. 4 (juvenile)	1
Ophiuroidea sp. 8 (postlarvae)	1
Unidentified Ophiuroidea	1
Aplacophora sp. 4	1
Thyasiridae sp. 2	1
Placopecten sp. 1	1
Bivalvia sp. 1	1
Scutopus sp. 1	1

Table A10. All 200 species on FeMn crusts and their frequency of occurrence (number of times they were found at any particular rock), Continued.

Taxa	***Frequency of occurrence***
Neolepetopsidae sp. 1	1
Gastropoda sp. 1	1
Gastropoda sp. 12	1
Gastropoda sp. 14	1
Gastropoda sp. 18	1
Gastropoda sp. 19	1
Gastropoda sp. 2	1
Gastropoda sp. 4	1
Gastropoda sp. 5	1
Gastropoda sp. 6	1
Gastropoda sp. 7	1
Gastropoda sp. 8	1
Limpet sp. 6	1
Limpet sp. 7	1
Limpet sp. 9 (juvenile)	1
Polyplacophora sp. 3	1
Spiomenia spiculata	1
Macrarelle sp. 1	1
Planaria	1
Abestopluma sp. 1	1
Hexactinella sp. 2	1
Hexactinella sp. 3	1
Hexactinella sp. 6	1
Hexactinella sp. 7	1
Hexactinella sp. 8	1
Porifera sp. 1	1
Porifera sp. 11	1
Porifera sp. 12	1
Porifera sp. 17	1
Porifera sp. 23	1
Porifera sp. 25	1
Porifera sp. 26	1
Porifera sp. 28	1
Porifera sp. 3	1
Porifera sp. 4	1
Porifera sp. 7	1

Table A11. Species unique to FeMn crusts and total number of individuals.

Phylum	***Species morphotype***	***Number of individuals***
Annelida	*Clymenella californica*	2
Annelida	Maldanidae sp. 3	1
Annelida	Lumbrineridae sp. 2	1
Annelida	Chrysopetalidae? sp. 1	1
Annelida	Phyllodocidae (fragment)	1
Annelida	Phyllodocidae sp. 1	1
Annelida	Polynoidae sp. 3	1
Annelida	Sphaerodoridae sp. 3	1
Annelida	*Dioplosyllis* sp. 3	2
Annelida	*Eusyllinae* sp. 1	1
Annelida	*Exogone* "*parexogone*"? sp. 1	1
Annelida	Exogoninae sp. 1	3
Annelida	Syllidae sp. 2 (juvenile)	1
Annelida	Syllidae sp. 3	2
Annelida	Syllidae sp. 6 (juvenile)	3
Annelida	*Protis*? sp. 1	1
Annelida	*Salmacina tribranchiata* sp. 1	3
Annelida	Serpulidae sp. 3	1
Annelida	Serpulidae sp. 5	2
Annelida	Serpulidae spp. (juvenile)	28
Annelida	*Laonice* nr. *nuchula*	1
Annelida	*Paraprionospio*? (juvenile)	1
Annelida	Spionidae (fragments)	1
Annelida	Ampharetidae sp. 1 (juvenile)	3
Annelida	*Aphelochaeta* spp. (juvenile)	3
Annelida	*Chaetozone* sp. 1	1
Annelida	*Trophoniella*? sp. 1	1
Annelida	Flabelligeridae fragment	1
Annelida	*Pista* nr. *elongata*	2
Annelida	Terebellidae spp. (juvenile)	1
Annelida	Polychaeta fragment	2
Arthropoda	Acari sp. 5	1
Arthropoda	Paradaliscidae sp. 1	1
Arthropoda	*Rhynohalicella hadona*	2
Arthropoda	Photidae sp. 1	29
Arthropoda	Stegocephalidae sp. 2	1
Arthropoda	Penaeidae sp. 1	1

Table A11. Species unique to FeMn crusts and total number of individuals, Continued.

Phylum	***Species morphotype***	***Number of individuals***
Arthropoda	Cirolanidae sp. 1	1
Arthropoda	*Desmosoma* sp. 1	1
Arthropoda	Haploniscidae sp. 1	2
Arthropoda	Haploniscidae sp. 2	1
Arthropoda	Nannoniscidae sp. 1	2
Arthropoda	Paramunnidae sp. 1	5
Arthropoda	*Tridentella glutocantha*	2
Arthropoda	Unid. Isopoda sp. 1	2
Arthropoda	*Paraleptognathia bisetulosa*	7
Arthropoda	Anarthruridae sp. 1	3
Arthropoda	*Araphura* sp. 2	3
Bryozoa	Bryozoa sp.6	4
Chordata	*Megalodicopia* sp.	1
Cnidaria	Actiniaria?	1
Cnidaria	Dendrophylliidae sp. 1	2
Echinodermata	*Ypsilothuria* sp. 1	1
Echinodermata	*Ophiacantha normani*	1
Echinodermata	Ophiuroidea sp. 1 (juvenile)	3
Echinodermata	Ophiuroidea sp. 14	1
Echinodermata	Ophiuroidea sp. 15	1
Echinodermata	Ophiuroidea sp. 3 (juvenile)	1
Echinodermata	Ophiuroidea sp. 4 (juvenile)	1
Echinodermata	Ophiuroidea sp. 8 (postlarvae)	2
Echinodermata	Unidentified Ophiuroidea	1
Mollusca	Aplacophora sp. 4	3
Mollusca	Tellinidae sp. 1	6
Mollusca	Thyasiridae sp. 2	1
Mollusca	Bivalvia sp. 1	1
Mollusca	*Scutopus* sp. 1	1
Mollusca	Neolepetopsidae sp. 1	1
Mollusca	Gastropoda sp. 1	1
Mollusca	Gastropoda sp. 12	1
Mollusca	Gastropoda sp. 18	1
Mollusca	Gastropoda sp. 19	2
Mollusca	Gastropoda sp. 2	1
Mollusca	Gastropoda sp. 22	3

Table A11. Species unique to FeMn crusts and total number of individuals, Continued.

Phylum	***Species morphotype***	***Number of individuals***
Mollusca	Gastropoda sp. 3	2
Mollusca	Gastropoda sp. 4	1
Mollusca	Gastropoda sp. 6	1
Mollusca	Gastropoda sp. 7	1
Mollusca	Gastropoda sp. 8	1
Mollusca	Limpet sp. 1	4
Mollusca	Limpet sp. 7	1
Mollusca	Limpet sp. 9 (juvenile)	1
Mollusca	Scaphopoda sp. 1	2
Mollusca	*Spiomenia spiculata*	2
Porifera	*Hexactinella* sp. 2	1
Porifera	*Hexactinella* sp. 3	1
Porifera	*Hexactinella* sp. 6	1
Porifera	Porifera sp. 11	1
Porifera	Porifera sp. 12	1
Porifera	Porifera sp. 17	1
Porifera	Porifera sp. 20	3
Porifera	Porifera sp. 23	1
Porifera	Porifera sp. 25	1
Porifera	Porifera sp. 26	1
Porifera	Porifera sp. 27	2
Porifera	Porifera sp. 28	1

Table A12. Species unique to phosphorite rocks and total number of individuals.

Phylum	***Species morphotype***	***Number of individuals***
Annelida	Amphinomidae sp. 1	3
Annelida	Notomastus spp. (juvenile)	1
Annelida	Maldanidae sp. 4	1
Annelida	Maldanidae sp. 5	2
Annelida	Paraonella? Sp. 1 (juvenile)	2
Annelida	Paraonidae sp. 1	5
Annelida	*Schistomeringos* sp. 1	2
Annelida	*Eunice* sp. 1	1
Annelida	*Lumbrineris californiensis*	1
Annelida	*Lumbrineris* nr. *japonica*	4
Annelida	Myzostomidae sp. 1	3
Annelida	*Scalibregma californicum*	1
Annelida	*Glycera nana*	1
Annelida	*Gyptis* spp.	1
Annelida	Nautiliniellidae? sp. 1	1
Annelida	*Nephtys* sp. 1	6
Annelida	*Phyllodoce* nr. *papillata*	1
Annelida	*Harmothoe fragilis*	8
Annelida	Polynoidae sp. 2	3
Annelida	*Eusyllis* nr. *blomstrandi*	2
Annelida	*Pionosyllis*? sp. 1	2
Annelida	Syllidae sp. 5	4
Annelida	Syllidae? sp. 4	1
Annelida	*Pseudopotamilla* sp. 1	3
Annelida	Sabellidae sp. 2	1
Annelida	Serpulidae sp. 1	2
Annelida	Serpulidae sp. 7	1
Annelida	*Pseudopolydora* sp. 1 (juvenile)	4
Annelida	*Prionospio ehlersi*	5
Annelida	*Spiophanes berkeleyorum*	1
Annelida	*Spiophanes*? sp. 2 (juvenile)	1
Annelida	Spionidae larvae	1
Annelida	*Cirriformia spirabrancha*	2
Annelida	*Pherusa neopapillata*	1
Annelida	*Pista* nr. *wui*	1
Annelida	*Scionella* nr. *japonica*	1

Table A12. Species unique to phosphorite rocks and total number of individuals, Continued.

Phylum	***Species morphotype***	***Number of individuals***
Annelida	Terebellidae sp. 1 (Neoamphitrite?)(Thelipus)	6
Annelida	Terebellides sp. 1	1
Annelida	*Octobranchus* sp. 1	1
Arthropoda	Leuconidae sp. 1	5
Arthropoda	Caprellidae sp. 2	5
Arthropoda	Caprellidae sp. 4	17
Arthropoda	Pleustidae sp. 1	6
Arthropoda	Unid. Gammaridea	6
Arthropoda	Majidae sp. 1	1
Arthropoda	*Gnathia tridens*	2
Arthropoda	Munnopsidae sp. 2	3
Arthropoda	"*Nannoniscus*" sp. 1	2
Arthropoda	Paramunnidae sp. 2	2
Arthropoda	Agathotanaidae sp. 1 (juvenile)	4
Arthropoda	Unid. Crustacea	1
Arthropoda	Pycnogonidae sp. 2	1
Bryozoa	Bryozoa sp. 10	2
Bryozoa	Bryozoa sp. 12	2
Bryozoa	Bryozoa sp. 7	4
Cnidaria	Stylasteridae	1
Echinodermata	Asteroidea	1
Echinodermata	*Ophiacantha diplasia*?	1
Echinodermata	*Ophiopholis longispana*	3
Echinodermata	*Ophiosphalma*? (postlarvae)	1
Echinodermata	Ophiuroidea sp. 16	4
Hemichordata	Hemichordata	1
Mollusca	Gastropoda sp. 16	1
Mollusca	Gastropoda sp. 20	1
Mollusca	Limpet sp. 2	3
Mollusca	Limpet sp. 3	1
Mollusca	Polyplacophora sp. 2	3
Mollusca	Scaphopoda sp. 2	2
Porifera	Hexactinella sp. 4	1
Porifera	Porifera sp. 13	1
Porifera	Porifera sp. 21	1
Porifera	Porifera sp. 24	1

Correlation plot.

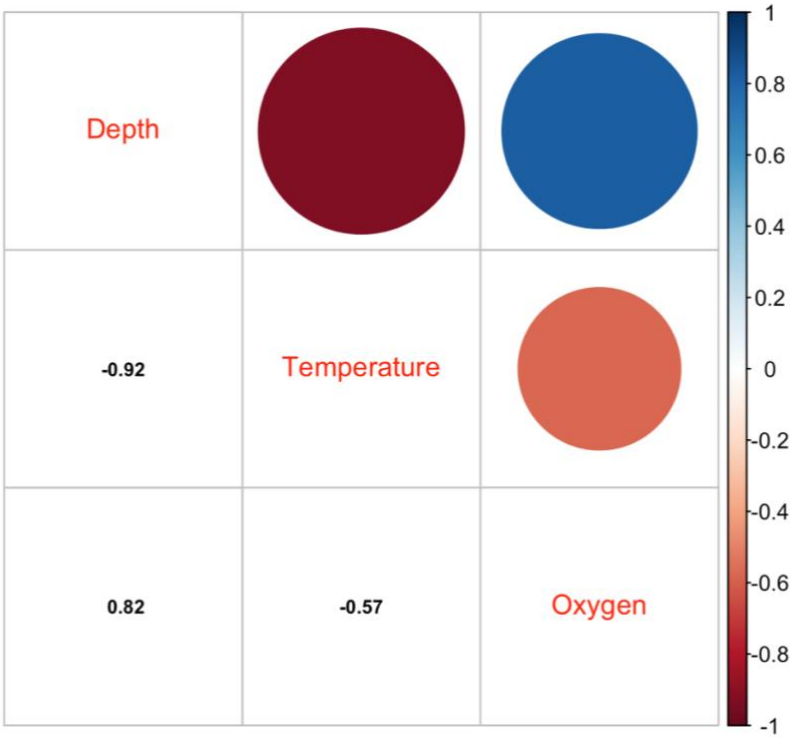

Figure A1. Correlation plot of depth, temperature and oxygen with correlation coefficients.

Plots of macrofaunal density by oxygen categories, depth categories, and within and outside the OMZ.

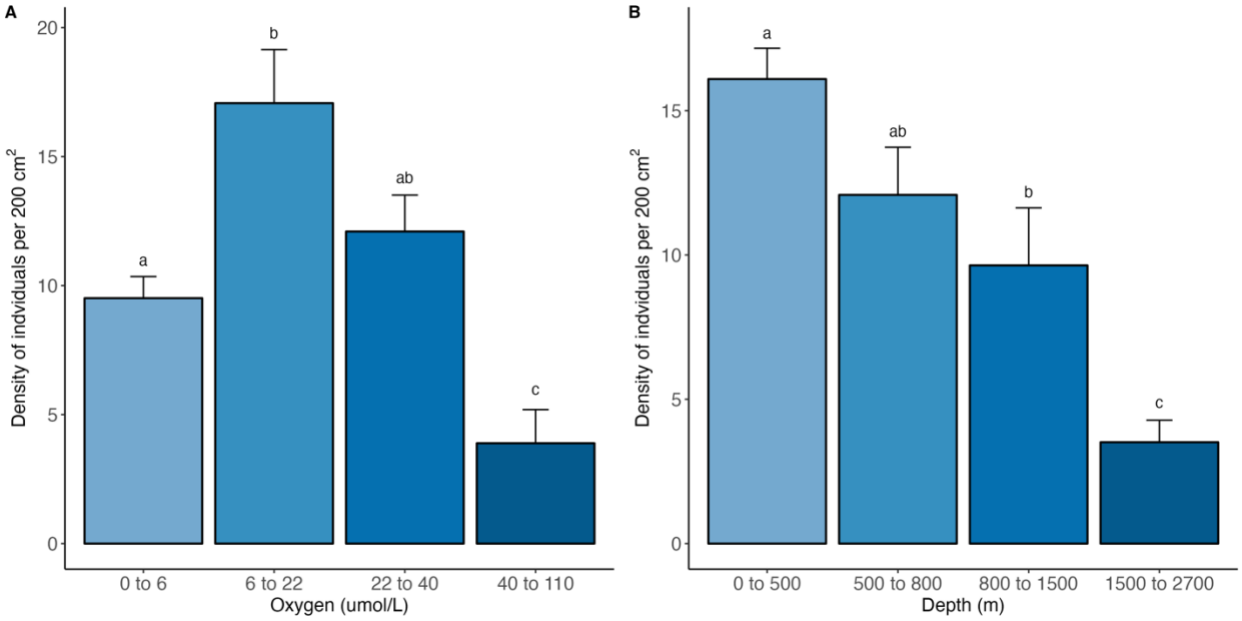

Figure A2. Average ± one standard error density of macrofauna per 200 cm^2 across A) oxygen categories, and B) depth categories.

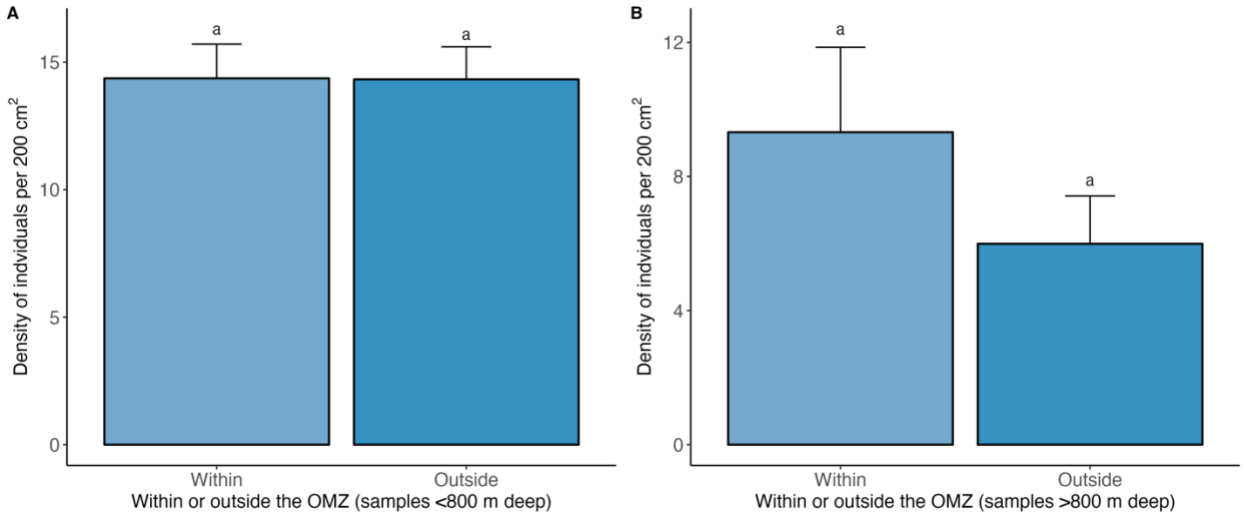

Figure A3. Average ± one standard error density of macrofauna per 200 cm^2 for A) within and outside the OMZ for samples <800 m deep, and B) within and outside the OMZ for samples >800 m deep.

Results from statistics performed on the densities and diversity of macrofauna communities across oxygen concentrations.

Table A13. P-values for Tukey multiple comparisons of density means between oxygen concentrations. Asterisks (*) indicate statistical significance at a 5% level.

Oxygen Category (μmol/L)	***0 to 6***	***22 to 40***	***40 to 110***
22 to 40	0.71		
40 to 110	0.0008*	0.00001*	
6 to 22	0.012*	0.11	0*

Table A14. Z-statistic and p-values for pairwise comparisons (Benjamini-Hochberg) between diversity (H') means of different oxygen concentration categories. Asterisks (*) indicate statistical significance at a 2.5% level.

Oxygen category (μmol/L)	***0 to 6***	***22 to 40***	***40 to 11***
22 to 40	Z: 2.97		
	p: 0.0029*		
40 to 11	Z: 5.16	Z: 2.72	
	p: 0.0000*	p: 0.0048*	
6 to 22	Z: 1.70	Z: -1.08	Z: -3.48
	p: 0.0526	p: 0.1383	p: 0.0007*

Results from statistics performed on the densities and diversity of macrofauna communities across depth.

Table A15. P-values for Tukey multiple comparisons of density means between depth categories. Asterisks (*) indicate statistical significance at a 5% level.

Depth (m)	*0 to 500*	*500 to 800*	*800 to 1500*
500 to 800	0.15		
800 to 1500	0.0006*	0.28	
1500 to 2700	0.0001*	0.000003*	0.001*

Table A16. Z-statistic and p-values for pairwise comparisons (Benjamini-Hochberg) between diversity means (H') of different depth categories. Asterisks (*) indicate statistical significance at a 2.5% level.

Depth (m)	*0 to 500*	*1500 to 2700*	*500 to 800*
1500 to 2700	Z: 4.39		
	p: 0.00001*		
500 to 800	Z: -1.16	Z: -5.19	
	p: 0.12	p: 0.00001*	
800 to 1500	Z: 3.12	Z: -1.38	Z: 4.03
	p: 0.0013*	p: 0.09	p: 0.0001*

Macrofauna average species richness (S), diversity (H'), evenness (J'), and $ES_{(20)}$ across different oxygen, depth and OMZ categories.

Table A17. Macrofauna average species richness (S), diversity (H'), evenness (J'), and $ES_{(20)}$ for each oxygen category. Chi Square and p values are given for Kruskal-Wallis test.

Oxygen (μmol/L)	*Species richness (S)*	*Shannon Index (H'_{loge})*	*Shannon Index (H'_{log10})*	*Evenness (J')*	*Rarefaction $ES_{(20)}$*
0 to 6	19.14 ± 1.87	2.67 ± 0.10	1.16 ± 0.04	0.94 ± 0.01	13.11 ± 0.67
6 to 22	19.11 ± 1.25	2.37 ± 0.11	1.03 ± 0.05	0.86 ± 0.02	10.56 ± 0.63
22 to 40	14.63 ± 1.21	2.16 ± 0.11	0.94 ± 0.05	0.84 ± 0.02	9.75 ± 0.54
40 to 110	6.33 ± 2.65	1.53 ± 0.15	0.67 ± 0.07	0.95 ± 0.02	5.84 ± 0.98
Chi-squared	25.28	27.81	27.81	27.71	30.49
df	3	3	3	3	3
p-value	1.34e-05	3.96e-06	3.96e-06	4.15e-06	1.08e-06

Table A18. Macrofauna average species richness (S), diversity (H'), evenness (J'), and ES(20) for each depth category. Chi Square and p values are given for Kruskal-Wallis test.

Depth (m)	*Species richness (S)*	*Shannon Index (H'_{loge})*	*Shannon Index (H'_{log10})*	*Evenness (J')*	*Rarefaction $ES_{(20)}$*
0 to 500	19.12 ± 1.34	2.52 ± 0.06	1.10 ± 0.03	0.87 ± 0.01	11.49 ± 0.34
500 to 800	21.15 ± 1.26	2.69 ± 0.11	1.17 ± 0.05	0.91 ± 0.02	13.04 ± 0.68
800 to 1500	11.25 ± 1.78	1.92 ± 0.13	0.83 ± 0.06	0.86 ± 0.03	8.47 ± 0.73
1500 to 2700	6.88 ± 2.18	1.56 ± 0.15	0.68 ± 0.06	0.93 ± 0.03	6.12 ± 0.94
Chi-squared	40.39	36.79	36.79	15.58	34.66
df	3	3	3	3	3
p-value	8.77e-09	5.09e-08	5.09e-08	0.001	1.43e-07

Table A19. Macrofauna average species richness (S), diversity (H'), evenness (J'), and ES(20) for within and outside the OMZ for samples >800 m deep and <800 m deep. U statistic and p-value given for Mann-Whitney U test.

OMZ >800	*Species richness (S)*	*Shannon Index (H'_{loge})*	*Shannon Index (H'_{log10})*	*Evenness (J')*	*Rarefaction $ES_{(20)}$*
Outside	7.65 ± 0.95[a]	1.60 ± 0.11[a]	0.69 ± 0.05[a]	0.88 ± 0.03[a]	6.58 ± 0.67[a]
Within	13.60 ± 4.11[b]	2.17 ± 0.15[b]	0.94 ± 0.07[b]	0.93 ± 0.02[a]	9.62 ± 1.07[b]
Mann-Whitney U statistic	73	55	55	121	60
p-value	0.04	0.008	0.008	0.7	0.01
OMZ <800	***Species richness (S)***	***Shannon Index (H'_{loge})***	***Shannon Index (H'_{log10})***	***Evenness (J')***	***$ES_{(20)}$***
Outside	18.19 ± 1.28[a]	2.49 ± 0.07[a]	1.08 ± 0.03[a]	0.87 ± 0.01[a]	11.24 ± 0.41[a]
Within	20.97 ± 1.50[a]	2.65 ± 0.08[a]	1.15 ± 0.03[a]	0.89 ± 0.02[b]	12.66 ± 0.50[b]
Mann-Whitney U statistic	194	165	165	152	144
p-value	0.29	0.08	0.08	0.04	0.02

Interaction effect between oxygen and depth categories for density and diversity of macrofaunal assemblages.

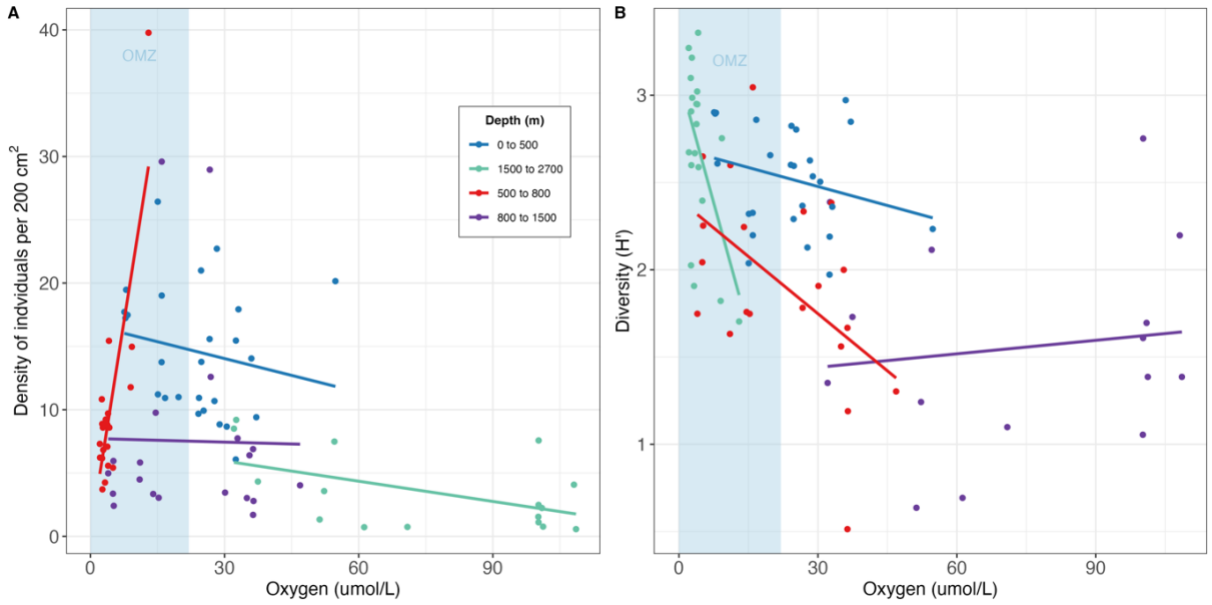

Figure A4. A) Scatter plot of density, and B) diversity (H') across different oxygen concentrations colored by depth to visualize the interaction effect between oxygen and depth categories. A) 0-500 m: R= 0.03, df = 24, p-value = 0.19, 500-800 m: R = 0.27, df = 18, p-value = 0.01, 800 to 1500 m: R = 0.22, df = 18, p-value: 0.01, 1500-2700 m: R = -0.05, df = 14, p-value = 0.63. B) 0-500 m: R = -0.003, df = 24, p-value = 0.34, 500-800 m: R = 0.65, df = 18, p-value = 1.05e-05, 800 to 1500 m: R = -0.05, df = 18, p-value: 0.94, 1500-2700 m: R = 0.2, df = 14, p-value = 0.04.

Density and diversity of macrofaunal communities by proximity to shore (offshore vs. inshore sites).

Table A20. Sites designated as inshore and offshore.

Sample	*Dive*	*Rock*	*Site*	*Proximity to shore*
HD1840-R2	HD1840	2	Patton Escarpment Central	Offshore
HD1840-R3	HD1840	3	Patton Escarpment Central	Offshore
HD1840-R4	HD1840	4	Patton Escarpment Central	Offshore
HD1840-R5	HD1840	5	Patton Escarpment Central	Offshore
HD1840-R6	HD1840	6	Patton Escarpment Central	Offshore
HD1841-R1	HD1841	1	San Juan Seamount Upper Flank	Offshore
HD1841-R3	HD1841	3	San Juan Seamount Upper Flank	Offshore
HD1841-R4	HD1841	4	San Juan Seamount Upper Flank	Offshore
HD1841-R5	HD1841	5	San Juan Seamount Upper Flank	Offshore
HD1841-R6	HD1841	6	San Juan Seamount Upper Flank	Offshore
HD1842-R1	HD1842	1	Northeast Bank	Offshore
HD1842-R2	HD1842	2	Northeast Bank	Offshore
HD1842-R3	HD1842	3	Northeast Bank	Offshore
HD1842-R4	HD1842	4	Northeast Bank	Offshore
HD1842-R5	HD1842	5	Northeast Bank	Offshore
HD1843-R1	HD1843	1	Cortes Bank	Offshore
HD1843-R3	HD1843	3	Cortes Bank	Offshore
HD1843-R4	HD1843	4	Cortes Bank	Offshore
HD1843-R5	HD1843	5	Cortes Bank	Offshore
HD1843-R6	HD1843	6	Cortes Bank	Offshore
HD1844-R2	HD1844	2	Patton Ridge South	Offshore
HD1844-R3	HD1844	3	Patton Ridge South	Offshore
HD1844-R4	HD1844	4	Patton Ridge South	Offshore
HD1844-R6	HD1844	6	Patton Ridge South	Offshore
HD1844-R7	HD1844	7	Patton Ridge South	Offshore
HD1845-R1	HD1845	1	40-Mile Bank	Inshore
HD1845-R2	HD1845	2	40-Mile Bank	Inshore
HD1845-R3	HD1845	3	40-Mile Bank	Inshore
HD1845-R5	HD1845	5	40-Mile Bank	Inshore
HD1845-R6	HD1845	6	40-Mile Bank	Inshore
HD1846-R1	HD1846	1	San Clemente Escarpment	Inshore

Table A20. Sites designated as inshore and offshore, Continued.

Sample	*Dive*	*Rock*	*Site*	*Proximity to shore*
HD1846-R2	HD1846	2	San Clemente Escarpment	Inshore
HD1846-R3	HD1846	3	San Clemente Escarpment	Inshore
HD1846-R4	HD1846	4	San Clemente Escarpment	Inshore
HD1846-R6	HD1846	6	San Clemente Escarpment	Inshore
HD1847-R2	HD1847	2	Osborn Bank Meso	Inshore
HD1847-R3	HD1847	3	Osborn Bank Meso	Inshore
HD1847-R5	HD1847	5	Osborn Bank Meso	Inshore
HD1847-R7	HD1847	7	Osborn Bank Meso	Inshore
SCB-006	S0440	1	Hancock Bank	Offshore
SCB-007	S0440	2	Hancock Bank	Offshore
SCB-010	S0440	3	Hancock Bank	Offshore
SCB-011	S0440	4	Hancock Bank	Offshore
SCB-015	S0440	5	Hancock Bank	Offshore
SCB-016	S0440	6	Hancock Bank	Offshore
SCB-019	S0440	7	Hancock Bank	Offshore
SCB-026	S0440	8	Hancock Bank	Offshore
SCB-075	S0443	1	San Juan Seamount North	Offshore
SCB-076	S0443	2	San Juan Seamount North	Offshore
SCB-077	S0443	3	San Juan Seamount North	Offshore
SCB-085	S0443	4	San Juan Seamount North	Offshore
SCB-087	S0443	5	San Juan Seamount North	Offshore
SCB-090	S0443	6	San Juan Seamount North	Offshore
SCB-095	S0443	7	San Juan Seamount North	Offshore
SCB-096	S0443	8	San Juan Seamount North	Offshore
SCB-099	S0444	1	Patton Escarpment	Offshore
SCB-107	S0444	3	Patton Escarpment	Offshore
SCB-116	S0444	4	Patton Escarpment	Offshore
SCB-117	S0444	5	Patton Escarpment	Offshore
SCB-119	S0444	6	Patton Escarpment	Offshore
SCB-127	S0444	8	Patton Escarpment	Offshore
SCB-134	S0445	1	Little Joe Seamount	Offshore
SCB-135	S0445	2	Little Joe Seamount	Offshore
SCB-145	S0445	3	Little Joe Seamount	Offshore
SCB-146	S0445	4	Little Joe Seamount	Offshore
SCB-151	S0445	5	Little Joe Seamount	Offshore
SCB-152	S0445	6	Little Joe Seamount	Offshore

Table A20. Sites designated as inshore and offshore, Continued.

Sample	*Dive*	*Rock*	*Site*	*Proximity to shore*
SCB-154	S0445	7	Little Joe Seamount	Offshore
SCB-155	S0445	8	Little Joe Seamount	Offshore
SCB-208	S0448	1	Crespi Knoll	Inshore
SCB-218	S0448	3	Crespi Knoll	Inshore
SCB-223	S0448	4	Crespi Knoll	Inshore
SCB-224	S0448	5	Crespi Knoll	Inshore
SCB-227	S0448	6	Crespi Knoll	Inshore
SCB-229	S0448	7	Crespi Knoll	Inshore
SCB-329	S0452	1	Coronado Escarpment	Inshore
SCB-330	S0452	2	Coronado Escarpment	Inshore
SCB-331	S0452	3	Coronado Escarpment	Inshore
SCB-332	S0452	4	Coronado Escarpment	Inshore
SCB-333	S0452	5	Coronado Escarpment	Inshore
SCB-342	S0452	6	Coronado Escarpment	Inshore
SCB-343	S0452	7	Coronado Escarpment	Inshore

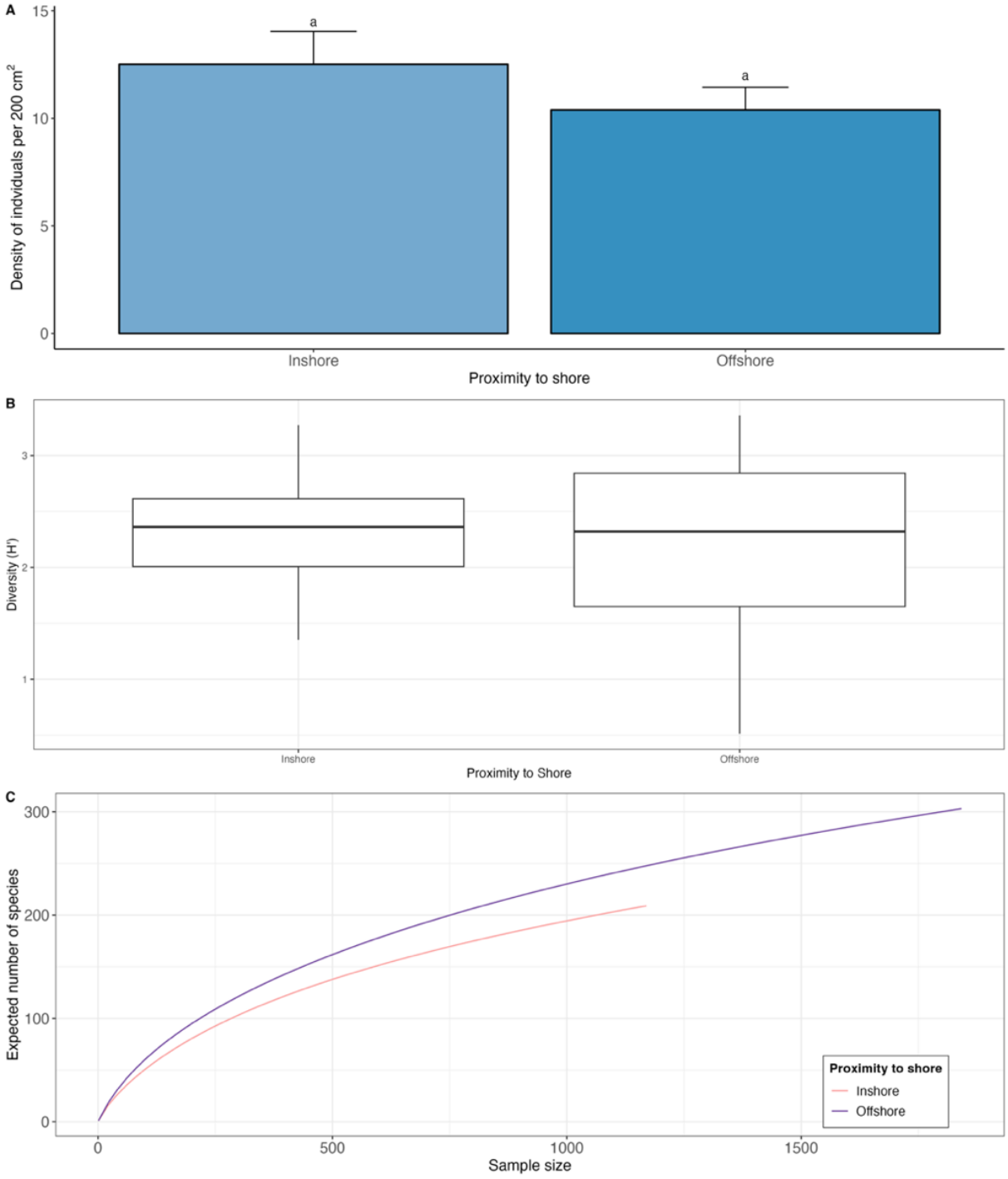

Figure A5. A) Average ± one standard error density of macrofauna per 200cm^2, B) Shannon Weiner diversity index with standard error, C) rarefaction curve (ES) for diversity across inshore vs offshore sites.

Table A21. Macrofauna average species richness (S), diversity (H'), evenness (J'), and $ES_{(20)}$ for rocks from inshore vs offshore sites. U statistic and p-value given for Mann-Whitney U test.

Proximity to shore	***Species richness (S)***	***Shannon Index (H'_{loge})***	***Shannon Index (H'_{log10})***	***Evenness (J')***	***Rarefaction $ES_{(20)}$***
Inshore	16.22 ± 1.29	2.31 ± 0.09	1.01 ± 0.04	0.86 ± 0.02	10.42 ± 0.51
Offshore	14.85 ± 1.40	2.18 ± 0.10	0.95 ± 0.04	0.90 ± 0.01	9.91 ± 0.58
Whitney U statistic	876	780	780	515	759
p-value	0.18	0.71	0.71	0.02	0.87

Density and diversity of macrofaunal communities by megafauna presence on the rock.

Table A22. Rocks with and without megafauna and the density of macrofauna communities per rock.

Sample	*Dive*	*Rock*	*Site*	*Macrofauna density*	*Macrofauna density /200 cm²*	*Megafauna presence*
HD1840-R2	HD1840	2	Patton Escarpment Central	48	14.28	No
HD1840-R3	HD1840	3	Patton Escarpment Central	73	9.95	No
HD1840-R4	HD1840	4	Patton Escarpment Central	20	11.20	No
HD1840-R5	HD1840	5	Patton Escarpment Central	42	10.56	Yes
HD1840-R6	HD1840	6	Patton Escarpment Central	41	11.69	No
HD1841-R1	HD1841	1	San Juan Seamount Upper Flank	13	3.34	No
HD1841-R3	HD1841	3	San Juan Seamount Upper Flank	22	8.22	No
HD1841-R4	HD1841	4	San Juan Seamount Upper Flank	35	7.55	No
HD1841-R5	HD1841	5	San Juan Seamount Upper Flank	85	14.03	No
HD1841-R6	HD1841	6	San Juan Seamount Upper Flank	70	10.62	No
HD1842-R1	HD1842	1	Northeast Bank	236	29.72	Yes
HD1842-R2	HD1842	2	Northeast Bank	15	7.46	No
HD1842-R3	HD1842	3	Northeast Bank	27	6.25	Yes
HD1842-R4	HD1842	4	Northeast Bank	20	7.07	No
HD1842-R5	HD1842	5	Northeast Bank	20	7.22	No
HD1843-R1	HD1843	1	Cortes Bank	141	19.61	No

Table A22. Rocks with and without megafauna and the density of macrofauna communities per rock, Continued.

Sample	*Dive*	*Rock*	*Site*	*Macrofauna density*	*Macrofauna density /200 cm²*	*Megafauna presence*
HD1843-R3	HD1843	3	Cortes Bank	196	19.96	Yes
HD1843-R4	HD1843	4	Cortes Bank	46	24.20	No
HD1843-R5	HD1843	5	Cortes Bank	41	19.36	No
HD1843-R6	HD1843	6	Cortes Bank	40	19.15	No
HD1844-R2	HD1844	2	Patton Ridge South	33	9.82	No
HD1844-R3	HD1844	3	Patton Ridge South	61	12.94	No
HD1844-R4	HD1844	4	Patton Ridge South	39	10.18	No
HD1844-R6	HD1844	6	Patton Ridge South	51	9.26	No
HD1844-R7	HD1844	7	Patton Ridge South	29	5.77	No
HD1845-R1	HD1845	1	40-Mile Bank	19	10.91	No
HD1845-R2	HD1845	2	40-Mile Bank	18	2.71	No
HD1845-R3	HD1845	3	40-Mile Bank	10	3.74	No
HD1845-R5	HD1845	5	40-Mile Bank	34	7.82	No
HD1845-R6	HD1845	6	40-Mile Bank	47	7.45	No
HD1846-R1	HD1846	1	San Clemente Escarpment	14	4.32	No
HD1846-R2	HD1846	2	San Clemente Escarpment	39	9.19	No
HD1846-R3	HD1846	3	San Clemente Escarpment	33	8.50	No
HD1846-R4	HD1846	4	San Clemente Escarpment	12	3.45	No
HD1846-R6	HD1846	6	San Clemente Escarpment	12	5.22	No
HD1847-R2	HD1847	2	Osborn Bank Meso	58	15.55	Yes
HD1847-R3	HD1847	3	Osborn Bank Meso	34	15.58	No
HD1847-R5	HD1847	5	Osborn Bank Meso	63	14.50	Yes
HD1847-R7	HD1847	7	Osborn Bank Meso	45	20.15	No
SCB-006	S0440	1	Hancock Bank	39	14.81	Yes

Table A22. Rocks with and without megafauna and the density of macrofauna communities per rock, Continued.

Sample	*Dive*	*Rock*	*Site*	*Macrofauna density*	*Macrofauna density /200 cm²*	*Megafauna presence*
SCB-007	S0440	2	Hancock Bank	60	15.48	No
SCB-010	S0440	3	Hancock Bank	45	11.73	No
SCB-011	S0440	4	Hancock Bank	51	26.42	Yes
SCB-015	S0440	5	Hancock Bank	46	17.57	Yes
SCB-016	S0440	6	Hancock Bank	32	23.40	Yes
SCB-019	S0440	7	Hancock Bank	61	11.90	Yes
SCB-026	S0440	8	Hancock Bank	49	10.01	Yes
SCB-075	S0443	1	San Juan Seamount North	6	3.02	No
SCB-076	S0443	2	San Juan Seamount North	24	6.88	No
SCB-077	S0443	3	San Juan Seamount North	8	1.69	Yes
SCB-085	S0443	4	San Juan Seamount North	29	7.42	Yes
SCB-087	S0443	5	San Juan Seamount North	38	12.25	No
SCB-090	S0443	6	San Juan Seamount North	35	4.65	No
SCB-095	S0443	7	San Juan Seamount North	138	31.71	Yes
SCB-096	S0443	8	San Juan Seamount North	70	24.48	No
SCB-099	S0444	1	Patton Escarpment	3	0.73	No
SCB-107	S0444	3	Patton Escarpment	2	0.72	No
SCB-116	S0444	4	Patton Escarpment	3	1.32	No

Table A22. Rocks with and without megafauna and the density of macrofauna communities per rock, Continued.

Sample	*Dive*	*Rock*	*Site*	*Macrofauna density*	*Macrofauna density /200 cm²*	*Megafauna presence*
SCB-117	S0444	5	Patton Escarpment	6	3.57	No
SCB-119	S0444	6	Patton Escarpment	19	7.48	No
SCB-127	S0444	8	Patton Escarpment	9	4.02	Yes
SCB-134	S0445	1	Little Joe Seamount	10	4.07	No
SCB-135	S0445	2	Little Joe Seamount	4	0.56	No
SCB-145	S0445	3	Little Joe Seamount	4	0.76	No
SCB-146	S0445	4	Little Joe Seamount	10	2.23	No
SCB-151	S0445	5	Little Joe Seamount	5	2.48	No
SCB-152	S0445	6	Little Joe Seamount	22	7.56	No
SCB-154	S0445	7	Little Joe Seamount	5	1.10	Yes
SCB-155	S0445	8	Little Joe Seamount	5	1.54	No
SCB-208	S0448	1	Crespi Knoll	229	39.77	No
SCB-218	S0448	3	Crespi Knoll	27	8.83	No
SCB-223	S0448	4	Crespi Knoll	38	18.92	No
SCB-224	S0448	5	Crespi Knoll	39	9.65	Yes
SCB-227	S0448	6	Crespi Knoll	31	19.16	No
SCB-229	S0448	7	Crespi Knoll	15	8.27	No
SCB-329	S0452	1	Coronado Escarpment	66	10.14	No
SCB-330	S0452	2	Coronado Escarpment	61	11.49	No
SCB-331	S0452	3	Coronado Escarpment	79	13.77	No
SCB-332	S0452	4	Coronado Escarpment	66	22.34	Yes
SCB-333	S0452	5	Coronado Escarpment	51	10.32	No
SCB-342	S0452	6	Coronado Escarpment	78	23.94	No
SCB-343	S0452	7	Coronado Escarpment	55	11.99	Yes

Table A23. Phylum and taxa of megafauna found on rocks across all substrate types.

Phylum	***Taxon***
Porifera	Rosselidae sp.
Porifera	Demosponge sp.
Cnidaria	*Anthoptilum* sp.
Cnidaria	Acanthagorgia sp.
Porifera	*Asbestopluma* sp.
Annelida	Terebellidae sp.
Cnidaria	Stylasteridae sp.2
Cnidaria	Heteropolypus sp.
Porifera	encrusting sponge
Echinodermata	*Psolus* sp.
Porifera	Unkown
Cnidaria	*Pennatulacea* sp.

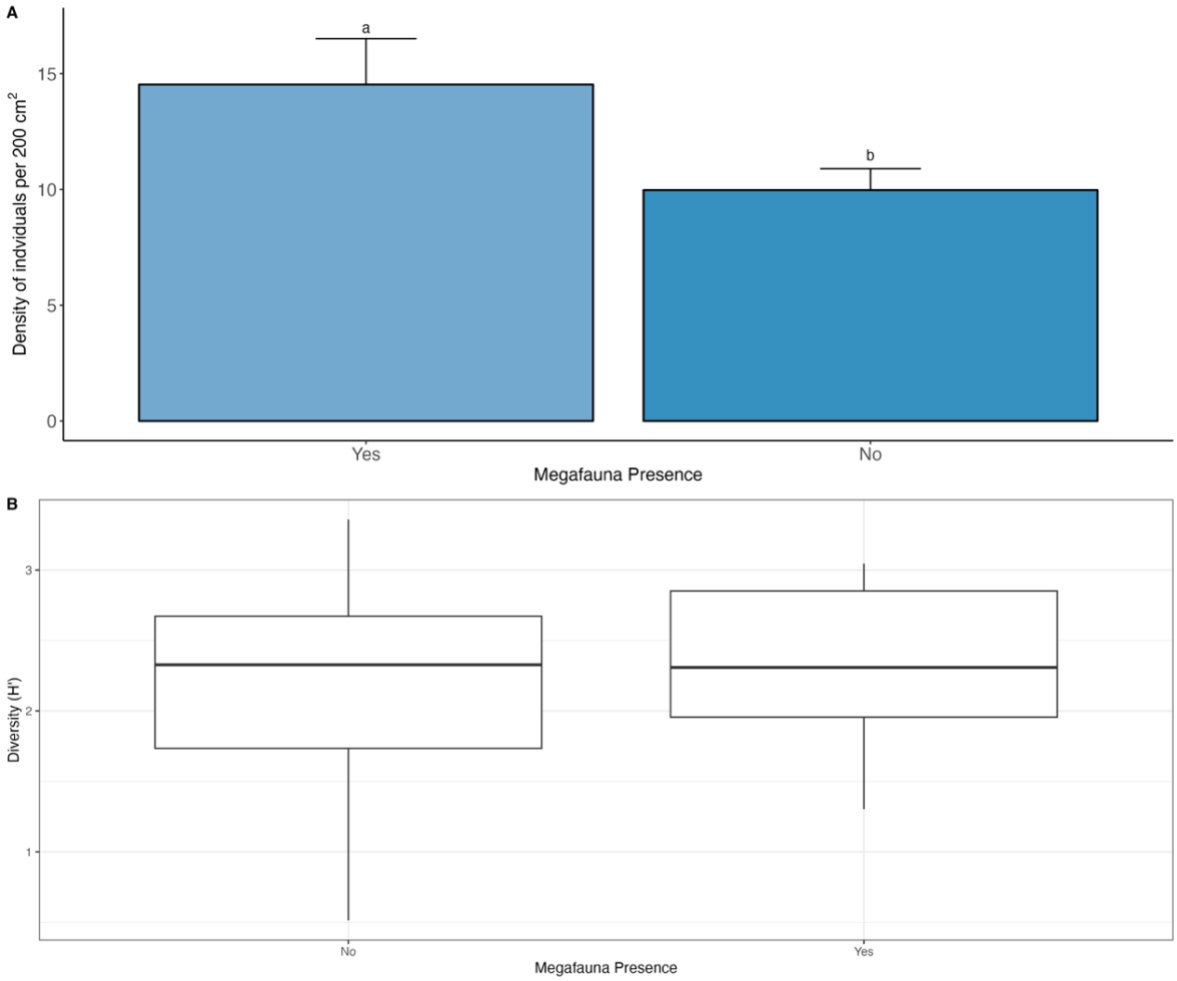

Figure A6. A) Average ± one standard error density of macrofauna per 200 cm^2 for all rocks, B) Shannon Weiner diversity index with standard error, across all rocks with and without megafauna.

Table A24. Macrofauna average species richness (S), diversity (H'), evenness (J'), and ES20 for rocks above 500 m with and without megafauna. U statistic and p-value given for Mann-Whitney U test.

Megafauna present	***Species richness (S)***	***Shannon Index (H'_{loge})***	***Shannon Index (H'_{log10})***	***Evenness (J')***	***$ES_{(20)}$***
No	17.8 ± 1.22	2.52 ± 0.07	0.95 ± 0.04	0.88 ± 0.01	11.54 ± 0.45
Yes	20.9 ± 2.69	2.52 ± 0.10	1.01 ± 0.05	0.84 ± 0.01	11.41 ± 0.54
Whitney U statistic	64.5	81	81	115	83
p-value	0.36	0.95	0.95	0.09	1

REFERENCES

Amon, D. J., Ziegler, A. F., Dahlgren, T. G., Glover, A. G., Goineau, A., Gooday, A. J., Wiklund, H., & Smith, C. R. (2016). Insights into the abundance and diversity of abyssal megafauna in a polymetallic-nodule region in the eastern Clarion-Clipperton Zone. *Scientific Reports*, *6*. https://doi.org/10.1038/srep30492

Baco, A., & Smith, C. (2003). High species richness in deep-sea chemoautotrophic whale skeleton communities. *Marine Ecology Progress Series*, *260*, 109–114. https://doi.org/10.3354/meps260109

Baker, M., Ramirez-Llodra, E., & Tyler, P. (2020). Natural Capital and Exploitation of the Deep Ocean. In *Natural Capital and Exploitation of the Deep Ocean*. Oxford University Press. https://doi.org/10.1093/oso/9780198841654.001.0001

Baldrighi, E., Lavaleye, M., Aliani, S., Conversi, A., & Manini, E. (2014). Large Spatial Scale Variability in Bathyal Macrobenthos Abundance, Biomass, α- and β-Diversity along the Mediterranean Continental Margin. *PLoS ONE*, *9*(9), e107261. https://doi.org/10.1371/journal.pone.0107261

Bax, N. (2011). *Review of* Deep-Sea Biodiversity: Pattern and Scale. *Oceanography*, *24*(01), 183–185. https://doi.org/10.5670/oceanog.2011.19

Benites, M., González, J., Hein, J., Marino, E., Reyes, J., Millo, C., & Jovane, L. (2023). Controls on the chemical composition of ferromanganese crusts from deep-water to the summit of the Rio Grande Rise, South Atlantic Ocean. *Marine Geology*, *462*, 107094. https://doi.org/10.1016/j.margeo.2023.107094

Bergo, N. M., Bendia, A. G., Ferreira, J. C. N., Murton, B. J., Brandini, F. P., & Pellizari, V. H. (2021). Microbial Diversity of Deep-Sea Ferromanganese Crust Field in the Rio Grande Rise, Southwestern Atlantic Ocean. *Microbial Ecology*, *82*(2), 344–355. https://doi.org/10.1007/s00248-020-01670-y

Bourque, J. R., Robertson, C. M., Brooke, S., & Demopoulos, A. W. J. (2017). Macrofaunal communities associated with chemosynthetic habitats from the U.S. Atlantic margin: A comparison among depth and habitat types. *Deep Sea Research Part II: Topical Studies in Oceanography*, *137*, 42–55. https://doi.org/10.1016/j.dsr2.2016.04.012

Breitburg, D., Levin, L. A., Oschlies, A., Grégoire, M., Chavez, F. P., Conley, D. J., Garçon, V., Gilbert, D., Gutiérrez, D., Isensee, K., Jacinto, G. S., Limburg, K. E., Montes, I., Naqvi, S. W. A., Pitcher, G. C., Rabalais, N. N., Roman, M. R., Rose, K. A., Seibel, B. A., Telszewski, M., Yasuhara, M., Zhang, J. (2018). Declining oxygen in the global ocean and coastal waters. *Science*, *359*(6371). https://doi.org/10.1126/science.aam7240

Buhl-Mortensen, L., Vanreusel, A., Gooday, A. J., Levin, L. A., Priede, I. G., Buhl-Mortensen, P., Gheerardyn, H., King, N. J., & Raes, M. (2010). Biological structures as a source of habitat heterogeneity and biodiversity on the deep ocean margins. *Marine Ecology*, *31*(1), 21–50. https://doi.org/10.1111/j.1439-0485.2010.00359.x

Carney, R. S. (1997). Basing conservation policies for the deep-sea floor on current-diversity concepts: a consideration of rarity.

Checkley, D. M., & Barth, J. A. (2009). Patterns and processes in the California Current System. *Progress in Oceanography*, *83*(1–4), 49–64. https://doi.org/10.1016/j.pocean.2009.07.028

Christodoulou, M., O'Hara, T. D., Hugall, A. F., & Arbizu, P. M. (2019). Dark Ophiuroid Biodiversity in a Prospective Abyssal Mine Field. *Current Biology*, *29*(22), 3909-3912.e3. https://doi.org/10.1016/j.cub.2019.09.012

Conrad, T., Hein, J. R., Paytan, A., & Clague, D. A. (2017). Formation of Fe-Mn crusts within a continental margin environment. *Ore Geology Reviews*, *87*, 25–40. https://doi.org/10.1016/j.oregeorev.2016.09.010

Corrêa, P. V. F., Jovane, L., Murton, B. J., & Sumida, P. Y. G. (2022). Benthic megafauna habitats, community structure and environmental drivers at Rio Grande Rise (SW Atlantic). *Deep Sea Research Part I: Oceanographic Research Papers*, *186*, 103811. https://doi.org/10.1016/j.dsr.2022.103811

Danovaro, R., Fanelli, E., Aguzzi, J., Billett, D., Carugati, L., Corinaldesi, C., Dell'Anno, A., Gjerde, K., Jamieson, A. J., Kark, S., McClain, C., Levin, L., Levin, N., Ramirez-Llodra, E., Ruhl, H., Smith, C. R., Snelgrove, P. V. R., Thomsen, L., Van Dover, C. L., & Yasuhara, M. (2020). Ecological variables for developing a global deep-ocean monitoring and conservation strategy. *Nature Ecology & Evolution*, *4*(2), 181–192. https://doi.org/10.1038/s41559-019-1091-z

Danovaro, R., Gambi, C., Dell'Anno, A., Corinaldesi, C., Fraschetti, S., Vanreusel, A., Vincx, M., & Gooday, A. J. (2008). Exponential Decline of Deep-Sea Ecosystem Functioning Linked to Benthic Biodiversity Loss. *Current Biology*, *18*(1), 1–8. https://doi.org/10.1016/j.cub.2007.11.056

De Smet, B., Pape, E., Riehl, T., Bonifácio, P., Colson, L., & Vanreusel, A. (2017). The community structure of deep-sea macrofauna associated with polymetallic nodules in the eastern part of the Clarion-Clipperton Fracture Zone. *Frontiers in Marine Science*, *4*(APR). https://doi.org/10.3389/fmars.2017.00103

De Smet, B., Simon-Lledó, E., Mevenkamp, L., Pape, E., Pasotti, F., Jones, D. O. B., & Vanreusel, A. (2021). The megafauna community from an abyssal area of interest for mining of polymetallic nodules. *Deep-Sea Research Part I: Oceanographic Research Papers*, *172*. https://doi.org/10.1016/j.dsr.2021.103530

Dong, D., Li, X., Yang, M., Gong, L., Li, Y., Sui, J., Gan, Z., Kou, Q., Xiao, N., & Zhang, J. (2021). Report of epibenthic macrofauna found from Haima cold seeps and adjacent deep-sea habitats, South China Sea. *Marine Life Science and Technology*, *3*(1). https://doi.org/10.1007/s42995-020-00073-9

Gage, J. D., & Tyler, P. A. (1991). *Deep-Sea Biology*. Cambridge University Press. https://doi.org/10.1017/CBO9781139163637

Gooday, A. J., Bett, B. J., Escobar, E., Ingole, B., Levin, L. A., Neira, C., Raman, A. V., & Sellanes, J. (2010). Habitat heterogeneity and its influence on benthic biodiversity in oxygen minimum zones. *Marine Ecology*, *31*(1), 125–147. https://doi.org/10.1111/j.1439-0485.2009.00348.x

Grigg, R. W., Malaboff, A., Chave, E. H., & Landahl, J. (2013). *Seamount Benthic Ecology and Potential Environmental Impact from Manganese Crust Mining in Hawaii* (pp. 379–390). https://doi.org/10.1029/GM043p0379

Hein, J., Koschinsky, A., Mikesell, M., Mizell, K., Glenn, C., & Wood, R. (2016). Marine Phosphorites as Potential Resources for Heavy Rare Earth Elements and Yttrium. *Minerals*, *6*(3), 88. https://doi.org/10.3390/min6030088

Hein, J. R., Mizell, K., Koschinsky, A., & Conrad, T. A. (2013). Deep-ocean mineral deposits as a source of critical metals for high- and green-technology applications: Comparison with land-based resources. In *Ore Geology Reviews* (Vol. 51, pp. 1–14). https://doi.org/10.1016/j.oregeorev.2012.12.001

Howard, E. M., Penn, J. L., Frenzel, H., Seibel, B. A., Bianchi, D., Renault, L., Kessouri, F., Sutula, M. A., McWilliams, J. C., & Deutsch, C. (2020). Climate-driven aerobic habitat loss in the California Current System. *Science Advances*, *6*(20). https://doi.org/10.1126/sciadv.aay3188

Jones, D. O. B., Amon, D. J., & Chapman, A. S. A. (2018). Mining Deep-Ocean Mineral Deposits: What are the Ecological Risks? *Elements*, *14*(5), 325–330. https://doi.org/10.2138/gselements.14.5.325

Kato, S., Okumura, T., Uematsu, K., Hirai, M., Iijima, K., Usui, A., & Suzuki, K. (2018). Heterogeneity of Microbial Communities on Deep-Sea Ferromanganese Crusts in the Takuyo-Daigo Seamount. *Microbes and Environments*, *33*(4), 366–377. https://doi.org/10.1264/jsme2.ME18090

Keeling, R. F., Körtzinger, A., & Gruber, N. (2010). Ocean Deoxygenation in a Warming World. *Annual Review of Marine Science*, *2*(1), 199–229. https://doi.org/10.1146/annurev.marine.010908.163855

Le, J. T., Levin, L. A., & Carson, R. T. (2017). Incorporating ecosystem services into environmental management of deep-seabed mining. *Deep Sea Research Part II: Topical Studies in Oceanography, 137*, 486–503. https://doi.org/10.1016/j.dsr2.2016.08.007

Leduc, D., Rowden, A. A., Torres, L. G., Nodder, S. D., & Pallentin, A. (2015). Distribution of macro-infaunal communities in phosphorite nodule deposits on Chatham Rise, Southwest Pacific: Implications for management of seabed mining. *Deep-Sea Research Part I: Oceanographic Research Papers*, *99*, 105–118. https://doi.org/10.1016/j.dsr.2015.01.006

Levin, L. A. (2003). Oxygen minimum zone benthos: adaptation and community response to hypoxia. In *Annual Review* (Vol. 41).

Levin, L. A., Etter, R. J., Rex, M. A., Gooday, A. J., Smith, C. R., Jes´, J., Pineda, J., Stuart, C. T., Hessler, R. R., & Pawson, D. (2001). Environmental influences on regional deep-sea species diversity.

Levin, L. A., Gage, J. D., Martin, C., & Lamont, P. A. (2000). Macrobenthic community structure within and beneath the oxygen minimum zone, NW Arabian Sea. In *A. Levin) Deep-Sea Research II* (Vol. 47).

Levin, L. A., Mendoza, G. F., & Grupe, B. M. (2017). Methane seepage effects on biodiversity and biological traits of macrofauna inhabiting authigenic carbonates. *Deep-Sea Research Part II: Topical Studies in Oceanography*, *137*, 26–41. https://doi.org/10.1016/j.dsr2.2016.05.021

Levin, L. A., Mendoza, G. F., Grupe, B. M., Gonzalez, J. P., Jellison, B., Rouse, G., Thurber, A. R., & Waren, A. (2015). Biodiversity on the rocks: Macrofauna inhabiting authigenic carbonate at Costa Rica methane seeps. *PLoS ONE*, *10*(7). https://doi.org/10.1371/journal.pone.0131080

Levin, L. A., Mengerink, K., Gjerde, K. M., Rowden, A. A., Van Dover, C. L., Clark, M. R., Ramirez-Llodra, E., Currie, B., Smith, C. R., Sato, K. N., Gallo, N., Sweetman, A. K., Lily, H., Armstrong, C. W., & Brider, J. (2016). Defining "serious harm" to the marine environment in the context of deep-seabed mining. *Marine Policy*, *74*, 245–259. https://doi.org/10.1016/j.marpol.2016.09.032

Levin, L., Gutiérrez, D., Rathburn, A., Neira C, C., Sellanes, J., Muñoz, P., Gallardo, V., & Salamanca, M. (2002). Benthic processes on the Peru margin: a transect across the oxygen minimum zone during the 1997-98 El Niño. In *Progress in Oceanography* (Vol. 53). www.elsevier.com/locate/pocean

Levint, L. A., Huggett, C. L., & Wishner, K. F. (1991). Previously published as Cynthia L. Thomas, 3. Graduate School of Oceanography. In *Journal of Marine Research* (Vol. 49). https://elischolar.library.yale.edu/

LI, X. (2017). Taxonomic research on deep-sea macrofauna in the South China Sea using the Chinese deep-sea submersible *Jiaolong*. *Integrative Zoology*, *12*(4), 270–282. https://doi.org/10.1111/1749-4877.12254

Ma, J., Song, J., Li, X., Wang, Q., Zhong, G., Yuan, H., Li, N., & Duan, L. (2021). The OMZ and Its Influence on POC in the Tropical Western Pacific Ocean: Based on the Survey in March 2018. *Frontiers in Earth Science*, *9*. https://doi.org/10.3389/feart.2021.632229

Macheriotou, L., Rigaux, A., Derycke, S., & Vanreusel, A. (2020). Phylogenetic clustering and rarity imply risk of local species extinction in prospective deep-sea mining areas of the Clarion–Clipperton Fracture Zone. *Proceedings of the Royal Society B: Biological Sciences*, *287*(1924), 20192666. https://doi.org/10.1098/rspb.2019.2666

Mizell, K., Hein, J. R., Lam, P. J., Koppers, A. A. P., & Staudigel, H. (2020). Geographic and Oceanographic Influences on Ferromanganese Crust Composition Along a Pacific Ocean Meridional Transect, 14 N to 14S. *Geochemistry, Geophysics, Geosystems*, *21*(2). https://doi.org/10.1029/2019GC008716

Montserrat, F., Guilhon, M., Corrêa, P. V. F., Bergo, N. M., Signori, C. N., Tura, P. M., Santos Maly, M. de los, Moura, D., Jovane, L., Pellizari, V., Sumida, P. Y. G., Brandini, F. P., & Turra, A. (2019). Deep-sea mining on the Rio Grande Rise (Southwestern Atlantic): A review on environmental baseline, ecosystem services and potential impacts. In *Deep-Sea Research Part I: Oceanographic Research Papers* (Vol. 145, pp. 31–58). Elsevier Ltd. https://doi.org/10.1016/j.dsr.2018.12.007

Mullineaux, L. S. (1987). Organisms living on manganese nodules and crusts: distribution and abundance at three North Pacific sites. In *Deep-Sea Research* (Vol. 34, Issue 2).

Mullineaux, L. S. (1989). Vertical distributions of the epifauna on manganese nodules: Implications for settlement and feeding. *Limnology and Oceanography*, *34*(7), 1247–1262. https://doi.org/10.4319/lo.1989.34.7.1247

Nahmani, J., & Lavelle, P. (2002). Effects of heavy metal pollution on soil macrofauna in a grassland of Northern France. *European Journal of Soil Biology*, *38*(3–4), 297–300. https://doi.org/10.1016/S1164-5563(02)01169-X

Oliver, T. H., Heard, M. S., Isaac, N. J. B., Roy, D. B., Procter, D., Eigenbrod, F., Freckleton, R., Hector, A., Orme, C. D. L., Petchey, O. L., Proença, V., Raffaelli, D., Suttle, K. B., Mace, G. M., Martín-López, B., Woodcock, B. A., & Bullock, J. M. (2015). Biodiversity and Resilience of Ecosystem Functions. In *Trends in Ecology and Evolution* (Vol. 30, Issue 11, pp. 673–684). Elsevier Ltd. https://doi.org/10.1016/j.tree.2015.08.009

Oschlies, A., Brandt, P., Stramma, L., & Schmidtko, S. (2018). Drivers and mechanisms of ocean deoxygenation. *Nature Geoscience*, *11*(7), 467–473. https://doi.org/10.1038/s41561-018-0152-2

Pereira, O. S., Gonzalez, J., Mendoza, G. F., Le, J., Coscino, C. L., Lee, R. W., Cortés, J., Cordes, E. E., & Levin, L. A. (2021). The dynamic influence of methane seepage on macrofauna inhabiting authigenic carbonates. *Ecosphere*, *12*(10). https://doi.org/10.1002/ecs2.3744

Pereira, O. S., Gonzalez, J., Mendoza, G., Le, J., McNeill, M., Ontiveros, J., Lee, R. W., Rouse, G. W., Cortés, J., & Levin, L. A. (2022). Does substrate matter in the deep sea? A comparison of bone, wood, and carbonate rock colonizers. *PLoS ONE*, *17*(7 July). https://doi.org/10.1371/journal.pone.0271635

Rabone, M., Wiethase, J. H., Simon-Lledó, E., Emery, A. M., Jones, D. O. B., Dahlgren, T. G., Bribiesca-Contreras, G., Wiklund, H., Horton, T., & Glover, A. G. (2023). How many metazoan species live in the world's largest mineral exploration region? *Current Biology*, *33*(12), 2383-2396.e5. https://doi.org/10.1016/j.cub.2023.04.052

Ramirez-Llodra, E., Brandt, A., Danovaro, R., De Mol, B., Escobar, E., German, C. R., Levin, L. A., Martinez Arbizu, P., Menot, L., Buhl-Mortensen, P., Narayanaswamy, B. E., Smith, C. R., Tittensor, D. P., Tyler, P. A., Vanreusel, A., & Vecchione, M. (2010). Deep, diverse and definitely different: unique attributes of the world's largest ecosystem. *Biogeosciences*, *7*(9), 2851–2899. https://doi.org/10.5194/bg-7-2851-2010

Ramirez-Llodra, E., Tyler, P. A., Baker, M. C., Bergstad, O. A., Clark, M. R., Escobar, E., Levin, L. A., Menot, L., Rowden, A. A., Smith, C. R., & Van Dover, C. L. (2011). Man and the Last Great Wilderness: Human Impact on the Deep Sea. *PLoS ONE*, *6*(8), e22588. https://doi.org/10.1371/journal.pone.0022588

Schlacher, T. A., Baco, A. R., Rowden, A. A., O'Hara, T. D., Clark, M. R., Kelley, C., & Dower, J. F. (2014). Seamount benthos in a cobalt-rich crust region of the central <scp>P</scp> acific: conservation challenges for future seabed mining. *Diversity and Distributions*, *20*(5), 491–502. https://doi.org/10.1111/ddi.12142

Schmidtko, S., Stramma, L., & Visbeck, M. (2017). Decline in global oceanic oxygen content during the past five decades. *Nature*, *542*(7641), 335–339. https://doi.org/10.1038/nature21399

Simon-Lledó, E., Bett, B. J., Huvenne, V. A. I., Schoening, T., Benoist, N. M. A., & Jones, D. O. B. (2019). Ecology of a polymetallic nodule occurrence gradient: Implications for deep-sea mining. *Limnology and Oceanography*, *64*(5), 1883–1894. https://doi.org/10.1002/lno.11157

Smith, C. R., & Hamilton, S. C. (1983). Epibenthic megafauna of a bathyal basin off southern California: patterns of abundance, biomass, and dispersion. *Deep Sea Research Part A. Oceanographic Research Papers*, *30*(9), 907–928. https://doi.org/10.1016/0198-0149(83)90048-1

Stramma, L., Schmidtko, S., Levin, L. A., & Johnson, G. C. (2010). Ocean oxygen minima expansions and their biological impacts. *Deep Sea Research Part I: Oceanographic Research Papers*, *57*(4), 587–595. https://doi.org/10.1016/j.dsr.2010.01.005

Thompson, J. B., Mullins, H. T., Newton, C. R., & Vercoutere, T. L. (1985). Alternative biofacies model for dysaerobic communities. *Lethaia*, *18*(2), 167–179. https://doi.org/10.1111/j.1502-3931.1985.tb00695.x

Thurber, A. R., Sweetman, A. K., Narayanaswamy, B. E., Jones, D. O. B., Ingels, J., & Hansman, R. L. (2014). Ecosystem function and services provided by the deep sea. *Biogeosciences*, *11*(14), 3941–3963. https://doi.org/10.5194/bg-11-3941-2014

Toscano, F., & Raspini, A. (2005). Epilithozoan fauna associated with ferromanganese crustgrounds on the continental slope segment between Capri and Li Galli Islands (Bay of Salerno, Northern Tyrrhenian Sea, Italy). *Facies*, *50*(3–4), 427–441. https://doi.org/10.1007/s10347-004-0036-3

Usui, A., Nishi, K., Sato, H., Nakasato, Y., Thornton, B., Kashiwabara, T., Tokumaru, A., Sakaguchi, A., Yamaoka, K., Kato, S., Nitahara, S., Suzuki, K., Iijima, K., & Urabe, T. (2017). Continuous growth of hydrogenetic ferromanganese crusts since 17 Myr ago on Takuyo-Daigo Seamount, NW Pacific, at water depths of 800–5500 m. *Ore Geology Reviews*, *87*, 71–87. https://doi.org/10.1016/j.oregeorev.2016.09.032

Vanreusel, A., Fonseca, G., Danovaro, R., Da Silva, M. C., Esteves, A. M., Ferrero, T., Gad, G., Galtsova, V., Gambi, C., Da Fonsêca Genevois, V., Ingels, J., Ingole, B., Lampadariou, N., Merckx, B., Miljutin, D., Miljutina, M., Muthumbi, A., Netto, S., Portnova, D., Radziejewska, T., Raes, M., Tchesunov, A., Vanaverbeke, J., Van, S.G., Venekey, V., Bezerra, T.N., Flint, H., Copley, J., Pape, E., Zeppilli, D., Martinez, P.A., Galeron, J. (2010). The contribution of deep-sea macrohabitat heterogeneity to global nematode diversity. *Marine Ecology*, *31*(1), 6–20. https://doi.org/10.1111/j.1439-0485.2009.00352.x

Veillette, J., Sarrazin, J., Gooday, A. J., Galéron, J., Caprais, J.-C., Vangriesheim, A., Étoubleau, J., Christian, J. R., & Kim Juniper, S. (2007). Ferromanganese nodule fauna in the Tropical North Pacific Ocean: Species richness, faunal cover and spatial distribution. *Deep Sea Research Part I: Oceanographic Research Papers*, *54*(11), 1912–1935. https://doi.org/10.1016/j.dsr.2007.06.011

Verlaan, P. A. (1992). Marine Biology Benthic recruitment and manganese crust formation on. In *Marine Biology* (Vol. 113).

Wei, C.-L., & Rowe, G. T. (2019). Productivity controls macrofauna diversity in the deep northern Gulf of Mexico. *Deep Sea Research Part I: Oceanographic Research Papers*, *143*, 17–27. https://doi.org/10.1016/j.dsr.2018.12.005

Wei, C.-L., Rowe, G. T., Escobar-Briones, E., Nunnally, C., Soliman, Y., & Ellis, N. (2012). Standing stocks and body size of deep-sea macrofauna: Predicting the baseline of 2010

Deepwater Horizon oil spill in the northern Gulf of Mexico. *Deep Sea Research Part I: Oceanographic Research Papers*, *69*, 82–99. https://doi.org/10.1016/j.dsr.2012.07.008